AD_____

Award Number:
W81XWH-06-1-0120

TITLE:
Evaluation of Genomic Instability in the Abnormal Prostate

PRINCIPAL INVESTIGATOR:
Christina Haaland-Pullus, A.S., B.S.
Jeffrey K Griffith, Ph D

CONTRACTING ORGANIZATION:
The University of New Mexico
Albuquerque, New Mexico 87131

REPORT DATE:
December 2008

TYPE OF REPORT:
Annual Summary

PREPARED FOR: U.S. Army Medical Research and Materiel Command
Fort Detrick, Maryland 21702-5012

REPORT DOCUMENTATION PAGE

Form Approved
OMB No. 0704-0188

1. REPORT DATE *(DD-MM-YYYY)*	2. REPORT TYPE	3. DATES COVERED *(From - To)*
01-12-2008	Annual Summary	1 Dec 2005- 30 Nov 2008

4. TITLE AND SUBTITLE
Evaluation of Genomic Instability in the Abnormal Prostate

5a. CONTRACT NUMBER

5b. GRANT NUMBER
W81XWH-06-1-0120

5c. PROGRAM ELEMENT NUMBER

6. AUTHOR(S)

Christina Haaland-Pullus, A.S., B.S.

Jeffrey K Griffith, Ph D

5d. PROJECT NUMBER

5e. TASK NUMBER

5f. WORK UNIT NUMBER

7. PERFORMING ORGANIZATION NAME(S) AND ADDRESS(ES)
The University of New Mexico

Albuquerque, New Mexico 87131

8. PERFORMING ORGANIZATION REPORT NUMBER

9. SPONSORING / MONITORING AGENCY NAME(S) AND ADDRESS(ES)
U.S. Army Medical Research and Materiel Command
Fort Detrick, Maryland 21702-5012

10. SPONSOR/MONITOR'S ACRONYM(S)

11. SPONSOR/MONITOR'S REPORT NUMBER(S)

12. DISTRIBUTION / AVAILABILITY STATEMENT
Approved for public release; distribution unlimited

13. SUPPLEMENTARY NOTES

14. ABSTRACT
The aim of this study is to investigate field effect in prostate cancer, the relationship between tumor and nearby histologically normal tissues compared to truly disease free prostate tissue. Identification of changes within tumor adjacent tissues has two possible clinical implications: prognosis and diagnosis. Several tools are being used to investigate this effect, specifically the assessment of telomere length, allelic imbalance, and methylation status, all markers of genomic instability. Microarray studies will be used to aid in the identification of additional gene expression changes occurring between tumor and histologically normal tissues compared to truly disease free tissue. While telomere length and allelic imbalance have been shown to correlate with outcome, it is expected that, when compared with truly normal tissue from disease-free prostates, several progressive changes will be seen, as has been found in prostate cancer cell lines. The proposed study will allow for interaction with other scientists, exposure to new technologies, teaching and continued patient interaction, all of which are important to the physician scientist.

15. SUBJECT TERMS
Prostate Cancer, Telomeres, Methylation, Micro array, Slot Blot, Allelic Imbalance

16. SECURITY CLASSIFICATION OF:			17. LIMITATION OF ABSTRACT	18. NUMBER OF PAGES	19a. NAME OF RESPONSIBLE PERSON
a. REPORT	b. ABSTRACT	c. THIS PAGE	UU	94	19b. TELEPHONE NUMBER *(include area code)*
unclassified	unclassified	unclassified			

Table of Contents

I. Introduction

The aim of this study is to investigate the relationship between tumor and tumor adjacent histologically normal (TAHN) prostate tissues, also referred to as the field effect. When compared with truly disease free prostate tissue, identification of changes within tumor adjacent tissues has two possible clinical implications: prognosis and diagnosis. Several tools are being used to investigate the field effect, specifically the assessment of telomere length, allelic imbalance, and methylation status, all markers of genomic instability. Microarray studies will be used to aid in the identification of additional gene expression changes occurring between tumor and histologically normal tissues compared to truly disease free tissue. While telomere length and allelic imbalance of tumor tissue have been shown to correlate with staging, it is expected that, when compared with truly normal tissue from disease-free prostates, changes will be seen in the nearby histologically normal tissues as well. The proposed study will allow for interaction with other scientists, exposure to new technologies, teaching and continued patient interaction, all of which are important to the physician scientist.

Hypothesis and Rationale

It is currently thought that a multi-step process is involved in the development of prostate cancer. Preliminary data from our laboratory suggest that telomere content (TC) and allelic imbalance (AI) are altered in both tumor and tumor adjacent tissue, and that these changes precede histologic changes. It is reasonable to extrapolate from this that normal appearing tissue may have diagnostic properties. Our data also suggest that there is a relationship between the level of genomic instability and prostate cancer relapse, indicating that this tissue may also have prognostic significance. Because the TC and AI modalities have previously shown correlation between staging and outcome, these will be used to determine the effectiveness of a PCR-based promoter methylation assay. Additionally, this study will incorporate microarray analysis to help guide the determination of where to look for changes in methylation status based on expression changes, as this will allow determination of expression differences between tumor, tumor adjacent tissues, and disease free prostate tissues.

Specific Aim #1: *Further assess and refine the use of the allelic imbalance assay in predicting potential disease relapse in retrospective and prospective studies of prostate cancer.*

Specific Aim #2: *Compare methylation states of genes known to be associated with prostate cancer, such as GSTP1, P504S, and CD44, between tumor cells, TAHN tissue and normal prostate tissue from men without cancer.*

Specific Aim #3: *Assess with microarray technology characteristic changes in gene expression relevant to prognosis in prostate cancer, and determine if this profile extends to surrounding histologically normal cells.*

II. Body

IIa. Materials and Methods

Patient Specimens:

Samples for use in all arms of the study have been identified and collected from the New Mexico Tumor Registry (NMTR), National Cancer Institute Cooperative Human Tissue Network (CHTN, Nashville, TN), Cooperative Prostate Cancer Tissue Resource (Pittsburg, PA) and the University of New Mexico School of Medicine (UNMSOM). Cases containing tumor adjacent histologically normal (TAHN) Biopsy, Cancerous Biopsy, TAHN (from prostatectomy), and Tumor (from prostatectomy) tissues were obtained from the Cooperative Prostate Cancer Tissue Resource (CPCTR, Pittsburg, Pennsylvania) for the TC (Table 2, 3) and AI studies (Table 4, 5). Control RNA, consisting of 9 pooled patients (from sudden death cases), was obtained from Ambion (Austin, TX) for use as the control in the microarray study.

Cell Lines:

DNA from cell lines (LnCaP, DU146, C4-2b, and PC-3) were used to determine if the primers and sodium bisulfite treatment were functioning properly. These lines represent a range of prostate cancer and gene promoter methylation.

Methylated DNA Control:

Universally methylated DNA (CpGenome™ Universal Methylated DNA) was obtained from Millipore (Temecula, CA) for use as a positive control in the methylation studies.

DNA Isolation:

All samples were fresh-frozen tissue with the exception of those from the CPCTR, from which DNA was isolated using a commercially available kit (DNeasy, Qiagen, Valencia, CA). The tissues from CPCTR were formalin-fixed, paraffin embedded sections, which were first deparaffinized and rehydrated prior to removal of the tissue from the slides, followed by DNA extraction in the same manner as the other samples. Following DNA isolation and in preparation for the Telomere Content (TC) assay, the dsDNA concentration was measured using PicoGreen (Quant-iT™ Picogreen ® dsDNA Kit, Molecular Probes, Eugene, OR) according to the manufacturer's protocol. For the Allelic Imbalance (AI) assay and methylation studies, DNA was quantified using a Thermo Scientific NanoDrop™ 1000 Spectrophotometer (Wilmington, DE).

RNA Isolation and Labeling:

RNA was isolated with commercially available kits (Qiashredder and RNeasy kits, Qiagen, Valencia, CA) from the set of 12 cases identified for use in the microarray study. RNA was assessed by NanoDrop™ (Thermo Scientific, Wilmington, DE) and the Agilent Bioanalyzer 2100 (Agilent, Foster City, CA) to determine quantity and quality of the RNA isolated.

RNA from 6 matched cases (*i.e.* a TAHN and Tumor sample from the same ~~one~~ patient) was then reverse transcribed into complementary DNA (cDNA) using the Retroscript™ RT Kit (Ambion, Austin, TX), followed by labeling with either Cy3 (pooled control RNA) or Cy5 (either tumor or TAHN pool) fluorescent cyanine dyes. Labeling was achieved by synthesizing the cDNAs in the presence of amino allyl dUTP (Sigma-Aldrich, St. Louis, MO) followed by chemically coupling of either Cy3 or Cy5 monofunctional dye (Amersham-Pharmacia Biotech, Arlington Heights, IL) to the cDNA. This process avoids biased incorporation of the dyes during reverse transcription. Dye incorporation was measured by NanoDrop™ (Thermo Scientific, Wilmington, DE) on an individual sample basis prior to pooling of the experimental groups in order to ensure equal representation of each sample in the pool.

Telomere Content (TC) Assay:

Assessment of TC was carried out as described previously (*1, 2*). Briefly, this is a blot assay that allows for chemiluminescent detection and quantitation of telomere content using a labeled telomere-specific probe.

Allelic Imbalance Assay:

Assessment of AI was performed as previously described (*3-5*) using the AmpFlSTR® kit (Applied Biosystems, Foster City, CA) which contains reagents that amplify 16 different short tandem repeat (i.e. microsatellite) loci within a single multiplex reaction.

Microarray Expression Analysis: (see Appendix B for complete manuscript)

Glass-slide-spotted-expression microarrays of the Qiagen Human Genome Oligo Set Version 3.0 (Qiagen) were used for this investigation. The arrays contained 37,123 transcripts, including 24,650 known genes, the rest being expressed sequence tags (ESTs) and controls. The design of these arrays is based on the Ensembl Human 13.31 Database (http://www.ensembl.org/) and on the Human Genome Sequencing Project. Equal parts of Cy3 and Cy5 labeled cDNAs were then combined and competitively hybridized to the microarray slides using the GeneTAC Genomic Solutions machine and protocol (Genomic Solutions Inc, Ann Arbor, MI). Following hybridization and washing, the slides were scanned at 532nm and 635nm using the Axon 4000A scanner (Axon Instruments, Union City, CA), and the signal data was processed using Axon GenePix Pro 5 software (Axon Instruments). Fluorescence intensities of the Cy3 and Cy5 dyes were determined for each oligonucleotide spot, followed by visual inspection prior to importing into Acuity 3.0 (Molecular Devices, Sunnyvale, CA). This program was utilized to normalize the data and allow for comparison between the replicates using standard quality calls (background removal, linear regression ratio >0.6, signal to noise ratio >3.0). Only data passing these quality filters were utilized in the present analysis. Sample groups, i.e. tumor and TAHN pools, were run in triplicate hybridizations.

Quantitative (real time) Reverse Transcriptase PCR:

Quantitative Real Time PCR (qRT-PCR) was used to verify the results of the microarray expression analyses. Samples from both the microarray (MA) and the independent validation array (VA) sets were individually analyzed in quadruplicate for each selected gene/primer set. Approximately 1 µg of RNA from the samples was converted to cDNA using the Retroscript™ RT Kit (Ambion) according to the manufacturer's protocol using random decamers. The cDNAs were subsequently diluted 1:5 for use in the PCR reactions.

The gene evaluated for mRNA expression to date is early growth response protein 1 (EGR-1). The sequence for PCR primers was previously published (*6*). mRNA levels were quantitated using the Sybr Green real-time PCR assay kit (Applied Biosystems, Foster City, CA) in a 25uL reaction, using 0.5uL of the diluted cDNA. Primers were used at a final concentration of 1 µmol for the forward and 1.5 µmol for the reverse in the PCR reaction. PCR reactions were carried out under the following cycling parameters: 95˚C for 10 minutes followed by 40 cycles of 95˚C for 15 seconds, and 60˚C for one minute using the Gene Amp® 7000 Sequence Detection System (Applied Biosystems). Baseline fluorescence was determined during cycles 6-15.

The levels of EGR-1 were determined using the ΔΔCt method, where the threshold of detection of the genes of interest were compared to the house keeping gene TATA binding protein (TBP). This method was chosen because the amplification efficiency of their primers was determined to be similar to that of the control transcript.

Sodium Bisulfite Treatment and Quantitative Methylation Specific PCR (Q-MSP):

Following DNA extraction, DNA was treated with the commercially available sodium bisulfite-based kit CpGenome fast DNA modification kit (Millipore, Temecula, CA) to cause deamination of unmethylated cytosines in the CpG repeats.

Primers used here were previously published (*7-9*) (Table 1). Semi-quantitative methylation specific PCR (QMSP) utilized methylated DNA specific TaqMan probes to detect methylated samples. In this technique, 1 uL of the sodium bisulfite treated DNA was combined with 10 uL of 2x TaqMan Universal PCR Kit (Applied Biosystems, Foster City, CA), 600 nmol of each primer, 200 nmol probe, and the remaining volume water for a total of 20 uL. The reactions were run on an ABI PRISM 7000 real time PCR machine with the following protocol: Initial denaturation at 95°C for 10 minutes followed by 50 cycles of 95°C for 15 seconds then 60°C for one minute (*8, 10, 11*). All samples were run in quadruplicate, and a promoter specific to unmethylated β-actin was used as the internal control. To determine levels of methylation, the delta Ct of a sample was divided by the delta Ct of β-actin and then multiplied by 100 to give a representative methylation level. Controls included a control reaction without template and a fully methylated DNA control (CpGenome™ Universal Methylated DNA, Millipore, Temecula, CA). In order for the data to be considered acceptable, there needed to be at least three interpretable results, which were then averaged and used in the calculation of relative methylation. Primers were designed to generate products between 80-200bp in size.

IIb. Results

Telomere Content Study

Telomere content in the six normal prostate tissues ranged from 94-121%. This agrees well with the previously reported range of 75-143%, that defines TC in 95% of 70 normal tissue samples from multiple organ sources (*4*).

Telomere content of the histologically normal tissue from biopsies (n=15) ranged from 25-217%, with a mean of 86% and median of 66%. Cancerous tissue from biopsy telomere content (n=40) ranged from 7-220%, with a mean of 74% and a median of 66%. The range for TAHN (n=33) was 17-355%, with a mean of 77% and a median of 58%. Finally, Tumor (n=39) ranged from 11-360% with a mean of 66% and a median of 59% (Figure 6).The median of all sample groupings fell below the experimentally determined normal telomere content range.

TC in TAHN and Tumor tissues in patient matched samples was strongly correlated (n=29, r^2=0.707, p=<0.0001, Figure 13) as was TC in TAHN and cancerous tissues from patient matched biopsy specimens (n=14, r^2=0.720, p=0.0001). Surprisingly, TC was neither correlated in TAHN tissues from patient matched biopsy and prostatectomy (n=11, r^2=0.012, p=0.7498), nor cancerous tissues from patient matched biopsy and prostatectomy (n=24, r^2=0.035, p=0.3823) (Figure 7).

To date, results of the TC studies are consistent with those previously published by this laboratory (*4, 12*). Specifically, TC in TAHN tissues is more similar to TC in tumor tissues than normal tissues, indicating the presence of a field of abnormal cells surrounding the tumor. However, the purpose of the current study is to verify these findings in an additional study cohort. Prospective samples are being collected, however the time frame of the study will not allow for follow up information to be collected. Instead a retrospective cohort (CPCTR) has been identified and is currently being analyzed.

Allelic Imbalance Study

Allelic Imbalance was investigated in a total of 143 samples, 24 histologically normal biopsy samples, 41 cancerous biopsy samples, 31 TAHN samples, 38 Tumor samples, and 9 disease-free prostate samples. Seven of the normal samples had zero sites of AI, and 2 samples had 1 site of AI for an average of 0.22 sites of AI per sample. These results were consistent with our previous study of 118 normal tissues from various organs. This demonstrated that approximately 75% and 25% of normal tissues have no sites and one site of AI, respectively. Only one sample (0.8%) had 2 sites of AI. Overall, there was an average of 0.27 sites of AI per sample (*13*).

In contrast to the normal tissues, the histologically normal biopsy samples had an average of 1.92 sites of AI (p=0.0049), while the cancerous biopsy samples had an average of 1.61 sites of AI (p=0.0001). Among the prostatectomy samples, TAHN tissues had an average of 2.23 sites of AI (p=0.0006) and the Tumor tissues had 2.71 sites of AI (p=<0.0001) on average (Figure 8).

With multiple patient matched specimens, the opportunity arose to investigate clonality between the field and the tumor cells populations. Additionally, because the patient cases included both biopsy and prostatectomy specimens, clonality could also be looked at over time, *i.e.* between biopsy and prostatectomy. We hypothesized that if a clonal relationship existed between the specimens, there would be matched sites of AI between them, *i.e.* the same locus would be imbalanced in both the TAHN and Tumor specimens. Analysis of the actual sites of AI was performed on three sub-populations: paired biopsy samples, paired prostatectomy samples, and matched samples with data for both biopsy and prostatectomy samples, resulting in groups of 4 pairs, 10 pairs, and 18 sets, respectively. Sites of AI in the patient matched cancerous biopsy specimens were compared to the histologically normal biopsy specimens and sites of AI found in patient matched tumor tissue were compared to TAHN (Table 6). While the four sets of matched histologically normal and cancerous biopsies did not contain and matched sites of AI, the 10 patient matched prostatectomy samples had 7 common sites of AI out of 17 possible instances (41.2%). In the 18 cases with all 4 tissues types providing data (Table 7), there were 12 instances of matched AI sites in the biopsy tissues out of 33 instances of AI in the Negative Biopsy samples (36.4%); 11 matched sites existed with 46 possible matches (23.9%) between tumor compared with TAHN. Nine sites of AI were found in 3 of the 4 tissue types (*i.e.* cancerous biopsy, TAHN, and tumor specimens), and 3 of these cases had 2 instances of the conserved sites. Most interesting was the finding of 2 cases with a conserved site of AI in all 4 samples.

Prospective samples are being collected, however the time frame of the study will not allow for follow up information to be collected. Instead a retrospective cohort (CPCTR) has been identified analyzed.

Microarray expression analysis. (See Appendix B for complete manuscript)

RNA expression levels are reported here as ratios of Cy3/Cy5 signals for individual transcripts, where the Cy3 and Cy5 fluorescent cyanine dyes were used to label cDNA from experimental (tumor or TAHN) and pooled cancer-free control tissues, respectively. While a ratio of 1.0 would thus indicate no change in expression compared to cancer-free controls, there is the possibility of dye bias due to differential incorporation of Cy3 and Cy5 during cDNA synthesis, or due to differential hybridization of Cy3- and Cy5-labeled cDNAs to target probes. To estimate the extent of potential dye bias, we labeled paired aliquots of control cDNA from cancer-free prostatic tissues with Cy3 and Cy5, combined equal amounts of the preparations, and hybridized them to a microarray set. Fluorescence analysis revealed a mean Cy3/Cy5 ratio of 1.27 ± 0.35 standard deviation (SD), a median ratio of 1.22, and a coefficient of variation of 27.3% for all transcripts (Appendix B, Table Table 3). In contrast, the means ± SD and coefficients of variation determined for the TAHN and tumor experimental sets were 1.58 ± 0.61 and 38.6%, and 1.63 ± 0.75 and 46.1%, respectively. Statistical analysis for the distribution of values for all detected transcripts revealed significant differences ($p<0.05$) for the tumor and TAHN microarray data from the Cy3/Cy5 dye bias test (Appendix B, Table 3). While this result indicated a minimal dye bias for Cy3 fluorescent cyanine cDNA incorporation and/or target hybridization, we considered all transcripts in the experimental sets with an expression ratio of <1.27 as equally or under-expressed compared to normal cancer-free prostatic tissues in order to avoid false positive assignment of over-expressed genes. Consideration of the Cy3/Cy5 dye bias is important because we focused our analyses of the microarray expression experiments on over-expressed transcripts, since over-expression of a protein marker in TAHN tissues would be amenable to positive identification and could thus be used in diagnostic tests.

In the microarrays, 3769 transcripts were mutually expressed in both tumor and TAHN tissues, 1810 of which were expressed above the Cy3/Cy5 dye bias of 1.27. We plotted the expression levels for these mutually expressed transcripts and analyzed their correlation between

tumor and TAHN tissues (graphically shown in Appendix B, Figure 2). Logistic regression analysis indicated a correlation coefficient R^2 of only 0.09, indicating overall poor concordance of the expression levels between tumor and TAHN tissues. The majority of these transcripts, i.e. 94% were expressed at <2.0xSD of the mean expression (see Appendix B, Table 3) of all transcripts expressed in tumor and TAHN tissues (i.e. <3.13 and <2.80, respectively), as shown in quadrant I of Figure 2 (Appendix B).

We used over-expression in the tumor tissues as a guide for the selection and further analysis of transcripts in the TAHN tissues. Accordingly, we identified the transcripts that were up-regulated in the tumor tissues at >2.0xSD of the mean, i.e. all transcripts with a ratio >3.13. Omitting expressed sequence tags (ESTs) and unknown open reading frames (ORFs), this identified 120 known transcripts up-regulated in tumor tissues. Of these, 97 transcripts were also expressed in the TAHN tissues, 70 of which were also expressed at >1.27, i.e. above the Cy3/Cy5 dye bias threshold (quadrants III + IV, Appendix B, Figure 2). Eighty-three transcripts were up-regulated in the TAHN tissues at >2.0xSD of the mean, i.e. all transcripts with a ratio >2.80 (quadrants II + III, Appendix B, Figure 2). Due to space limits, we show the top 40 unique transcripts mutually up-regulated in tumor and TAHN tissues resulting from these analyses in Table IV. The number of mutually expressed and known transcripts at >2.0xSD for both tumor and TAHN tissues was 10 (quadrants III, Appendix B, Figure 2).

qRT-PCR validation of microarrays. As shown in Figure 2, microarray analysis indicated extensive heterogeneity of expression between tumor and TAHN tissues for the majority of transcripts. However, our microarray expression results represent mean values generated using pooled RNA populations. Therefore, it was important to estimate the extent of heterogeneity in individual samples. For this, we used qRT-PCR to test and validate the findings of the microarray expression analysis on selected transcripts in RNA samples of tumor and TAHN tissues compared to normal cancer-free prostate tissues. To better characterize the extent and heterogeneity of prostatic field cancerization in individual samples, we deliberately chose transcripts from above, below and at the 2.0xSD threshold of the mean in TAHN transcripts (i.e. ~2.8-fold up-regulated compared to cancer-free tissues, as defined in Appendix B, Table 3). Early growth response protein 1 (EGR-1) represents the transcript most up-regulated (8.92-fold) in TAHN tissues and has been previously implicated in prostate tumorigenesis (13-20). Its expression in tumor tissue was 9.27-fold (Appendix B, Table 4). Testican, also known as SPOCK-1, was up-regulated at 4.29-fold and 1.73-fold in tumor and TAHN tissues, respectively. Testican has recently been shown to be expressed in prostatic tissues (*14*). Fatty acid synthase (FAS) represents an expected change in tumorigenesis of the prostate (*15, 16*) and was up-regulated at 5.31-fold and 1.93-fold in tumor and TAHN tissues, respectively. In contrast, tristetraprolin (TTP) has not been previously reported to be associated with prostate tumorigenesis and may thus represent a novel finding. It was expressed at 5.81-fold and 2.75-fold in tumor and TAHN prostatic tissues, respectively (Table IV). For control purposes, we also included two transcripts that were equally or under-expressed in either tumor or TAHN tissues, i.e. tissue inhibitor of metalloproteinase 2 (TIMP2) and superoxide dismutase 2 (SOD2), expressed at 0.46-fold and 1.06-fold, and at 1.04-fold and 0.42-fold in tumor and TAHN tissues, respectively.

qRT-PCR validation was first performed on the six individual RNA samples pooled and used in the microarray expression analysis, the microarray (MA) set (Appendix B, Figure 3). In this analysis, the expression levels were compared to 6 normal cancer-free prostate control samples. Although variation was observed, mean expression of FAS, TTP, EGR-1 and testican in TAHN tissues was significantly different from normal controls ($p<0.05$; p range = 0.01-0.03). Similarly, mean expression for these transcripts in tumor tissues was significantly different from normal controls ($p<0.05$; p range = <0.01-0.03). In contrast, and as expected, mean expression of the control transcripts TIMP2 and SOD2, which were equally or under-expressed in either tumor or TAHN tissues in the microarray experiments, was similar in TAHN and tumor tissues, as well as in normal controls ($p>0.05$; p range = 0.27-0.70). Although not necessarily expected

due to a higher degree of heterogeneity in cancerous tissues, expression of all of these transcripts was similar in TAHN and tumor tissues ($p>0.05$; p range = 0.07-0.59), with the exception of FAS ($p=0.02$). Thus, the results obtained with six individual RNA samples analyzed by qRT-PCR confirm the conclusions drawn from the analysis of pooled RNA by microarray expression analysis.

To corroborate these findings from the MA set, we also individually analyzed RNA from six independent tumors and patient matched TAHN tissues, the validation (VA) set. As in the MA set, mean expression of FAS, TTP, EGR-1 and testican in TAHN tissues was significantly different from normal controls ($p<0.05$; p range = <0.01-0.03), demonstrating a consistent gene expression signature in TAHN tissues. In the VA set, mean expression of these transcripts in tumor tissues showed extensive variation when compared to normal controls, with EGR-1 and TTP showing significant and near significant differential expression ($p<0.01$ and $p=0.06$, respectively), and FAS and testican showing similar expression ($p=0.10$ and $p=0.27$, respectively). As expected, the control transcripts TIMP2 and SOD2 showed similar expression in TAHN and tumor tissues, and in normal controls ($p>0.05$; p range = 0.28-1.00). Collectively, the qRT-PCR data (Appendix B, Figure 3) was in excellent agreement with the data from the microarrays, thereby indicating the occurrence of field cancerization for the selected transcripts in TAHN when compared to tumor and cancer-free tissues.

Methylation Study

Gene promoter methylation was found to be highly variable between the cells lines (LnCap, PC-3, DU-145, and C4-2b) investigated (Figure 1). In all eight instances, normal DNA was found to lack methylation at the promoters of the genes of interest (Figure 2), and all normal samples were unmethylated for β-actin.

Tumor and TAHN samples showed methylation for some genes and not others (Figure 3). While the GSTP1 assay successfully identified methylation in cell lines, it did not detect methylation in patient samples, contrary to previously published studies of GSTP1 methylation in cancer. Troubleshooting is underway to determine why these results are inconsistent. Rar-β2 was found to be methylated in one instance of tumor DNA. APC was methylated in four tumor samples, but none of the TAHN samples (Figure 5). RassF1A was showed frequent promoter methylation in tumor samples (Figure 3), and was also found in four samples to be methylated in the matched TAHN tissues (Figure 4).

IIc. Discussion

Telomere Content Study

The results of these studies are similar to those reported previously for cancerous breast samples (*4*, *12*, *17*) and cancerous prostate tissues (*12*, *18*). Our prior studies demonstrated that TC in tissues obtained from radical mastectomy and prostatectomy was significantly reduced compared to disease-free prostate and breast tissues. More importantly, these studies also found that the histologically normal tissue adjacent to the tumor had significantly reduced TC compared to disease-free tissues.

The current study confirmed those findings in prostatectomy tissue, and extended them to biopsy tissue. As expected, the findings were similar in the biopsy tissues to those in prostatectomy tissues. Specifically, cancerous tissue from biopsy TC was significantly reduced compared to disease-free tissue, and histologically normal tissue from biopsy tissue was also significantly reduced in matched patient samples. These findings indicate that TC in biopsy tissues may be informative of the presence of prostate cancer. These findings indicate that it may be possible to detect abnormalities in biopsy tissue indicative of cancer, potentially avoiding repeated biopsies and leading to earlier treatment in cases that would otherwise have been missed on the basis of histology.

The matched biopsy and prostatectomy samples used in this study enabled, for the first time, an evaluation of two separate time points in patient matched samples. The results

demonstrate that TC in tissues from biopsy and prostatectomy specimens is informative, regardless of histology. However, TC was not correlated between paired histologically normal or cancerous biopsy and prostatectomy specimens. There are two possible explanations for this: a) Temporal alterations and/or b) spatial alterations. It is possible that telomere length is highly dynamic and constantly changing. The time between biopsy and prostatectomy was unknown for the samples in this study, so it is possible that the findings reflect ongoing changes in the abnormal cells. It is also possible that the differences are due to the physical location within the prostate of the sample collected. Biopsy samples are taken in a grid pattern and only sample a small portion of the prostate, however, the general sampling area changes very little from patient to patient. Tissues collected from prostatectomy specimens can come from any location within the prostate. Additionally, unpublished data from our laboratory has found a high level of heterogeneity within the prostate itself regarding TC. Based on that previous work revealing a range of TC variation throughout the cancerous prostate and the findings of TC correlation in prostatectomy specimens found by this study, it is more likely that the TC correlation observed is due to spatial variation. However, temporal effects cannot be ruled out, due to the lack of data regarding time between biopsy and prostatectomy. More research will be needed to further elucidate this point.

Allelic Imbalance Study

Genomic instability is a common occurrence in cancer (*19-21*). Instability can be reflected in loss of heterozigosity, and so other studies have endeavored to determine if loss of heterozigosity at specific loci can be used to detect prostate cancer (*22, 23*). However, this approach assumes that the genomic changes are consistent from case to case of prostate cancer. Viewed from the perspective that the entire genome becomes unstable during carcinogenesis, the assay employed by our laboratory reflects genome-wide genomic instability as opposed to locus-specific instability. Additionally, our assay avoids the requirement of a ‘normal’ control sample, reducing the amount of tissue or other biologic samples required from the patient, and permitting evaluation of archival tissues where patient-matched normal tissue may not be available. Because the assay is PCR based, only a small amount if tissue is required, such as a biopsy needle core. Previous studies from our laboratory in both breast and prostate cancers have demonstrated the presence of a field of genetically altered cells surrounding the tumor as demonstrated by both altered TC and allelic imbalance (*4, 13*). Taken together, these results demonstrate that AI in histologically normal tissue from a cancerous prostate is indeed informative regarding genomic instability and the likelihood of cancerous alterations being present, and does demonstrate the presence of a field of altered cells is present. The current study confirmed this finding.

While this study originally proposed to look for prostate cancer specific microsatellite markers, it makes more sense to use an assay that is general to more than one cancer. Additionally, the commercial availability of the AmpFlSTR® kit (Applied Biosystems, Foster City, CA) makes it the type of assay that can easily move into the clinical setting. For these reasons, the study has evolved to validating the use of the AI assay for possible clinical use.

This is the first study to compare nonspecific sites of allelic imbalance in patient matched biopsy and prostatectomy specimens using the assay developed within our laboratory. AI was detected in both cancerous and histologically normal tissues from both biopsy and prostatectomy specimens. Moreover, the numbers of sites of AI exceeded those found in normal tissues and overlapped those found in cancers. These findings indicate two things: a) a field of genetically altered cells are present at the time of biopsy in cores determined to be histologically normal, and b) the number of sites of AI in both cancerous and histologically normal tissues from needle core biopsies is informative of a cancer diagnosis. However, it is important to point out that all of the patients in this cohort went on to prostatectomy due to the presence of prostate cancer. We have not yet performed a comparable analysis of biopsies that did not result in a cancer diagnosis or that contained only BPH or PIN. Thus, the conclusions of this investigation must be viewed provisionally.

The interesting finding of this study arises from the finding of matched sites of AI in patient matched tissues, such as TAHN and tumor specimens and biopsy and prostatectomy specimens. These findings imply that the tumor cells may arise from a clone found in the field of histologically normal, though genetically altered cells. Further, these findings support the theory of clonal selection in cancer progression, evidenced by the maintenance of a cell population containing specific genomic alterations. We interpret instances in which site of AI were present in TAHN tissue but not in the matched Tumor tissue to reflect genetically altered clones that did not give rise to the tumor, *i.e.* clones that were not selected and constituted either a minority of the cell population or that were lost completely. Most intriguing was the finding of conserved sites of AI in all for specimens of a single case. The likelihood of conservation of a single site within all 4 specimens was determined to be 0.01% and 0.02% for the 2 cases, providing further evidence that AI maintenance is not attributable to chance alone. The intriguing finding of conserved sites of imbalance between samples supports the theory of clonality of cancer cells and their precancerous progenitors. The results suggest that the abnormal field of cells arise early, and eventually gives rise to the tumor, accumulating mutations over time.

Microarray Study (See Appendix B for the complete manuscript)

The major finding of this study is the occurrence of up-regulated transcripts in tumor adjacent histologically normal (TAHN) human prostatic tissues, as shown by microarray and qRT-PCR expression analysis of 12 mostly early stage (T2-T3) and low grade (Gleason sum 6-7) prostate tumors. While the study was not designed to provide a comprehensive signature of prostatic TAHN tissues, it does provide a strong indication of prostatic field cancerization and emphasizes its potential as a source of markers to be further verified in larger cohorts. We focused on the identification of transcripts that were up-regulated in both tumor and TAHN prostatic tissues, as such transcripts may have important clinical applications, especially for the alternative or adjunct diagnosis of prostatic malignancy after inconclusive or false negative biopsy assessment.

Few expression studies have reported molecular signatures and individual markers characteristic of prostatic TAHN tissues. Field cancerization is however evident at the genetic as well as the epigenetic level, as we have shown by altered telomeres in whole tissue TAHN extracts (*12*) and as shown by others by gene promoter methylation of APC, RARβ2, and RASSF1A (*24*). We also conducted a detailed review of the Gene Expression Omnibus (GEO) microarray data sets from the National Center for Biotechnology Information (NCBI) available at http://www.ncbi.nlm.nih.gov/geo/. We thereby focused on our top transcripts mutually up-regulated in tumor and corresponding TAHN tissues, as well on the transcripts validated by qRT-PCR (Appendix B, Table IV). This review revealed one data set, GSE6919 that matched our criteria of comparing cancer-free normal (n=18), TAHN (n=63), and tumor tissues (n=65 for primary and n=25 for metastatic) with similar tissue collection procedure and pathological assessment to exclude any obvious neoplastic alterations in TAHN and normal tissues. Despite a higher number of samples, expression levels for EGR-1, c-Fos, FAS, GDF-15, metallothionein 1E (MT-1E), and testican showed high levels of heterogeneity. Nevertheless, expression of EGR-1, c-Fos, FAS, and testican were elevated in both tumor and TAHN tissues, while GDF-15 and MT-1E were not. The reported values compared to our own data are shown in Figure 4 (Appendix B). Together, these comparisons validate our findings, and lead us to conclude that field cancerization is a rather strong and robust manifestation in prostatic tumors.

In the present study, we chose to use bulk tissue that was not microdissected in order to include both glandular (epithelial) as well as stromal (fibroblastic) compartments. This approach also demonstrates that the identified gene expression changes could potentially be identified in biopsy samples. In the present study, we pooled samples for the microarray analysis in order to minimize effects of sample heterogeneity. The authenticity of our findings, however, was confirmed by qRT-PCR using RNA from individual samples. Although heterogeneity from patient to patient was observed, data validity was corroborated in an additional independent set of patient samples. The up-regulated transcripts observed in both tumor and TAHN tissues were

identified in comparison to a mutually shared and appropriate background control, i.e. prostatic tissues from cancer-free deceased individuals with a similar age range.

Albeit not comprehensive, Table IV (Appendix B) indicates part of a signature that may be characteristic of prostatic field cancerized tissues. It is conceivable that some of the listed transcripts could have an important role in prostatic TAHN tissues, either a causative one as drivers of pre-malignancy or as a reaction to the presence of the tumor, or both. Among the highest up-regulated transcripts in TAHN tissues were EGR-1, c-Fos, and the growth/differentiation factor 15 (GDF-15), also called macrophage inhibitory cytokine-1 (MIC1). EGR-1 has been strongly implicated in prostate cancer (*15, 25-27*) and regulates multiple target genes that in turn have a potential role in prostatic carcinogenesis and progression, such as epidermal growth factor receptor (EGFR), platelet derived growth factor (PDGF), and human telomerase reverse transcriptase (hTERT), thereby regulating a spectrum of cellular responses, including growth and growth arrest, survival and apoptosis, and differentiation and transformation (*28, 29*).

To further estimate the extent and heterogeneity of prostatic field cancerization, we also chose transcripts that were less up-regulated in TAHN tissues, such as TTP, FAS, and testican. TTP expression is not specific to prostatic tissues. However, it is an ubiquitously expressed AU-rich element (ARE) binding protein and a regulator of mRNA stability, including of pro-inflammatory proteins, such as tumor necrosis alpha (TNFα) (*30*), which plays an important role in prostate adenocarcinoma (*31*). It is possible that TNFα is produced by inflammatory cells in TAHN tissues in agreement with the prominent role of inflammation as proposed by De Marzo and colleagues (*32*). TNFα is a classical activator of the nuclear factor kappa B (NFκB) pathway which is constitutively activated in prostate cancer with prominent downstream targets that support an activated cellular state, including EGR-1 (*28, 33*). FAS has been termed a “metabolic oncogene” and may reflect a prostate cell’s energetic switch to a more anaerobic yet more reductive physiologic state, which is a hallmark of prostate cancer progression (*15, 16*). In addition, FAS has been shown to positively affect NFκB nuclear translocation in cancer cells leading to an anti-apoptotic effect (*34*). Finally, testican (SPOCK-1) belongs to the fibulin protein family of extracellular matrix proteins which influence cell adhesion and migration, and have thus been associated with progression of several cancer types (*35*), including prostate cancer, in which it has recently been shown to be up-regulated (*14*).

Collectively, our data adds to and partially confirms previously published, yet rather scarce reports that support the occurrence of field cancerization in prostatic tissues. This study warrants further investigations in larger cohorts of tissue samples collected at defined distances from tumor margins (1cm in this study), and into its underlying mechanisms, as well as potential clinical use of representative transcripts towards an improved prostate cancer detection and patient outcome.

Methylation Study

While data regarding the methylation of cell lines is included here, the cell lines themselves are only suitable for determining if the assay itself is working, as cell line methylation is variable between cell lines and over time (*36*). Additional samples from the CPCTR cohort were evaluated for suitability for methylation evaluation. However, due to the age and fixing processes of these samples, the DNA was either too degraded to begin with or was degraded beyond use by the sodium bisulfite treatment. Additional sources of suitable DNA are being investigated, including the prospective study.

While global de-methylation is associated with the cancer genome, it is well known that methylation silencing of individual genes is also common. GSTP1 methylation is a well established phenomenon in cancer cells (*10, 37*). However, while several studies have evaluated many genes, including GSTP1, RassF1A, Rar-β2, and APC (*7-11, 37-39*), these studies have been plagued by a lack of proper controls, in that studies need to include truly normal, disease-free tissue, not tumor adjacent tissues, for establishing a base line level of methylation. This is particularly important in methylation studies where variable levels of methylation have been

observed not only in tumors but in other pathologies of the prostate as well. This study endeavored to demonstrate why this is important by showing the existence of a field of altered cells in the tissues surrounding the tumor. As illustrated by the Rar-β2 results, this field of alteration does exist around a tumor, but as evidenced by the APC results, the extent of alterations in adjacent tissue is variable. While this study is not definitive, it does agree with published data, particularly a recent study focusing on field effect and the same four genes (*24*), and indicates that further investigation of these genes is warranted. Further investigation may lead to a new diagnostic tool to detect prostate cancer with out the presence of tumor cells in a biopsy, as well as differentiate between cancer and other pathologies such as PIN and BPH.

III. Key Research Accomplishments

IIIa. Research Accomplishments

- The assay for detecting methylation at specific gene promoters has been developed (table 1).
- Methylation of prostate cancer cell line models has been characterized for specific promoters. (Appendix A, figure 1).
- Methylation of normal prostate has been characterized. (Appendix A, figure 2).
- Gene promoter methylation of prostate tumor and tumor adjacent tissue in a collection of matched samples has been characterized for 3 sets of genes. (Appendix A, figure 3, 4, 5).
- Methylation within the set of cases currently characterized has shown changes between tumor and tumor adjacent tissues. (Appendix A, figures 4, 5).
- Characterization by microarray and validation of the results has been completed. (Appendix B).
- TC was found to be reduced in all case specimens with the exception of TAHN biopsy (Figure 6).
- TC was found to correlate between TAHN and Tumor, as well as TAHN and Cancerous Biopsies, but not between TAHN and TAHN biopsy or Tumor and Cancerous biopsy specimens (Figure 7).
- AI was shown to be increased not only in TAHN and Tumor specimens, but also in TAHN biopsy and Cancerous biopsy specimens as well (Figure 8).
- Data has been presented at several conferences.
- A paper has been submitted by the candidate regarding the microarray study and is currently be revised for resubmission (Appendix B).
- A paper has been co-authored by the candidate regarding field effect in breast tissue. (Appendix C).
- A paper has been co-authored by the candidate demonstrating the use of allelic imbalance as a measurement of genomic instability. (Appendix D).

IIb. Training and Educational Accomplishments

The student has had continuing opportunities to work and interact with oncologists, pathologists and other PhD scientists who specialize in prostate cancer. These interactions have occurred through tumor board meetings, journal clubs, urology rounds, special seminars and direct interaction within the clinical setting as well as the laboratory. Training in microscopy has taught the student recognition of the various pathologies of the prostate. Additionally, she has been active in patient enrollment for prognostic studies and has learned how to design a study, and the administrative requirements associated with clinical research. This type of interaction is also valuable, as it provides ongoing interaction with patients, something the student feels is important to her career as a physician scientist.

On an educational level, the student has completed all required course work for completion of a PhD degree. The student has also completed her Comprehensive Exam in September of 2007 and is scheduled to defend on January 9, 2009. The student has also assisted in the writing and the co-instruction of a section of the upper-level undergraduate course, Biochemical Laboratory Methods. The student has aspirations of continuing her career in research and remaining in academia and felt teaching provided an opportunity to develop the essential teaching skills need for her chosen career path as a physician scientist.

Training and Educational Milestones (3 tasks)

Task 1: -Develop ability to identify the morphology and characteristics of prostate tissue from normal to metastatic cancer. Learn the use of special stains and histological markers in prostate pathology. This will be done under the instruction of Dr. Nancy Joste, Chief of Surgical Pathology.
Months 1-12 **Completed with modification**

The student has learned identification of various stages of prostate cancer, as well as the normal pathology of the prostate gland. The training was carried out at the Veteran's Affairs Hospital (VAH) in Albuquerque in the pathology department with Dr. Massie. This modification occurred as the VAH has more prostate cases and the student has been enrolling patients here and Dr. Massie, the head of the Pathology Department, has been providing pathologic information regarding study subjects.

Task 2: -Attend clinics with oncologists (Dr. Ian Rabinowitz, Dr. Anthony Smith) at the University of New Mexico Hospital for the purpose of directly observing current detection, diagnosis, and treatment of prostate cancer, and to learn about the patient's interactions, perceptions and concerns with these current modalities. Attend oncology rounds and meetings at the Cancer Research and Treatment Center to expand general and detailed knowledge base of oncology.
Months 1-36 **Completed with modification**

The student has observed surgeries at the VAH with Dr. Michael Davis. This change was made due to the higher frequency of prostatectomies at the VAH. The student has attended urology and oncology rounds as well as directly interacting with prostate cancer patients.

Task 3: -Present ongoing work at local and national meetings.
Months 12-36 **Completed**

The student has presented at several conferences, including the MD/PhD conference in Keystone, Colorado and IMPaCT meeting in Atlanta, Georgia.

IV. Reportable Outcomes

Abstracts

Sevilleta Annual Biochemistry Retreat, April 21, 2007, Sevilleta, NM

The Evaluation of Genomic Instability by Methylation Status in the Abnormal Prostate
Christina Haaland, Christopher Heaphy, Jeffrey Griffith, PhD

Introduction
Prostate cancer is the second most common cause of cancer related death in men after lung cancer, and the incidence of prostate cancer increases significantly with advanced age. It is currently accepted that tumorigenesis is a multi-step process where there is accumulation of genetic and epigenetic changes, altering the normal cellular regulatory mechanisms. Previously our laboratory has shown that telomere content (TC) and allelic imbalance (AI), both measures of genomic instability, correlate strongly with clinical outcome in prostate and breast cancers. More importantly, we have demonstrated that the changes observed in tumors are also present in tumor adjacent histologically normal (TAHN) tissues, indicating that genetic changes indicative of tumor progression precede histological differentiation. Further, these changes imply that markers of genetic instability in seemingly normal tissue proximal to prostate tumors also have prognostic significance.
Purpose
This leads to the question are these genetic changes in the TAHN prostate tissues limited to TC and AI, or do they include epigenetic changes as well? Evaluation of promoter methylation may allow for the evaluation of new markers for diagnostic or prognostic use in tissue obtained from needle core biopsies.
Methods
Detection of methylation status is a PCR-based assay performed through the use of specific primers designed for regions of DNA where methylation occurs. These areas are the CG repeats found mainly within the promoters of genes. Following treatment with sodium bisulfite, CG repeats without methylation, those promoters that are transciptionally functional, are chemically changed into TG repeats, allowing for selective detection.
Results
Currently we have also characterized the methylation status of the genes GSTP1, Rar-β2, APC, and RassF1A in prostate cancer model cell lines, disease free prostate tissue and patient samples of both tumor and matched TAHN tissues. β-actin was used as the unmethylated internal reference gene. Cell lines included PC-3, DU145, LnCaP and C4-2b. Four disease free samples were obtained from autopsy material of disease free prostates. Eight matched patient samples have been characterized to date. Cell lines demonstrated high levels of methylation. Disease free prostates demonstrate a lack of methylation for all genes. Methylation levels are more variable in the matched patient samples, and more samples are being characterized to evaluate potential patterns.
Future Directions
Additional samples and genes are being identified to clarify the significance of methylation in tumor and TAHN tissues of the prostate.

Medical Scientist Training Program Annual MD/PhD Student Conference, July 27-29, 2007, Keystone Colorado

The Evaluation of mRNA Expression and Methylation Status in the Abnormal Prostate
HAALAND, C.M.*, HEAPHY, C.M., GRIFFITH, J.K.

Prostate cancer is the second most common cause of cancer related death in men and the incidence increases significantly with advancing age. Tumorigenesis is a multi-step process characterized by the accumulation of genetic and epigenetic changes, thus altering the normal cellular regulatory mechanisms. However, these histological changes may be missed in a needle core biopsy of the prostate; therefore, molecular markers are needed to increase the accuracy of diagnosis.
Our laboratory has shown that telomere content (TC) and allelic imbalance (AI), both markers of genomic instability, are altered within tumor tissue and correlate strongly with clinical outcome measures in prostate and breast cancers. More importantly, we have demonstrated that these changes are also present in tumor adjacent histologically normal (TAHN) tissues located 1 cm from the tumor margin, implying that these markers exist in seemingly normal prostate tissues which may have prognostic and diagnostic significance.
We hypothesize that the changes in TAHN tissues are not limited to TC and AI, and may include epigenetic and gene expression changes. Methylation of gene promoters causes gene silencing and is associated with tumors, resulting in alterations of gene expression. Evaluation of expressional differences and promoter methylation may lead to the evaluation of new markers for diagnostic or prognostic use in tissue obtained from needle core biopsies.
We have evaluated a pool of six matched patient tumor and TAHN samples by microarray analysis. RNA expression between the two sample pools was found to be altered when compared to disease-free prostate gene expression. We have also characterized the methylation status of the genes GSTP1, Rar-β2, APC, and RassF1A in prostate cancer cell lines (PC-3, DU145, LnCaP and C4-2b), four disease-free prostate tissues (from autopsy material) and eight matched patient tumor and TAHN tissue samples. The cell lines demonstrated high levels of methylation, whereas the disease-free prostates demonstrated a lack of methylation for all genes. Methylation levels were more variable in the matched patient samples, and more samples are being characterized to evaluate potential patterns.
We conclude that in addition to genomic instability, alterations in mRNA expression and the methylation status of gene promoters are occurring in TAHN tissues and display potential clinical implications.

Innovative Minds in Prostate Cancer Today (IMPaCT), September 5-8, 2007, Atlanta, Georgia

Evaluation of Genomic Instability by Methylation Status in the Abnormal Prostate
Christina M Haaland; Christopher Heaphy; Kimberly Butler; Marco Bisoffi; Jeffrey Griffith

Abstract:
Prostate cancer is the second most common cause of cancer related death in men after lung cancer, with incidence of prostate cancer increasing significantly with advanced age. It is currently accepted that tumorigenesis is a multi-step process where there is accumulation of genetic and epigenetic changes that alter the normal regulatory mechanisms controlling cellular proliferation. However, not enough is yet known about the processes of tumorigenesis and disease progression, creating limitations in detection, treatment and prevention of this cancer. This study is designed to look for better methods of detection and prognostic markers regarding prostate cancer to reduce the risk of mortality associated with current treatment modalities.
In retrospective studies, our laboratory has shown that telomere content (TC), a proxy for telomere length, correlates strongly with clinical outcome in prostate and breast cancers. Additionally, studies within our lab suggest that the extent of allelic imbalance (AI), another marker of genomic instability where microsatellite repeats are measured for changes in heterozigosity, is associated with both TC and prognosis in prostate cancers. Most importantly, we have shown that the changes in TC and AI observed in tumors are also present in tumor adjacent histologically normal (TAHN) tissues. This suggests that genetic changes indicative of

tumor progression precede histological differentiation, and further implies that markers of genetic instability in seemingly normal tissue proximal to prostate tumors also have prognostic significance.
Another important question is whether the genetic changes in the TAHN prostate tissues are limited to TC and AI, or also include epigenetic changes, particularly methylation of key genes. Methylation of gene promoters causes their expression to be silenced. Detection of the methylation status is done through the use of very specific primers design for the regions where methylation occurs-CG repeats found mainly within the promoters of genes. Following treatment with sodium bisulfite, CG repeats without methylation are changed into TG repeats, allowing for this selective detection. Evaluation of promoter methylation, if differential, may allow for several new markers to be evaluated for diagnostic or prognostic use in tissue obtained from needle core biopsies. Currently we have characterized the methylation status of the genes GSTP1, Rar-beta2, APC, and RassF1A in both prostate cancer model cell lines and patient samples of both tumor and matched nearby histologically normal tissues. While there is increasing levels of methylation with increasingly aggressive tumor cell lines, the picture is more variable in the matched patient samples. However none of these genes is methylated in normal prostate tissue samples. Methylation studies are also ongoing to determine how methylation changes in tumor and nearby histologically normal tissues of the abnormal prostate, and how these changes may be relevant to detection of prostate cancer. Additionally, microarray studies are being used to help determine future investigations. These are being carried out with pooled, matched samples of tumor and nearby normal prostate tissue samples from six patients.

IMPACT statement: The results of this work will impact patient care and treatment through more sensitive detection methods and tailoring of individual patient care through outcome prediction.

Journal Articles

C.M. Haaland, C.M. Heaphy, K.S. Butler, E. G. Fischer, J.K. Griffith, and M. Bisoffi. Differential Gene Expression in Tumor Adjacent Histologically Normal Prostatic Tissue Indicates Field Cancerization.
Under revision for resubmission to the journal Prostate. (Appendix B)

C.M. Heaphy, M.Bisoffi, C.A. Fordyce, **C.M. Haaland**, W.C. Hines, N.E. Joste and J.K. Griffith. Telomere DNA content and allelic imbalance demonstrate field cancerization in histologically normal tissue adjacent to breast tumors. International Journal of Cancer, 119:108-116, 2006. (Appendix C). Note: Ms. Haaland's participation in this project occurred prior to her receipt of the PCRP Award.

C.M. Heaphy, W.C. Hines, K.S. Butler, **C.M. Haaland**, G. Heywood, E.G. Fischer, M. Bisoffi and J.K. Griffith. Measurement of Genome-wide Allelic Imbalance in Human Tissue Using a Multiplex PCR System. Journal of Molecular Diagnostics, 9:266-271, 2007. (Appendix D).

V. Conclusions

TC and AI studies are ongoing regarding the prospective arm of specific aim one, and completed for the retrospective aspect of the same aim. TC in biopsy samples was found to be altered and more similar to prostatectomy specimens than disease-free specimens, suggesting that TC may be used to examine biopsy specimens. Additionally, TC was found to correlate between TAHN and tumor specimens, as well as TAHN and cancerous biopsy specimens, but not between TAHN and TAHN biopsy or tumor and cancerous biopsy specimens. This most likely is due to differences in spatial orientation during sampling, but may also be due to temporal effects as the time between biopsy and prostatectomy is unknown. Similar findings were also found when analyzing AI, specifically that biopsy specimens were more similar to prostatectomy specimens than disease-free specimens. Surprisingly, sites of AI were conserved between multiple specimens from the same case in several instances. This finding suggests that clonality may play a role in cancer development, and that some genetic alterations may be preserved in cases were they are (presumably) beneficial. Finally, both TC and AI may prove useful in regards to improving diagnosis at the time of biopsy, as both assays revealed that biopsies from patients with prostate cancer resembled assay results from prostatectomy specimens but not truly disease-free specimens.

Regarding specific aim 2 and the methylation studies, it has been found that there is altered methylation within the field of histologically normal tissues. Additional samples are being analyzed to verify these findings. It has also been shown that methylation of normal, disease-free tissue in not found at the gene promoters under investigation.

Microarray studies are now complete and the results have been validated. Of note is the finding that Egr-1 is elevated not only in prostate tumor tissue, but also in the histologically normal tissues surrounding the tumor, indicating that Egr-1 may have potential as a biomarker. However, the results of this study fully support the finding of a unique field of altered cells surrounding a focus of tumor, and that these alterations are detectable in bulk tissue.

References

(1) Bryant, J., Hutchings, KG, Moyzis, RK, Griffith, JK. (1997) Measurement of telomeric DNA content in human tissues. *BioTechniques 23*, 476-8, 480, 482.

(2) Fordyce, C., Heaphy, CM, Griffith, JK. (2002) Chemiluminescent Measurement of Telomere DNA Content in Biopsies. *BioTechniques 33*, 144-146, 148.

(3) Skotheim RI, D. C., Kraggerud SM, Jakobsen KS, Lothe RA. (2001) Evaluation of loss of heterozygosity/allelic imbalance scoring in tumor DNA. *Cancer Genet Cytogenet 127*, 64-70.

(4) Heaphy CM, B. M., Fordyce CA, Haaland CM, Hines WC, Joste NE, Griffith JK. (2006) Telomere DNA content and allelic imbalance demonstrate field cancerization in histologicalle normal tissue adjacent to breast tumors. *International journal of cancer 119*, 108-116.

(5) Sgueglia JB, G. S., Davis J. (2003) Precision studies using the ABI prism 3100 genetic analyzer for forensic DNA analysis. *Anal Bioanal Chem 376*, 1247-54.

(6) Ogishima, T., Shiina, H., Breault, J.E., Terashima, M., Honda, S., Enokida, H., Urakami, S., Tokizane, T., Kawakami, T., Ribeiro-Filho, L.A., Fujime, M., Kane, C.J., Carroll, P.R., Igawa, M., Dahiya, R. (2005) Promoter CpG hypomethylation and transcription factor EGR1 hyperactivate heparanase expression in bladder cancer. *Oncogene 24*, 6765-6772.

(7) Eads, C. A., Lord, R.V., Wickramasinghe, K., Long, T.I., Kurumboor, S.K., Bernstein, L., Peters, J.H., DeMeester, S.R., DeMeester, T.R., Skinner, K.A., Laird, P.W. (2001) Epigenetic Patterns in the Progression of Esophageal Adenocarcinoma. *Cancer Research 61*, 3410–3418.

(8) Jero´nimo, C., Henrique, R., Hoque, M.O., Mambo, E., Ribeiro, F.R., Varzim, G., Oliveira, J., Teixeira, M.R., Lopes, C., Sidransky, D. (2004) A Quantitative Promoter Methylation Profile of Prostate Cancer. *Clinical Cancer Research 10*, 8472–8478.

(9) Jero´nimo, C., Henrique, R., Hoque, M.O., Ribeiro, F.R., Oliveira, J., Fonseca, D., Teixeira, M.R., Lopes, C., Sidransky, D. (2004) Quantitative RARbeta2 Hypermethylation: A Promising Prostate Cancer Marker. *Clinical Cancer Research 10*, 4010-4014.

(10) Esteller, M., Corn, P.G., Baylin, S. B., and Herman, J.G. (2001) A Gene Hypermethylation Profile of Human Cancer. *Cancer Research 61*, 3225-3229.

(11) Henrique, R., Jero´nimo, C., Teixeira, M.R., Hoque, M.O., Carvalho, A.L., Pais, I., Ribeiro, F.R., Oliveira, J.R., Lopes, C, Sidransky, D. (2006) Epigenetic Heterogeneity of High-Grade Prostatic Intraepithelial Neoplasia: Clues for Clonal Progression in Prostate Carcinogenesis. *Molecular Cancer Research 4*.

(12) Fordyce, C., Heaphy, CM, Joste, NE, Smith, AY, Hunt, WC, Griffith, JK. (2005) Association Between Cancer-free Survival and Telomere DNA Content in Prostate Tumors. *The journal of urology 173*, 610-614.

(13) Heaphy, C. M., Hines, W.C., Butler, K.S., Haaland, C.M., Heywood, G., Fischer, E.G., Bisoffi M, Griffith, J.K. (2007) Assessment of the Frequency of Allelic Imbalance in Human Tissue Using a Multiplex Polymerase Chain Reaction System. *Jounral of Molecular Diagnostics 9*, 266-271.

(14) Wlazlinski, A., Engers, R., Hoffmann, M. J., Hader, C., Jung, V., Muller, M., and Schulz, W. A. (2007) Downregulation of several fibulin genes in prostate cancer. *Prostate 67*, 1770-80.

(15) Baron, A., Migita, T., Tang, D., and Loda, M. (2004) Fatty acid synthase: a metabolic oncogene in prostate cancer? *J Cell Biochem 91*, 47-53.

(16) Kuhajda, F. P. (2006) Fatty acid synthase and cancer: new application of an old pathway. *Cancer Res 66*, 5977-80.

(17) Griffith, J. K., Bryant JE, Fordyce CA, Gilliland FD, Joste NE, Moyzis RK. (1999) Reduced telomere DNA content is correlated with genomic instability and metastasis in invasive human breast carcinoma. *Breast Cancer Res Treat 54*, 59-64.
(18) Donaldson, L., Fordyce C, Gilliland F, Smith A, Feddersen R, Joste N, Moyzis R, Griffith J. (1999) Association between outcome and telomere DNA content in prostate cancer. *J Urol 162*, 1788-92.
(19) Lengauer C., K. K. W., Vogelstein B. (1997) Genetic instability in colorectal cancers. *Nature 386*, 623-627.
(20) De Wever O, M. M. (2003) Role of tissue stroma in cancer cell invasion. *Journal of pathology 200*, 429-447.
(21) Hanahan, D., Weinberg, R.A. (2000) The Hallmarks of Cancer. *Cell 100*, 57-70.
(22) Müller, I., Beeger, C., Alix-Panabières, C., Rebillard, X., Pantel, K., Schwarzenbach, H. (2008) Identification of loss of heterozygosity on circulating free DNA in peripheral blood of prostate cancer patients: potential and technical improvements. *Clinical Chemistry 54*, 688-96.
(23) Lieberfarb, M. E., Lin, M., Lechpammer, M., Li, C., Tanenbaum, D.M., Febbo, P.G., Wright, R.L., Shim, J., Kantoff, P.W., Loda, M., Meyerson, M., Sellers, W.R. (2003) Genome-wide loss of heterozygosity analysis from laser capture microdissected prostate cancer using single nucleotide polymorphic allele (SNP) arrays and a novel bioinformatics platform dChipSNP. *Cancer Research 63*, 4781-5.
(24) Mehrotra, J., Varde, S., Wang, H., Chiu, H., Vargo, J., Gray, K., Nagle, R.B., Neri, J.R., Mazumder, A. (2007) Quantitative, spatial resolution of the epigenetic field effect in prostate cancer. *Prostate 68*, 152-60.
(25) Thigpen AE, C. K., Guileyardo JM, Molberg KH, McConnell JD, Russell DW. (1996) Increased expression of early growth response-1 messenger ribonucleic acid in prostatic adenocarcinoma. *The journal of urology 155*, 975-981.
(26) Virolle T, K.-H. A., Baron V, De Gregorio G, Adamson ED, Mercola D. (2003) Egr-1 promotes growth and survival of prostate cancer cells. Identification of novel Egr-1 target genes. *The journal of biological chemistry 278*, 11802-11810.
(27) Mora GR, O. K., Mitchell RF, Jr., Jenkins RB, Tindall DJ. (2005) Regulation of expression of the early growth response gene-1 (EGR-1) in malignant and benign cells of thhe prostate. *The prostate 63*, 198-207.
(28) Thiel, G., and Cibelli, G. (2002) Regulation of life and death by the zinc finger transcription factor Egr-1. *J Cell Physiol 193*, 287-92.
(29) Khachigian, L. M., and Collins, T. (1998) Early growth response factor 1: a pleiotropic mediator of inducible gene expression. *J Mol Med 76*, 613-6.
(30) Zhang, T., Kruys, V., Huez, G., and Gueydan, C. (2002) AU-rich element-mediated translational control: complexity and multiple activities of trans-activating factors. *Biochem Soc Trans 30*, 952-8.
(31) Bouraoui, Y., Ricote, M., Garcia-Tunon, I., Rodriguez-Berriguete, G., Touffehi, M., Rais, N. B., Fraile, B., Paniagua, R., Oueslati, R., and Royuela, M. (2008) Pro-inflammatory cytokines and prostate-specific antigen in hyperplasia and human prostate cancer. *Cancer Detect Prev 32*, 23-32.
(32) DeMarzo, A. M., Nelson, W. G., Isaacs, W. B., and Epstein, J. I. (2003) Pathological and molecular aspects of prostate cancer. *Lancet 361*, 955-64.
(33) Suh, J., and Rabson, A. B. (2004) NF-kappaB activation in human prostate cancer: important mediator or epiphenomenon? *J Cell Biochem 91*, 100-17.
(34) Menendez, J. A., Mehmi, I., Atlas, E., Colomer, R., and Lupu, R. (2004) Novel signaling molecules implicated in tumor-associated fatty acid synthase-dependent breast cancer cell proliferation and survival: Role of exogenous dietary fatty acids, p53-p21WAF1/CIP1, ERK1/2 MAPK, p27KIP1, BRCA1, and NF-kappaB. *Int J Oncol 24*, 591-608.
(35) Gallagher, W. M., Currid, C. A., and Whelan, L. C. (2005) Fibulins and cancer: friend or foe? *Trends Mol Med 11*, 336-40.

(36) Smiraglia, D. J., Rush L.J., Frühwald, M.C., Dai, Z., Held, W.A., Costello, J.F., Lang, J.C., Eng, C, Li, B., Wright, F.A., Caligiuri, M.A., Plass, C. (2001) Excessive CpG island methylation in cancer cell lines versus primary human malignancies. *Human Molecular Genetics 10*, 1413-1419.

(37) Nakayama M., G. M. L., Yegnasubramanian S., Lin X., DeMarzo A.M., Nelson, W.G. (2004) GSTP1 CpG island hypermethylation as a molecular biomarker for prostate cancer. *J Cell Biochem 91*, 540-553.

(38) Hanson JA, G. J., Grover A, Tangrea MA, Chuaqui RF, Emmert-Buck MR, Tangrea JA, Libutti SK, Linehan WM, Woodson KG. (2006) Gene promoter methylation in prostate tumor-associated stromal cells. *Jounral of the national cancer institute 98*, 255-261.

(39) Li, L.-C., Okino, S.T., Dahiya, R. (2004) DNA methylation in prostate cancer. *Biochimica et Biophysica Acta 1704*, 87-102.

Appendix A

Figure 1

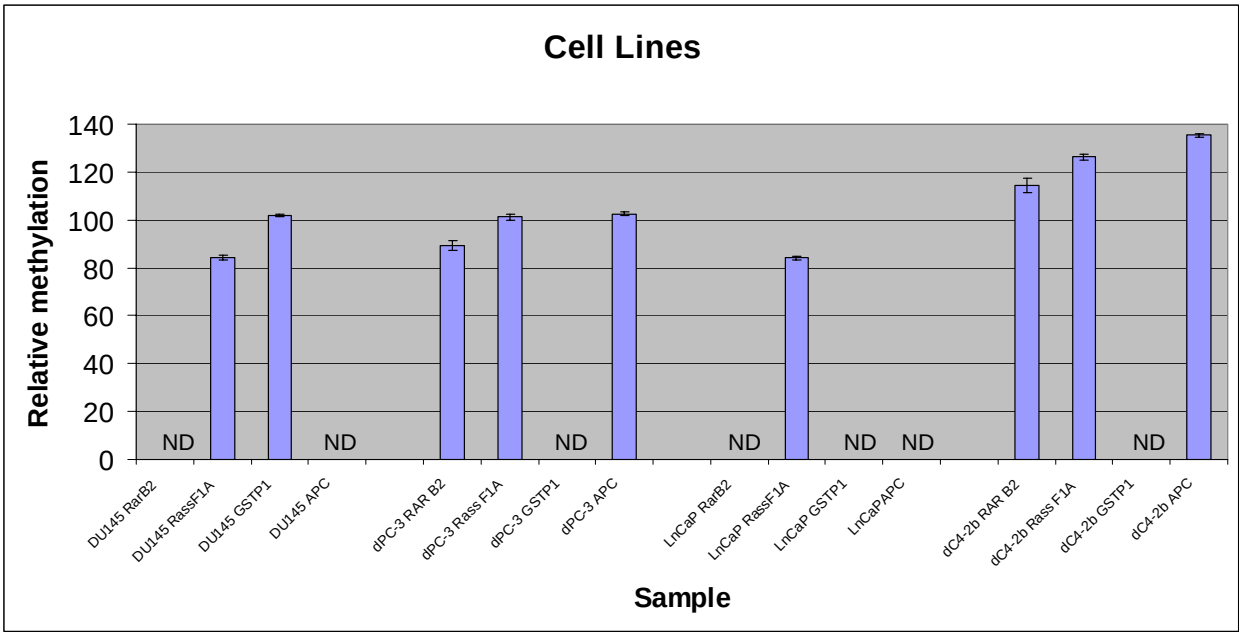

Figure 1. The methylation status of 4 prostate cancer cell line models: DU-145, derived from a brain metastasis and hormone insensitive, PC-3, an androgen independent model derived from a bone metastasis, LnCaP, lymph node derived and hormone sensitive, and C4-2b, a bone metastasis, androgen independent cell line. The promoter methylation status for the genes Rar-B2, APC, Rass F1A, and GSTP-1 have been analyzed in these cell lines. B-actin is used as an internal reference to normalize the assay (not shown). ND=none detected.

Figure 2

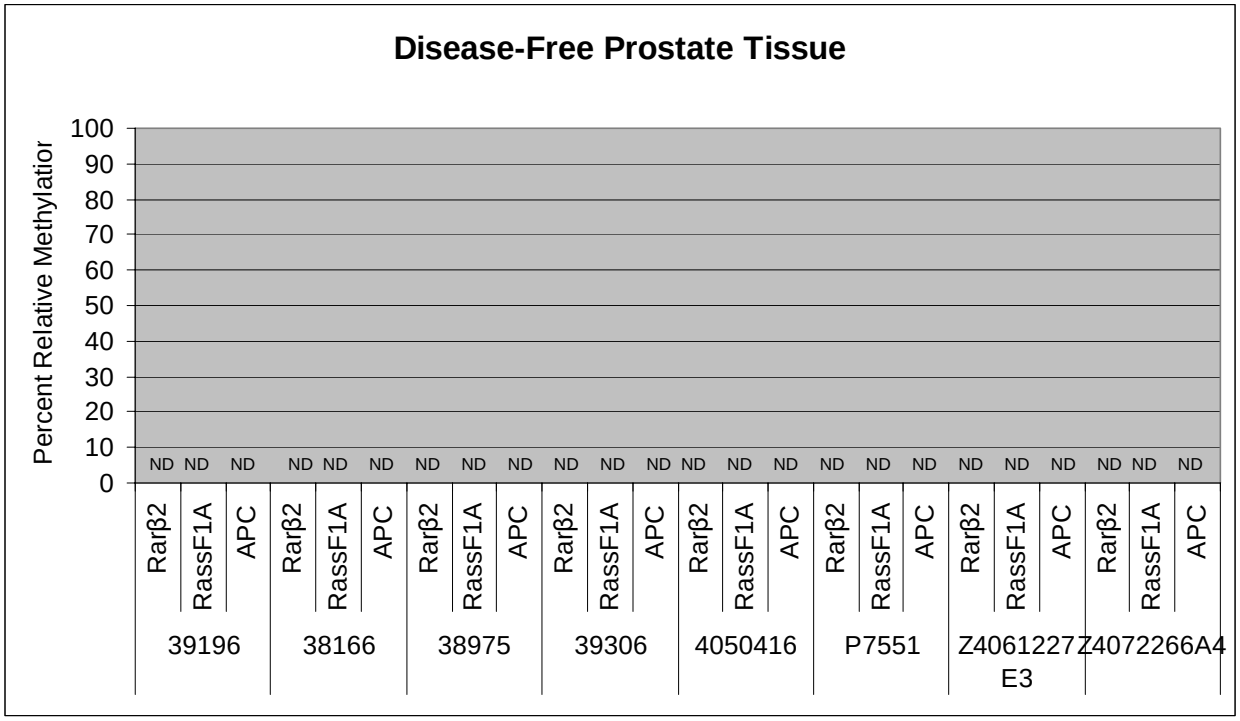

Figure 2. DNA from disease-free prostate tissues. Included are a post-mortem DNA sample of prostate tissue from an infant (P7551), and six post-mortem DNA samples from adults shown to be free of prostate disease (39306, 39196, 38166, 28975, 29206, Z4061227E3, Z4072255A4). All samples were analyzed for methylation with the promoters for Rar-B2, APC, Rass F1A, and GSTP-1. In all cases all gene promoters were found to be unmethylated. B-actin was the internal reference control used to normalize assay results (not shown). ND=none detected.

Figure 3

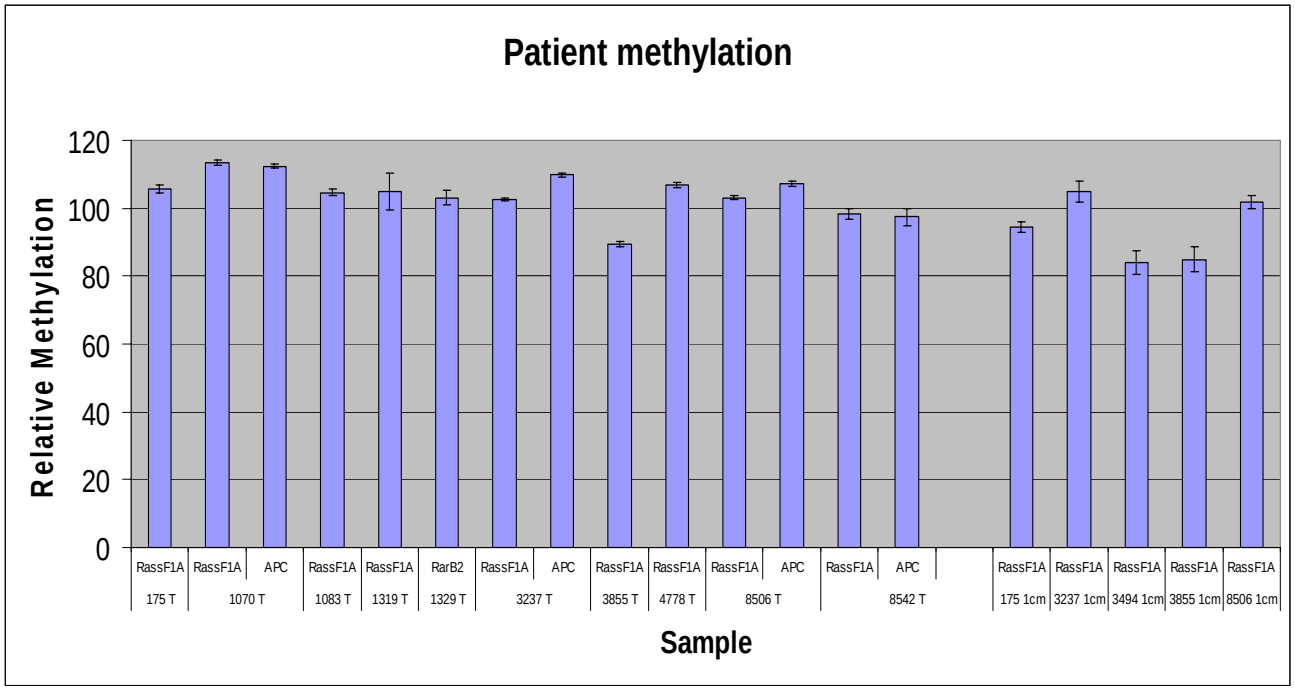

Figure 3. Graph represents all instances of promoter methylation found for RassF1A, APC, or Rar-β2 among 12 matched patient sample sets. Methylation relative to B-actin is shown on the left of the graph, sample designation is shown along the bottom. 'T' indicates tumor tissue, '1cm' indicates nearby histologically normal tissue. Tumor tissue (T) methylation levels are shown on the left, nearby histologically normal tissues (1cm) are on the right. B-actin was used as the internal control (not shown).

Figure 4

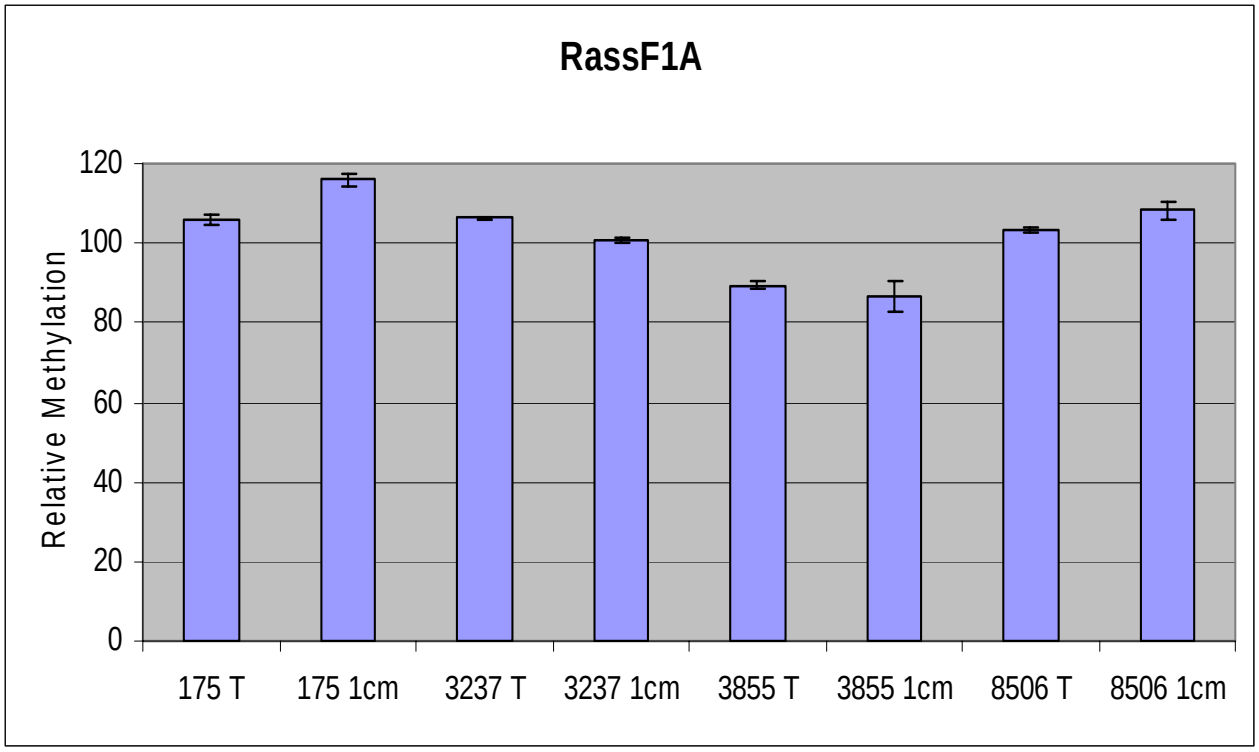

Figure 4. Promoter methylation found for the RassF1A promoter. Methylation relative to B-actin is shown on the left of the graph, sample designation is shown along the bottom. 'T' indicates tumor tissue, '1cm' indicates nearby histologically normal tissue. RassF1A was found to be methylated not only in the tumor tissue, but also the matched nearby histologically normal tissue of 4 of the patient samples examined. These findings indicate that epigenetic alterations exist beyond the tumor. B-actin was used as the internal control (not shown).

Figure 5

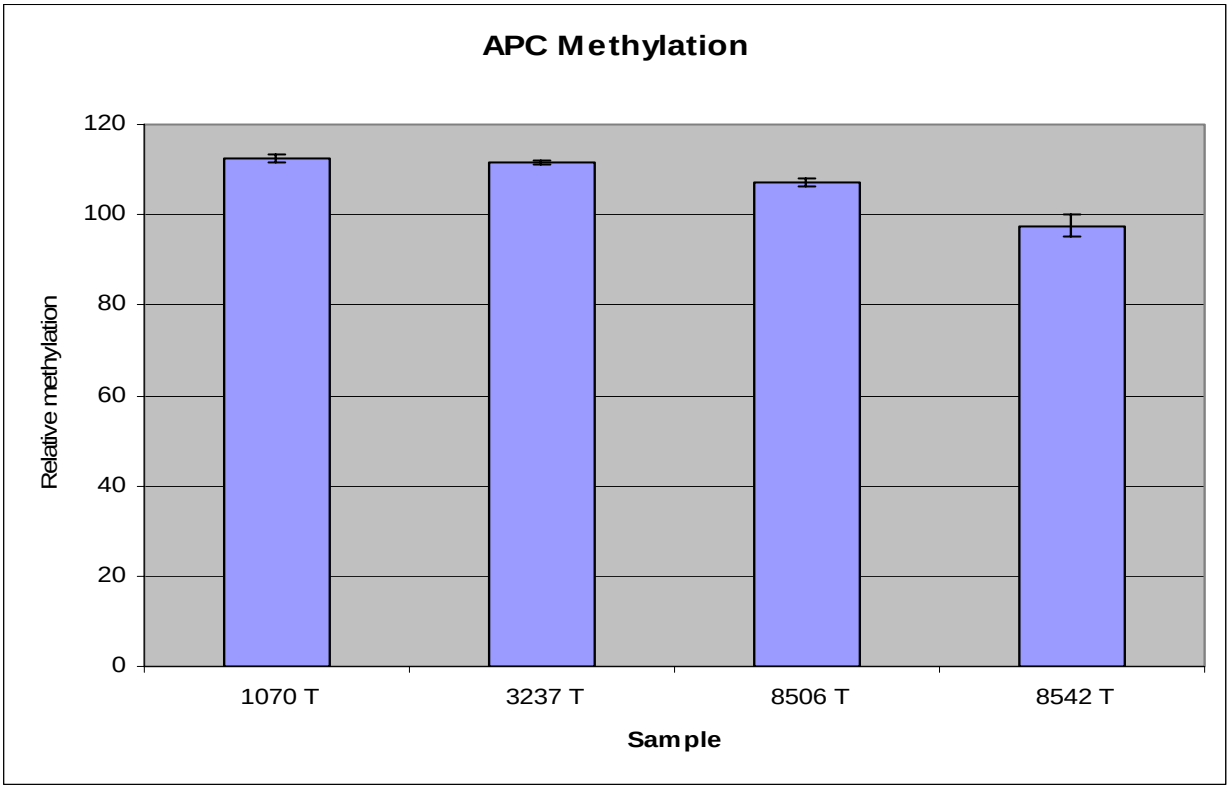

Figure 5. Promoter methylation results for APC. Methylation relative to B-actin is shown on the left of the graph, sample designation is shown along the bottom. 'T' indicates tumor tissue. The gene promoter was found to be methylated in the above tumor tissues, however not in the nearby histologically normal tissues of any patient samples examined. B-actin was used as the internal control (not shown).

Figure 6

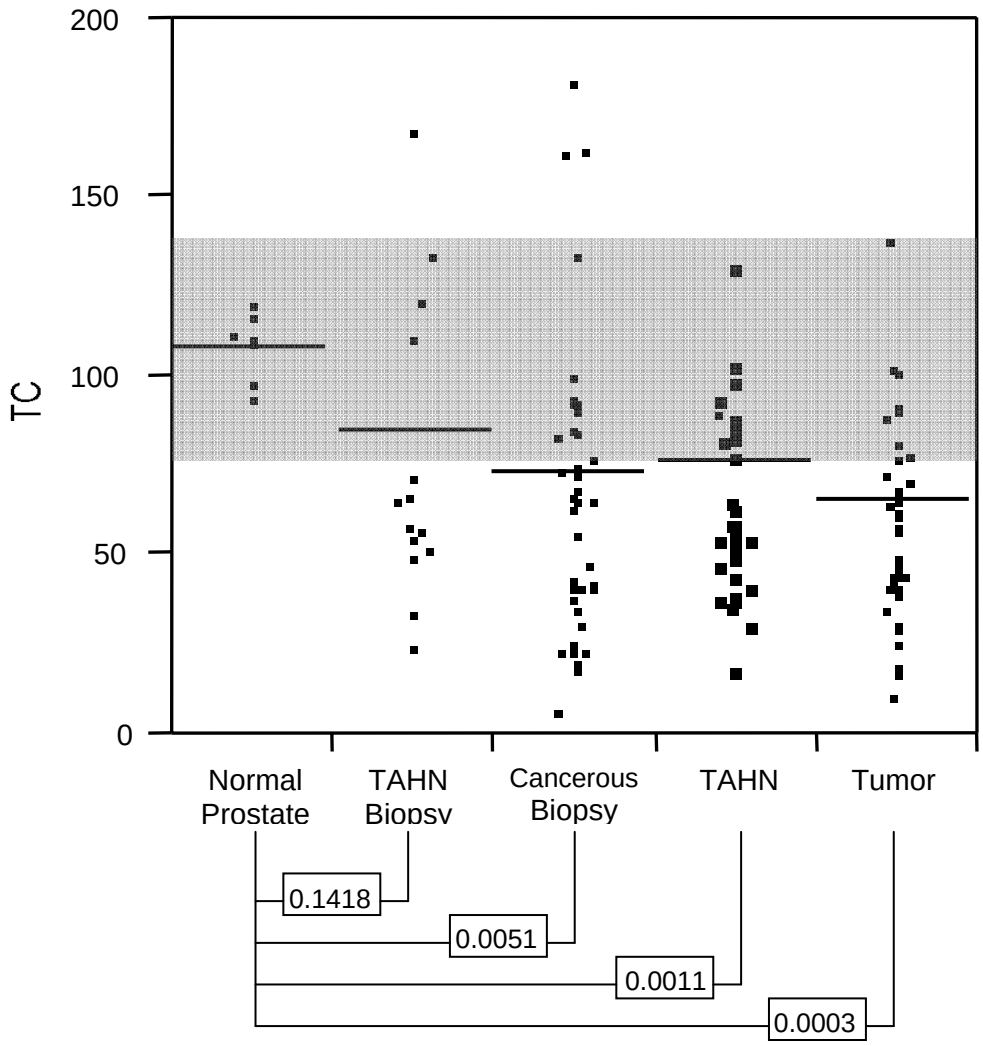

Figure 6. Telomere Content of samples by tissue source. The gray box indicates the 95% range of normal tissues as determined experimentally. Boxes contain the *p*-values between the sample groups (Student's *t*-test). The mean values of cancerous biopsy, TAHN, and Tumor were below the 95% range of normal disease-free tissue.

Figure 7

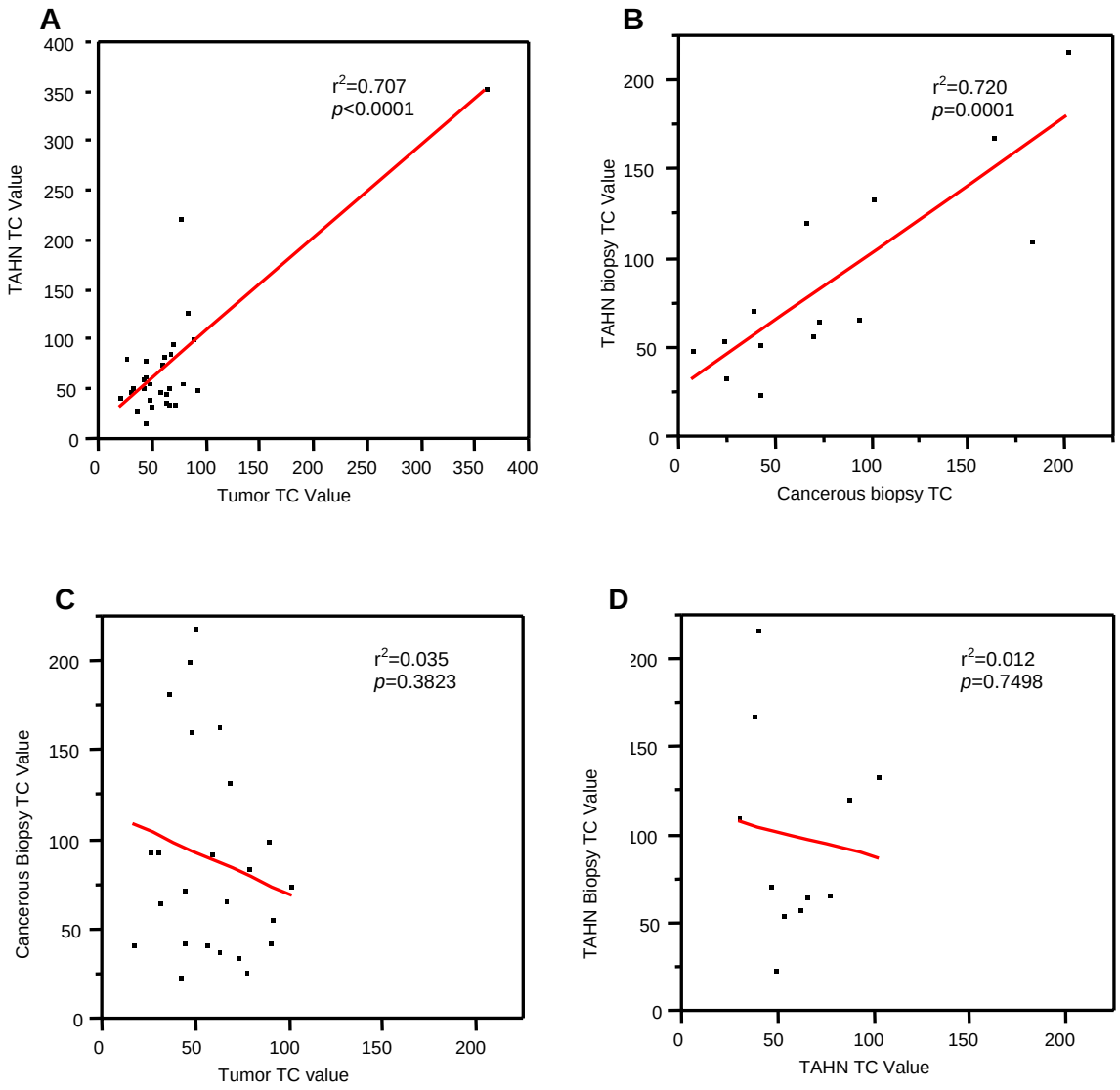

Figure 7. Correlation of samples by tissue source. Paired samples by prostatectomy or biopsy, and compared by relative tissue type. Panel A shows the TC relationship between TAHN and Tumor tissues. Panel shows the TC relationship between TAHN and Cancerous Biopsy tissues. Panel C shows the lack of TC correlation between Cancerous Biopsy and Tumor tissues. Panel D shows the lack of TC correlation between TAHN Biopsy and TAHN tissues.

Figure 8

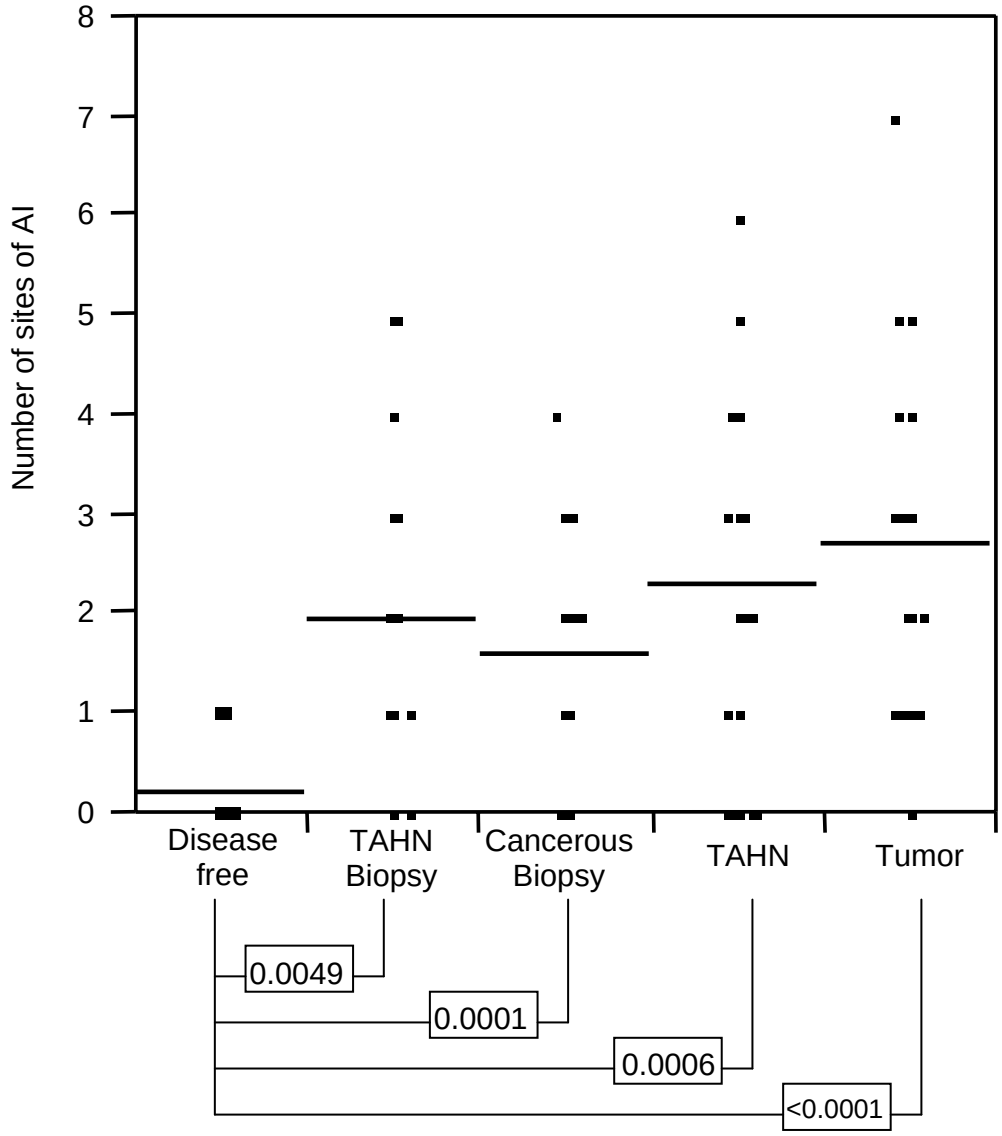

Figure 8. Allelic Imbalance. Allelic Imbalance of study cohort compared to normal disease-free prostate tissues. Boxes indicate significance as determined by the Student's *t*-test. Normal disease-free tissue was found to have 1 or fewer sites of AI. The mean number of sites of AI for all other tissue types was above 1, with TAHN and Tumor specimens having the highest mean at greater than 2 sites per specimen on average.

Table 1

Designation	Oligonucleotide Sequence
Rar-β2 Forward	5'-CGA GAA CGC GAG CGA TTC-3'
Rar-β2 Reverse	5'-CAA ACT TAC TCG ACC AAT CCA ACC-3'
Rar-β2 Probe	5'-6-FAM-TCG GAA CGT ATT CGG AAG GTT TTT TGT AAG TAT TT-6-TAMSp-3'
β-actin Forward	5'-TGG TGA TGG AGG AGG TTT AGT AAG-3'
β-actin Reverse	5'-ACC CAA TAA AAC CTA CTC CTC CCT TAA-3'
β-actin Probe	5'-6-FAM-ACC ACC ACC CAA CAC ACA ATA ACA AAC ACA-6-TAMSp-3'
GSTP-1 Forward	5'-AGT TGC CGC GCG ATT-3'
GSTP-1 Reverse	5'-GCC CCA ATA CTA AAT CAC GAC G-3'
GSTP-1 Probe	5'-6-FAM-CGG TCG ACG TTC GGG GTG TAG CG-6-TAMSp-3'
RassF1A Forward	5'-GCG TTG AAG TCG GGG TTC-3'
RassF1A Reverse	5'-CCC GTA CTT CGC TAA CTT TAA ACG-3'
RassF1A Probe	5'-6-FAM-ACA AAC GCG AAC CGA ACG AAA CCA-6-TAMSp-3'
APC Forward	5'-GAA CCA AAA CGC TCC CCA T-3'
APC Reverse	5'-TTA TAT GTC GGT TAC GTG CGT TTA TAT-3'
APC Probe	5'-6-FAM-CCC GTC GAA AAC CCG CCG ATT A-6-TAMSp-3'

Table 1. Primers and probes used for Q-MSP. The left column indicates the primer/probe designation, the right column indicates the sequence of the oligonucleotide and fluorescent labels (for the probes).

Table 2

Patient demographics (*n*=56)	
Caucasian	48
African American	8
Age at Prostatectomy (in years)	
Range	47-79
Median	63.5
Mean	62.9
Gleason Score	
5	2
6	22
7	30
8	2
Stage	
T2a/b	46
T3	10

Table 2. Characteristics of the Telomere Content (TC) study cohort. Of the 56 cases analyzed, 48 were Caucasian and 8 were African American. Age at prostatectomy ranged from 47 to 79 years of age, with a median of 63.5 years and mean of 62.9 years. The Gleason score of specimens ranged from 5 to 8, with the majority being scored 6 (*n*=22) or 7 (*n*=30). Staging was either T2a or b (*n*=46) or T3 (*n*=10).

Table 3

	Number of patients	Median time to outcome (months)	Mean (months)	Min (months)	Max (months)
Recurrence	25	27	35.8	14	109
No Recurrence	31	62	58.8	17	134

Table 3. Recurrence/follow up information of the Telomere Content (TC) study. 25 of the cases recurred, with a median time to recurrence of 27 months and a range of 14 to 109 months. Mean time to recurrence was 35.8 months. Of the 31 cases that did not recur, median time of follow up was 62 months, with a mean of 58.8 months and a range of 17 to 134 months of follow up.

Table 4

Patient demographics (*n*=56)	
Caucasian	49
African American	7
Age at Prostatectomy (in years)	
Range	47-79
Median	63
Mean	62.68
Gleason Score	
5	2
6	22
7	30
8	2
Stage	
T2a/b	45
T3a/b	11

Table 4. Patient cohort of the Allelic Imbalance study. 56 cases were analyzed in the allelic imbalance (AI) study, of which 49 were Caucasian and 7 were African American. Age at prostatectomy ranged from 47 to 79 years of age, with a median age of 63 years and a mean of 62.68 years. Gleason scores of the patients ranged from 5 to 8, with the majority of Gleason scores being 6 (*n*=22) or 7 (*n*=30). The majority of cases were staged T2a or b (*n*=45), with the remainder being staged T3a or b (*n*=11).

Table 5

	Number of patients	Median time to outcome (months)	Mean (months)	Min (months)	Max (months)
Recurrence	25	27	35.9	14	109
No Recurrence	31	62	59.5	17	134

Table 5. Recurrence/follow up data of the Allelic Imbalance (AI) study cohort. 25 of the cases recurred, with a median time to recurrence of 27 months and a range of 14 to 109 months. Mean time to recurrence was 35.9 months. Of the 31 cases that did not recur, median time of follow up was 62 months, with a mean of 59.5 months and a range of 17 to 134 months of follow up.

Table 6

		1	2	3	4	5	6	7	8	9	10	11	12	13	14	15
1	Neg Bx															
	Pos Bx															
2	Neg Bx															
	Pos Bx															
3	Neg Bx															
	Pos Bx															
4	Neg Bx															
	Pos Bx															
5	TAHN															
	Tumor															
6	TAHN															
	Tumor															
7	TAHN															
	Tumor															
8	TAHN															
	Tumor															
9	TAHN															
	Tumor															
10	TAHN															
	Tumor															
11	TAHN															
	Tumor															
12	TAHN															
	Tumor															
13	TAHN															
	Tumor															
14	TAHN															
	Tumor															

Table 6. Clonality of allelic imbalance. Matched samples, either Negative and Positive Biopsy or TAHN and Tumor. The lightest gray boxes indicate a heterozygous or non-informative allele, the darker gray boxes indicate a site of imbalance. The darkest boxes indicate a matched site of imbalance in the two tissue types. The numbers at the left of the table indicate the case number. The following column notates the sample type. The numbers across the top correlate to the allele tested. Amelogenin was not included in the table as the entire cohort is male. 1-D8S1179; 2-D21S11; 3-D7S820; 4-CSF1PO; 5-D3S1358; 6-THO1; 7-D13S317; 8-D16S539; 9-D2S1338; 10-D19S433; 11-vWA; 12-TPOX; 13-D18S51; 14-D5S818; 15-FGA.

Table 7

		1	2	3	4	5	6	7	8	9	10	11	12	13	14	15
15	Neg Bx															
	Pos Bx															
	TAHN															
	Tumor															
16	Neg Bx															
	Pos Bx															
	TAHN											0.12				
	Tumor					0.08										
17	Neg Bx															
	Pos Bx															
	TAHN															
	Tumor															
18	Neg Bx															
	Pos Bx															
	TAHN															
	Tumor										0.01					
19	Neg Bx															
	Pos Bx															
	TAHN															
	Tumor											0.08			0.22	
20	Neg Bx															
	Pos Bx															
	TAHN															
	Tumor															
21	Neg Bx															
	Pos Bx															
	TAHN															
	Tumor		0.10												0.09	
22	Neg Bx															
	Pos Bx															
	TAHN															
	Tumor					0.02										
23	Neg Bx															
	Pos Bx															
	TAHN															
	Tumor															
24	Neg Bx															
	Pos Bx															
	TAHN															
	Tumor														0.15	
25	Neg Bx															
	Pos Bx															
	TAHN															
	Tumor															
26	Neg Bx															
	Pos Bx															
	TAHN															
	Tumor											0.05				
27	Neg Bx															
	Pos Bx															
	TAHN															
	Tumor															

28	**Neg Bx**	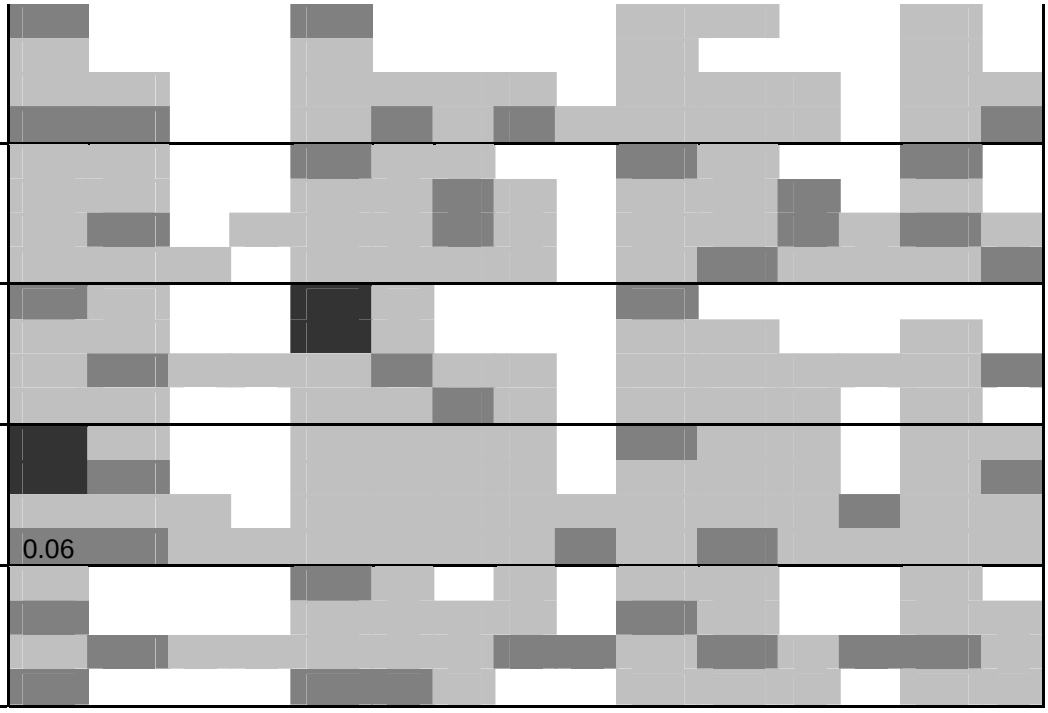
	Pos Bx	
	TAHN	
	Tumor	
29	**Neg Bx**	
	Pos Bx	
	TAHN	
	Tumor	
30	**Neg Bx**	
	Pos Bx	
	TAHN	
	Tumor	
31	**Neg Bx**	
	Pos Bx	
	TAHN	
	Tumor	0.06
32	**Neg Bx**	
	Pos Bx	
	TAHN	
	Tumor	

Table 7. Clonaity at two time points. Cases including all four sample types: Negative Biopsy, Positive Biopsy, TAHN, and Tumor tissue. The lightest gray boxes indicate sites of heterozigosity or homozygous/non-informative alleles. Darker gray boxes indicate sites of allelic imbalance. The darkest boxes indicate paired sites of allelic imbalance between either Negative Biopsy and Positive Biopsy tissues or TAHN and Tumor tissues. In cases with three common sites of imbalance between the sample types, the number indicates the likelihood of imbalance between the three sample types. The numbers at the left of the table indicate the case number. The following column notates the sample type. The numbers across the top correlate to the allele tested. Amelogenin was not included in the table as the entire cohort is male. 1-D8S1179; 2-D21S11; 3-D7S820; 4-CSF1PO; 5-D3S1358; 6-THO1; 7-D13S317; 8-D16S539; 9-D2S1338; 10-D19S433; 11-vWA; 12-TPOX; 13-D18S51; 14-D5S818; 15-FGA. The numbers in the box indicate the percent likelihood of the site of AI matching in three or four specimens for that case.

Appendix B

Differential Gene Expression in Tumor Adjacent Histologically Normal Prostatic Tissue Indicates Field Cancerization

Christina M. Haaland,[1] Christopher M. Heaphy,[1] Kimberly S. Butler,[1] Edgar G. Fischer,[2] Jeffrey K. Griffith,[1,3] and Marco Bisoffi[1,3,*]

University of New Mexico School of Medicine, [1]Department of Biochemistry and Molecular Biology, [2]Department of Pathology, [3]Cancer Research and Treatment Center, Albuquerque, New Mexico.

Running Title: Field Cancerization in Prostatic Tissues.

Abbreviations: AI, allelic imbalance; AP-1, activator protein 1; ARE, AU-rich element; BPH, benign prostatic hyperplasia; DRE, digital rectal examination; EGFR, epidermal growth factor receptor; EGR-1, early growth response protein 1; EPCA, early prostate cancer antigen; EST, expressed sequence tag; FAS, fatty acid synthase; GAPDH, glyceraldehyde 3-phosphate dehydrogenase; GDF-15, growth/differentiation factor 15; H&E, hematoxylin & eosin; hTERT, human telomerase reverse transcriptase; MIC1, macrophage inhibitory cytokine-1; NFκB, nuclear factor kappa B; ORF, open reading frame; PDGF, platelet derived growth factor; PSA, prostate specific antigen; qRT-PCR, quantitative reverse transcriptase PCR; SOD2, superoxide dismutase 2; TAHN, tumor adjacent histologically normal; TBP, TATA binding protein; TC, telomere DNA content; TIMP2, tissue inhibitor of metalloproteinase 2; TNFα, tumor necrosis factor alpha; TTP, tristetraprolin.

Correspondence to: Marco Bisoffi, University of New Mexico School of Medicine Department of Biochemistry and Molecular Biology, MSC08 4670, 1 University of New Mexico, Albuquerque, NM 87131. Tel. (505) 272-8157. Fax (505) 272-6587. Email: mbisoffi@salud.unm.edu

Note: Current address for C.M. Heaphy: The Johns Hopkins Medical Institutions, Department of Pathology, Baltimore, MD 21224.

Support: This work is supported by the Department of Defense Award W81XWH-06-1-0120 (C.M. Haaland), the NIH-IDeA Network of Biomedical Research Excellence Awards P20-RR016480 (M. Bisoffi) and P20-RR0164880 (J.K. Griffith).

Abstract

BACKGROUND. Field cancerization denotes the occurrence of aberrant cells in tumor adjacent histologically normal tissues (TAHN). Field cancerization in prostatic tissues has not been described in detail. Markers of field cancerization could be of clinical utility: (i) For the diagnosis and confirmation of cancer in prostate biopsies after abnormal prostate specific antigen (PSA) and digital rectal examination (DRE), and independent of histology, and (ii) as early targets for chemopreventive intervention in pre-malignant disease.

METHODS. Pooled RNA from paired patient tumor and TAHN tissues excised at 1cm from the tumor margin from patient prostatectomies were subjected to microarray expression analysis and compared to RNA from normal cancer-free prostatic tissues. Quantitative reverse transcriptase PCR (qRT-PCR) was performed on the individual RNA samples used for microarray analysis, and on an independent set, to validate and confirm the results.

RESULTS. We chose transcripts in tumors to guide the selection of genes that were up-regulated at different levels in TAHN tissues for validation by qRT-PCR, and for characterizing the extent of field cancerization. We report expression levels for early growth response protein 1 (EGR-1), tristetraprolin (TTP), testican, and fatty acid synthase (FAS) in individual and independent tumor and TAHN tissues.

CONCLUSIONS. This study offers novel and partially confirmatory proof of previously reported expressional changes in field cancerized human prostatic TAHN tissues at defined distances from tumor margins. Despite tissue heterogeneity, field cancerized prostatic tissues represent a source of protein biomarkers that could be used for early diagnosis of disease in prostatic biopsies in combination with, or independent of, histological assessment.

Keywords: Prostate, field cancerization, tumor adjacent histologically normal, gene expression.

Introduction

The terms “field cancerization” or “field effect” were first introduced in tumors of the head and neck to describe the occurrence of genetic alterations in histologically normal tissues adjacent to tumors (1-4). Such alterations outside of the histologically visible tumor margins could result from pre-existing fields of genetically compromised cells in which the tumor develops. Alternatively, the tumor could influence the surrounding tissue, or it may reflect a combination of these two scenarios. While the underlying mechanisms of field cancerization remain unclear, its occurrence has been described in several epithelial cell derived tumors, including but not limited to lung, esophageal, colorectal, breast, and skin cancers (1,4,5). In contrast, relatively little is known about field cancerization in prostate cancer, perhaps due to its previously reported multifocal nature (5,6). In addition, prostate cancer is often present in the setting of other benign prostatic conditions, most frequently benign prostatic hyperplasia (BPH), which could influence adjacent cells and thus affect the characterization of field cancerized tissue. Finally, due to the relatively small size of the human prostate, the entire organ may be affected, either genetically or biochemically, excluding the existence of matched, truly normal, i.e. entirely unaffected tissue from the same patient.

Field cancerization is of clinical importance (5). In prostate cancer, markers of field cancerization may be important for confirming or detecting disease in biopsies after abnormal prostate specific antigen (PSA) and/or digital rectal examination (DRE), the current standard of care for detecting prostate cancer. PSA screening has led to earlier detection and an overall decrease in prostate cancer specific mortality, emphasizing the importance of prostate biopsies (7,8). However, biopsy tissue represents a very small portion of the prostate and consists primarily of tumor adjacent histologically normal (TAHN) tissue. In spite of ultrasound

guidance, it is easy to miss a small focal malignancy. The current accuracy of prostate cancer detection/confirmation by biopsy is approximately 25% with the rest representing false negative diagnoses (9,10). In the presence of an abnormal PSA and/or DRE, this represents a dilemma for the patient and his physician. Therefore, biomarkers that are indicative of disease, yet independent of histology, i.e. present in field cancerized TAHN tissue, could greatly increase the accuracy of early prostate cancer detection in biopsies (5).

Our laboratory has previously investigated the nature of field cancerization in both prostate and breast cancers using markers of genomic instability, including telomere DNA content (TC), an established surrogate measure of telomere length, and the extent of allelic imbalance (AI) (11,12). These studies have shown telomere alterations and the presence of AI in both tumor and TAHN tissues. In particular, alterations in TC seen in prostate tumors were frequently mimicked in the matched TAHN tissues, indicating prostatic field cancerization (11). Based on these observations, we hypothesized that the molecular changes would not be limited to genomic instability, but may include consistent alterations in gene expression. To test this hypothesis, we have conducted a study utilizing microarray expression analysis of cancerous and TAHN prostatic tissues isolated at 1cm from the visible tumor margin. We report here the identification of consistently altered gene expression in TAHN tissues indicative of field cancerization in prostate cancer.

Materials and Methods

Prostate sample collection, preparation, and demographics. Twelve matched prostate tumors and TAHN tissues excised at 1cm from the visible tumor margin (approximately 150 mg each), resulting in a total of 24 samples, were obtained from the University of New Mexico Hospital Pathology Laboratory in agreement with all University, State and Federal laws. The median age of the cohort was 57 years with a range was 51-71 years; all samples had Gleason scores of 3+3 or 3+4, and a Stage of T2 with the exception of two T3 cases; all samples were node negative (Table I). Tissue samples were snap frozen in liquid nitrogen immediately after collection and stored at -70˚C. A portion of the frozen tissues (approximately 50 mg) was homogenized and RNA was isolated and resuspended in RNase-free water (Qiashredder and RNeasy Kits Qiagen, Valencia, CA). In order to characterize the tissue portions used for RNA isolation by histopathology, directly adjacent tissue portions (approximately 50 mg per sample) were formalin fixed and paraffin embedded for sectioning and hematoxylin & eosin (H&E) staining for independent pathological review (Fig. 1). Samples were randomized into 2 groups, the microarray set (MA set, Table I) and the validation set (VA set, Table I). Each group consisted of 6 patient matched tumor and TAHN samples; the MA samples were those designated 1-6, while the VA set were the samples designated 7-12 in Table I. For the six cases chosen for microarray analysis, a total of 1µg of the isolated RNA was pooled to generate the MA set, while the remaining RNAs, and RNAs from six additional cases (independent VA set) were stored separately.

Six prostate samples from cancer-free controls (unrelated death cases) were obtained from the National Cancer Institute Cooperative Human Tissue Network (CHTN; Nashville, TN), stored at -70˚C, and subjected to RNA extraction and histological review. The latter confirmed

these samples to be cancer-free and also free of BPH (Fig. 1). The median age of this set was 44.5 years, with a range of 26-79 years (Table I).

Microarray expression analysis. RNA integrity was analyzed using the Agilent Bioanalyzer 2100 (Agilent, Foster City, CA). RNAs from six matched tumor and TAHN tissues were selected to be prepared for microarray analysis based on RNA quality and quantity (the MA set). RNA from the selected samples was combined in equal parts to a total of 1µg to generate the tumor and TAHN pools for the MA set. Control RNA for microarray analysis was obtained from Ambion (Austin, TX) as a customized service, and consisted of RNA pooled from 9 deceased organ donors of Caucasian descent. Great care was taken in choosing cases with a similar age range (median age was 70 years, the range was 45-79 years), and cause of death unrelated to prostatic disease; in fact, the majority of cases were victims of myocardial infarction and cardiac arrest. RNA was reverse transcribed into complementary DNA (cDNA) using the Retroscript™ RT Kit (Ambion, Austin, TX), followed by labeling with either Cy3 (pooled control RNA) or Cy5 (either tumor or TAHN pool) fluorescent cyanine dyes. Labeling was achieved by synthesizing the cDNAs in the presence of amino allyl dUTP (Sigma-Aldrich, St. Louis, MO) followed by chemically coupling of either Cy3 or Cy5 monofunctional dye (Amersham-Pharmacia Biotech, Arlington Heights, IL) to the cDNA. This process avoids biased incorporation of the dyes during reverse transcription.

Glass-slide-spotted-expression microarrays of the Qiagen Human Genome Oligo Set Version 3.0 (Qiagen) were used for this investigation. The arrays contained 37,123 transcripts, including 24,650 known genes, the rest being expressed sequence tags (ESTs) and controls. The design of these arrays is based on the Ensembl Human 13.31 Database

(http://www.ensembl.org/) and on the Human Genome Sequencing Project. Equal parts of Cy3 and Cy5 labeled cDNAs were then combined and competitively hybridized to the microarray slides using the GeneTAC Genomic Solutions machine and protocol (Genomic Solutions Inc, Ann Arbor, MI). Following hybridization and washing, the slides were scanned at 532nm and 635nm using the Axon 4000A scanner (Axon Instruments, Union City, CA), and the signal data was processed using Axon GenePix Pro 5 software (Axon Instruments). Fluorescence intensities of the Cy3 and Cy5 dyes were determined for each oligonucleotide spot, followed by visual inspection prior to importing into Acuity 3.0 (Molecular Devices, Sunnyvale, CA). This program was utilized to normalize the data and allow for comparison between the replicates using standard quality calls (background removal, linear regression ratio >0.6, signal to noise ratio >3.0). Only data passing these quality filters were utilized in the present analysis. Sample groups, i.e. tumor and TAHN pools, were run in triplicate hybridizations.

Quantitative (real time) reverse transcriptase PCR. Quantitative Real Time PCR (qRT-PCR) was used to verify the results of the microarray expression analyses. Samples from both the MA and the independent VA sets were individually analyzed in quadruplicate for each selected gene/primer set. Approximately 1 µg of RNA from the samples was converted to cDNA using the Retroscript™ RT Kit (Ambion) according to the manufacturer's protocol using random decamers. The cDNAs were subsequently diluted 1:5 for use in the PCR reactions.

Genes included in mRNA expression evaluation included early growth response protein 1 (EGR-1), tristetraprolin (TTP), testican, fatty acid synthase (FAS), tissue inhibitor of metalloproteinase 2 (TIMP2), and superoxide dismutase 2 (SOD2). mRNA levels were quantitated using the Sybr Green real-time PCR assay kit (Applied Biosystems, Foster City, CA)

in a 25uL reaction, using 0.5uL of the diluted cDNA. Primers were used at a final concentration of 400 uM for both the forward or reverse in each reaction with the exception of EGR-1, for which the forward primer was used at a final concentration of 1 µmol, the reverse at a final concentration of 1.5 µmol in the PCR reaction. The primers' sequences are listed in Table II. PCR reactions were carried out under the following cycling parameters: 95˚C for 10 minutes followed by 40 cycles of 95˚C for 15 seconds, and 60˚C for one minute using the Gene Amp® 7000 Sequence Detection System (Applied Biosystems). Baseline fluorescence was determined during cycles 6-15.

The levels of EGR-1, TIMP2, and SOD2 were determined using the ΔΔCt method, where the threshold of detection of the genes of interest were compared to a house keeping gene, either the TATA binding protein (TBP) (for EGR-1), or glyceraldehyde 3-phosphate dehydrogenase (GAPDH) (for TIMP2 and SOD2). This method was chosen because the amplification efficiencies of their primers were determined to be similar to the ones of the control transcripts. The remaining genes, i.e. FAS, TTP, and testican, were evaluated using quantitation compared to serial dilutions of plasmids carrying cDNAs for these transcripts. Expression level calculations were controlled by the PCR efficiency corrected comparative quantitation method. Plasmids containing FAS, TTP, testican, and TBP PCR fragments were constructed using the pGem T-Easy vector (Promega Corporation, Madison, WI), and the PCR product incorporation was verified by sequencing. The data was reported as relative expression of genes of interest in tumor and TAHN RNA compared to expression levels in the pooled control prostate RNA.

Statistics. qRT-PCR results obtained from the microarray and validation sets were analyzed using JMP IN version 3.2.1 from Statistical Analysis Software (SAS; Cary, NC).

Differences in the means between tumor or TAHN and cancer-free samples were analyzed using unpaired two sample *t*-test; differences between matched tumor and TAHN samples were analyzed using paired two sample *t*-test; differences with $p<0.05$ were considered statistically significant.

Results

Microarray expression analysis. We report RNA expression levels as ratios of Cy3/Cy5 signals for individual transcripts, where the Cy3 and Cy5 fluorescent cyanine dyes were used to label cDNA from experimental (tumor or TAHN) and pooled cancer-free control tissues, respectively. While a ratio of 1.0 would thus indicate no change in expression compared to cancer-free controls, there is the possibility of dye bias due to differential incorporation of Cy3 and Cy5 during cDNA synthesis, or due to differential hybridization of Cy3- and Cy5-labeled cDNAs to target probes. To estimate the extent of potential dye bias, we labeled paired aliquots of control cDNA from cancer-free prostatic tissues with Cy3 and Cy5, combined equal amounts of the preparations, and hybridized them to a microarray set. Fluorescence analysis revealed a mean Cy3/Cy5 ratio of 1.27 ± 0.35 standard deviation (SD), a median ratio of 1.22, and a coefficient of variation of 27.3% for all transcripts (Table III). In contrast, the means ± SD and coefficients of variation determined for the TAHN and tumor experimental sets were 1.58 ± 0.61 and 38.6%, and 1.63 ± 0.75 and 46.1%, respectively. Statistical analysis for the distribution of values for all detected transcripts revealed significant differences ($p<0.05$) for the tumor and TAHN microarray data from the Cy3/Cy5 dye bias test (Table III). While this result indicated a minimal dye bias for Cy3 fluorescent cyanine cDNA incorporation and/or target hybridization, we considered all transcripts in the experimental sets with an expression ratio of <1.27 as equally or under-expressed compared to normal cancer-free prostatic tissues in order to avoid false positive assignment of up-regulated genes. Consideration of the Cy3/Cy5 dye bias is important because we focused our analyses of the microarray expression experiments on up-regulated transcripts, since over-expression of a protein marker in TAHN tissues would be amenable to positive identification and could thus be used in diagnostic tests.

In the microarrays, 3769 transcripts were mutually expressed in both tumor and TAHN tissues, 1810 of which were expressed above the Cy3/Cy5 dye bias of 1.27. We plotted the expression levels for these mutually expressed transcripts and analyzed their correlation between tumor and TAHN tissues (graphically shown Figure 2). Logistic regression analysis indicated a correlation coefficient R^2 of only 0.09, indicating overall poor concordance of the expression levels between tumor and TAHN tissues. The majority of these transcripts, i.e. 94% were expressed at <2.0xSD of the mean expression (see Table III) of all transcripts expressed in tumor and TAHN tissues (i.e. <3.13 and <2.80, respectively), as shown in quadrant I of Figure 2.

We used over-expression in the tumor tissues as a guide for the selection and further analysis of transcripts in the TAHN tissues. Accordingly, we identified the transcripts that were up-regulated in the tumor tissues at >2.0xSD of the mean, i.e. all transcripts with a ratio >3.13. Omitting expressed sequence tags (ESTs) and unknown open reading frames (ORFs), this identified 120 known transcripts up-regulated in tumor tissues. Of these, 97 transcripts were also expressed in the TAHN tissues, 70 of which were also expressed at >1.27, i.e. above the Cy3/Cy5 dye bias threshold (quadrants III + IV, Figure 2). Eighty-three transcripts were up-regulated in the TAHN tissues at >2.0xSD of the mean, i.e. all transcripts with a ratio >2.80 (quadrants II + III, Figure 2). Due to space limits, we show the top 40 unique transcripts mutually up-regulated in tumor and TAHN tissues resulting from these analyses in Table IV. The number of mutually expressed and known transcripts at >2.0xSD for both tumor and TAHN tissues was 10 (quadrants III, Figure 2).

qRT-PCR validation of microarrays. As shown in Figure 2, microarray analysis indicated extensive heterogeneity of expression between tumor and TAHN tissues for the

majority of transcripts. However, our microarray expression results represent mean values generated using pooled RNA populations. Therefore, it was important to estimate the extent of heterogeneity in individual samples. For this, we used qRT-PCR to test and validate the findings of the microarray expression analysis on selected transcripts in RNA samples of tumor and TAHN tissues compared to normal cancer-free prostate tissues. To better characterize the extent and heterogeneity of prostatic field cancerization in individual samples, we deliberately chose transcripts from above, below and at the 2.0xSD threshold of the mean in TAHN transcripts (i.e. ~2.8-fold up-regulated compared to cancer-free tissues, as defined in Table III). Early growth response protein 1 (EGR-1) represents the transcript most up-regulated (8.92-fold) in TAHN tissues and has been previously implicated in prostate tumorigenesis (13-20). Its expression in tumor tissue was 9.27-fold (Table IV). Testican, also known as SPOCK-1, was up-regulated at 4.29-fold and 1.73-fold in tumor and TAHN tissues, respectively. Testican has recently been shown to be expressed in prostatic tissues (21). Fatty acid synthase (FAS) represents an expected change in tumorigenesis of the prostate (22,23) and was up-regulated at 5.31-fold and 1.93-fold in tumor and TAHN tissues, respectively. In contrast, tristetraprolin (TTP) has not been previously reported to be associated with prostate tumorigenesis and may thus represent a novel finding. It was expressed at 5.81-fold and 2.75-fold in tumor and TAHN prostatic tissues, respectively (Table IV). For control purposes, we also included two transcripts that were equally or under-expressed in either tumor or TAHN tissues, i.e. tissue inhibitor of metalloproteinase 2 (TIMP2) and superoxide dismutase 2 (SOD2), expressed at 0.46-fold and 1.06-fold, and at 1.04-fold and 0.42-fold in tumor and TAHN tissues, respectively.

qRT-PCR validation was first performed on the six individual RNA samples pooled and used in the microarray expression analysis, the microarray (MA) set (Figure 3). In this analysis,

the expression levels were compared to 6 normal cancer-free prostate control samples. Although variation was observed, mean expression of FAS, TTP, EGR-1 and testican in TAHN tissues was significantly different from normal controls ($p<0.05$; p range = 0.01-0.03). Similarly, mean expression for these transcripts in tumor tissues was significantly different from normal controls ($p<0.05$; p range = <0.01-0.03). In contrast, and as expected, mean expression of the control transcripts TIMP2 and SOD2, which were equally or under-expressed in either tumor or TAHN tissues in the microarray experiments, was similar in TAHN and tumor tissues, as well as in normal controls ($p>0.05$; p range = 0.27-0.70). Although not necessarily expected due to a higher degree of heterogeneity in cancerous tissues, expression of all of these transcripts was similar in TAHN and tumor tissues ($p>0.05$; p range = 0.07-0.59), with the exception of FAS ($p=0.02$). Thus, the results obtained with six individual RNA samples analyzed by qRT-PCR confirm the conclusions drawn from the analysis of pooled RNA by microarray expression analysis.

To corroborate these findings from the MA set, we also individually analyzed RNA from six independent tumors and patient matched TAHN tissues, the validation (VA) set. As in the MA set, mean expression of FAS, TTP, EGR-1 and testican in TAHN tissues was significantly different from normal controls ($p<0.05$; p range = <0.01-0.03), demonstrating a consistent gene expression signature in TAHN tissues. In the VA set, mean expression of these transcripts in tumor tissues showed extensive variation when compared to normal controls, with EGR-1 and TTP showing significant and near significant differential expression ($p<0.01$ and $p=0.06$, respectively), and FAS and testican showing similar expression ($p=0.10$ and $p=0.27$, respectively). As expected, the control transcripts TIMP2 and SOD2 showed similar expression in TAHN and tumor tissues, and in normal controls ($p>0.05$; p range = 0.28-1.00). Collectively, the qRT-PCR data (Figure 3) was in excellent agreement with the data from the microarrays,

thereby indicating the occurrence of field cancerization for the selected transcripts in TAHN when compared to tumor and cancer-free tissues.

Discussion

The major finding of this study is the occurrence of up-regulated transcripts in tumor adjacent histologically normal (TAHN) human prostatic tissues, as shown by microarray and qRT-PCR expression analysis of 12 mostly early stage (T2-T3) and low grade (Gleason sum 6-7) prostate tumors. While the study was not designed to provide a comprehensive signature of prostatic TAHN tissues, it does provide a strong indication of prostatic field cancerization and emphasizes its potential as a source of markers to be further verified in larger cohorts. We focused on the identification of transcripts that were up-regulated in both tumor and TAHN prostatic tissues, as such transcripts may have important clinical applications, especially for the alternative or adjunct diagnosis of prostatic malignancy after inconclusive or false negative biopsy assessment. Dhir and colleagues have reported on the identification of early prostate cancer antigen (EPCA), a biomarker that is expressed throughout the prostate of individuals with prostate cancer but not in those without the disease, also indicating field cancerization (24). The authors of that study showed that EPCA staining by quantitative immunohistochemistry resulted in minimal overlap between samples from patients with prostate carcinoma and controls, and reported a sensitivity of 84% and a specificity of 85% in identifying individuals with prostate cancer >5 years earlier than currently used diagnostics.

Several expression studies have reported unique molecular signatures for prostate cancer by comparing cancerous to histologically cancer-free adjacent tissues and attempting to link the gene profiles to clinicopathological patient information such as stage and Gleason sum scoring (25-32). However, the use of matched tissues as appropriate controls has been questioned due to field cancerized cells harboring genetic and biochemical alterations (33). This is supported by our prior (11,12) and present results. In contrast, few expression studies have reported molecular

signatures and individual markers characteristic of prostatic TAHN tissues. Field cancerization is however evident at the genetic as well as the epigenetic level, as we have shown by altered telomeres in whole tissue TAHN extracts (11) and as shown by others by gene promoter methylation of APC, RARβ2, and RASSF1A (34). Field cancerization in prostatic tissues is also evidenced by RNA/protein expression analysis (35,36). In a similar study with a focus on signatures rather than single transcripts and without validation by qRT-PCR, Chandran and colleagues reported on up to 254 differentially expressed transcripts when comparing tumor associated matched tissues to cancer-free controls utilizing an Affymetrix platform of ~63,000 probes (35). Of note, the authors claim that the majority of these transcripts would not be identified as differentially expressed when compared to tumors. Due to different platforms, patient populations, and sample preparations, it is difficult to compare findings between studies. For example, while the exact distance of TAHN tissue from the tumor is not known in most published studies, we have carefully chosen a defined distance of 1cm. Despite differences, similarities reported by different groups corroborate the occurrence of field cancerization. Accordingly, Yu and colleagues have recently shown field cancerization in prostatic tissues at the expression level using gene chip technology on a set of 152 samples (36). Although these authors were mainly concerned with the comparison between tumor and matched tissues, they also reported expressional differences between prostatic TAHN and tissues from cancer-free control donors. Of interest in their study, the transcription factor c-Fos was up-regulated 2.55-6.80 and 4.67-6.67 in TAHN and tumor tissues, respectively. This is similar to our own findings of 4.13-fold and 9.50-fold over-expression in TAHN and tumor tissues, respectively (Table IV). We also conducted a detailed review of the Gene Expression Omnibus (GEO) microarray data sets from the National Center for Biotechnology Information (NCBI) available at

http://www.ncbi.nlm.nih.gov/geo/. We thereby focused on our top transcripts mutually up-regulated in tumor and corresponding TAHN tissues, as well on the transcripts validated by qRT-PCR (Table IV). This review revealed one data set, GSE6919 that matched our criteria of comparing cancer-free normal (n=18), TAHN (n=63), and tumor tissues (n=65 for primary and n=25 for metastatic) with similar tissue collection procedure and pathological assessment to exclude any obvious neoplastic alterations in TAHN and normal tissues. Despite a higher number of samples, expression levels for EGR-1, c-Fos, FAS, GDF-15, metallothionein 1E (MT-1E), and testican showed high levels of heterogeneity. Nevertheless, expression of EGR-1, c-Fos, FAS, and testican were elevated in both tumor and TAHN tissues, while GDF-15 and MT-1E were not. The reported values compared to our own data are shown in Figure 4. Together, these comparisons validate our findings, and lead us to conclude that field cancerization is a rather strong and robust manifestation in prostatic tumors.

In the present study, we chose to use bulk tissue that was not microdissected in order to include both glandular (epithelial) as well as stromal (fibroblastic) compartments. While prostate adenocarcinoma is ultimately an epithelial disease, it is widely accepted that the stroma is involved in initiating, maintaining, and promoting a malignant phenotype through inter-cell signaling (37,38). These processes may also occur in TAHN tissues, as shown by Hanson and colleagues, who have reported promoter methylation for GSTP1, RARβ2, and CD44 in stromal cells associated with tumors (39). Additionally, this approach also demonstrates that the identified gene expression changes could potentially be identified in biopsy samples. In the present study, we pooled samples for the microarray analysis in order to minimize effects of sample heterogeneity. The authenticity of our findings, however, was confirmed by qRT-PCR using RNA from individual samples. Although heterogeneity from patient to patient was

observed, data validity was corroborated in an additional independent set of patient samples. The up-regulated transcripts observed in both tumor and TAHN tissues were identified in comparison to a mutually shared and appropriate background control, i.e. prostatic tissues from cancer-free deceased individuals with a similar age range.

Albeit not comprehensive, Table IV indicates part of a signature that may be characteristic of prostatic field cancerized tissues. It is conceivable that some of the listed transcripts could have an important role in prostatic TAHN tissues, either a causative one as drivers of pre-malignancy or as a reaction to the presence of the tumor, or both. Among the highest up-regulated transcripts in TAHN tissues were EGR-1, c-Fos, and the growth/differentiation factor 15 (GDF-15), also called macrophage inhibitory cytokine-1 (MIC1). EGR-1 has been strongly implicated in prostate cancer (13-20) and regulates multiple target genes that in turn have a potential role in prostatic carcinogenesis and progression, such as epidermal growth factor receptor (EGFR), platelet derived growth factor (PDGF), and human telomerase reverse transcriptase (hTERT), thereby regulating a spectrum of cellular responses, including growth and growth arrest, survival and apoptosis, and differentiation and transformation (40,41). The involvement of c-Fos as part of the transcription factor activator protein 1 (AP-1) that is activated downstream of many growth factors is supported by a large body of literature on oncogenesis and metastasis (42,43). GDF-15 (MIC1) is a member of the transforming growth factor β (TGFβ) family and is known to be up-regulated in prostate cancer (44,45). In addition, increased levels of GDF-15 have also been correlated with metastasis and the development of sclerotic bone lesions, which are typical for prostate cancer (45). It has also been shown to contribute to chemotherapeutic drug resistance (46). Important to this study, and in contrast to the NCBI GEO data set, GDF-15 expression was previously detected in benign

tissue areas of prostate cancers affected with Gleason sum scores 5-8 disease (47). Similarly, elevated expression of metallothioneins (MT) was recently shown in tissues adjacent to head and neck cancers and breast adenocarcinomas, especially in the presence of affected lymph nodes (48), leading these authors to speculate that MT expression in normal tissues signals the presence of a tumor.

To further estimate the extent and heterogeneity of prostatic field cancerization, we also chose transcripts that were less up-regulated in TAHN tissues, such as TTP, FAS, and testican. TTP expression is not specific to prostatic tissues. However, it is an ubiquitously expressed AU-rich element (ARE) binding protein and a regulator of mRNA stability, including of pro-inflammatory proteins, such as tumor necrosis alpha (TNFα) (49), which plays an important role in prostate adenocarcinoma (50). It is possible that TNFα is produced by inflammatory cells in TAHN tissues in agreement with the prominent role of inflammation as proposed by De Marzo and colleagues (51). TNFα is a classical activator of the nuclear factor kappa B (NFκB) pathway which is constitutively activated in prostate cancer with prominent downstream targets that support an activated cellular state, including EGR-1 (40,52). FAS has been termed a “metabolic oncogene” and may reflect a prostate cell’s energetic switch to a more anaerobic yet more reductive physiologic state, which is a hallmark of prostate cancer progression (22,23). In addition, FAS has been shown to positively affect NFκB nuclear translocation in cancer cells leading to an anti-apoptotic effect (53). Finally, testican (SPOCK-1) belongs to the fibulin protein family of extracellular matrix proteins which influence cell adhesion and migration, and have thus been associated with progression of several cancer types (54), including prostate cancer, in which it has recently been shown to be up-regulated (21).

Collectively, our data adds to and partially confirms previously published, yet rather scarce reports that support the occurrence of field cancerization in prostatic tissues. This study warrants further investigations in larger cohorts of tissue samples collected at defined distances from tumor margins (1cm in this study), and into its underlying mechanisms, as well as potential clinical use of representative transcripts towards an improved prostate cancer detection and patient outcome.

Acknowledgements

We would like to thank Dr. Rick Lyons, Barbara Griffith, Ryan Peters and Philip Enriquez III from the UNM Experimental Pathology Laboratory for providing the printed microarray slides and their technical support. Some experiments used the facilities or services provided by the Keck-UNM Genomics Resource, a facility supported by a grant from the WM Keck Foundation as well as the State of New Mexico, the UNM Cancer Research and Treatment Center and the New Mexico Center for Environmental Health Sciences. We thank Terry Mulcahy and Phillip Enriquez III from DNA Research Services of the University of New Mexico Health Sciences Center for plasmid sequence verification. The UNM Biochemistry and Molecular Biology Department is acknowledged for administrative support. This work is supported by the Department of Defense Award W81XWH-06-1-0120 (C.M. Haaland), the NIH-IDeA Network of Biomedical Research Excellence Awards P20-RR016480 (M. Bisoffi) and P20-RR0164880 (J.K. Griffith).

References

1. Braakhuis BJ, Tabor MP, Kummer JA, Leemans CR, Brakenhoff RH. A genetic explanation of Slaughter's concept of field cancerization: evidence and clinical implications. Cancer research 2003;63(8):1727-1730.
2. Ha PK, Califano JA. The molecular biology of mucosal field cancerization of the head and neck. Crit Rev Oral Biol Med 2003;14(5):363-369.
3. Slaughter DP, Southwick HW, Smejkal W. Field cancerization in oral stratified squamous epithelium; clinical implications of multicentric origin. Cancer 1953;6(5):963-968.
4. Hockel M, Dornhofer N. The hydra phenomenon of cancer: why tumors recur locally after microscopically complete resection. Cancer research 2005;65(8):2997-3002.
5. Dakubo GD, Jakupciak JP, Birch-Machin MA, Parr RL. Clinical implications and utility of field cancerization. Cancer cell international 2007;7:2.
6. Bostwick DG, Shan A, Qian J, Darson M, Maihle NJ, Jenkins RB, Cheng L. Independent origin of multiple foci of prostatic intraepithelial neoplasia: comparison with matched foci of prostate carcinoma. Cancer 1998;83(9):1995-2002.
7. Collin SM, Martin RM, Metcalfe C, Gunnell D, Albertsen PC, Neal D, Hamdy F, Stephens P, Lane JA, Moore R, Donovan J. Prostate-cancer mortality in the USA and UK in 1975-2004: an ecological study. The lancet oncology 2008;9(5):445-452.
8. McDavid K, Lee J, Fulton JP, Tonita J, Thompson TD. Prostate cancer incidence and mortality rates and trends in the United States and Canada. Public Health Rep 2004;119(2):174-186.
9. Rabbani F, Stroumbakis N, Kava BR, Cookson MS, Fair WR. Incidence and clinical significance of false-negative sextant prostate biopsies. The Journal of urology 1998;159(4):1247-1250.
10. Stamey TA. Making the most out of six systematic sextant biopsies. Urology 1995;45(1):2-12.
11. Fordyce CA, Heaphy CM, Joste NE, Smith AY, Hunt WC, Griffith JK. Association between cancer-free survival and telomere DNA content in prostate tumors. The Journal of urology 2005;173(2):610-614.
12. Heaphy CM, Bisoffi M, Fordyce CA, Haaland CM, Hines WC, Joste NE, Griffith JK. Telomere DNA content and allelic imbalance demonstrate field cancerization in histologically normal tissue adjacent to breast tumors. International journal of cancer 2006;119(1):108-116.
13. Adamson ED, Mercola D. Egr1 transcription factor: multiple roles in prostate tumor cell growth and survival. Tumour Biol 2002;23(2):93-102.
14. Eid MA, Kumar MV, Iczkowski KA, Bostwick DG, Tindall DJ. Expression of early growth response genes in human prostate cancer. Cancer research 1998;58(11):2461-2468.
15. Thigpen AE, Cala KM, Guileyardo JM, Molberg KH, McConnell JD, Russell DW. Increased expression of early growth response-1 messenger ribonucleic acid in prostatic adenocarcinoma. The Journal of urology 1996;155(3):975-981.
16. Virolle T, Krones-Herzig A, Baron V, De Gregorio G, Adamson ED, Mercola D. Egr1 promotes growth and survival of prostate cancer cells. Identification of novel Egr1 target genes. The Journal of biological chemistry 2003;278(14):11802-11810.

17. Baron V, De Gregorio G, Krones-Herzig A, Virolle T, Calogero A, Urcis R, Mercola D. Inhibition of Egr-1 expression reverses transformation of prostate cancer cells in vitro and in vivo. Oncogene 2003;22(27):4194-4204.
18. Baron V, Duss S, Rhim J, Mercola D. Antisense to the early growth response-1 gene (Egr-1) inhibits prostate tumor development in TRAMP mice. Annals of the New York Academy of Sciences 2003;1002:197-216.
19. Adamson E, de Belle I, Mittal S, Wang Y, Hayakawa J, Korkmaz K, O'Hagan D, McClelland M, Mercola D. Egr1 signaling in prostate cancer. Cancer biology & therapy 2003;2(6):617-622.
20. Mora GR, Olivier KR, Mitchell RF, Jr., Jenkins RB, Tindall DJ. Regulation of expression of the early growth response gene-1 (EGR-1) in malignant and benign cells of the prostate. The Prostate 2005;63(2):198-207.
21. Wlazlinski A, Engers R, Hoffmann MJ, Hader C, Jung V, Muller M, Schulz WA. Downregulation of several fibulin genes in prostate cancer. The Prostate 2007;67(16):1770-1780.
22. Baron A, Migita T, Tang D, Loda M. Fatty acid synthase: a metabolic oncogene in prostate cancer? Journal of cellular biochemistry 2004;91(1):47-53.
23. Kuhajda FP. Fatty acid synthase and cancer: new application of an old pathway. Cancer research 2006;66(12):5977-5980.
24. Dhir R, Vietmeier B, Arlotti J, Acquafondata M, Landsittel D, Masterson R, Getzenberg RH. Early identification of individuals with prostate cancer in negative biopsies. The Journal of urology 2004;171(4):1419-1423.
25. Dhanasekaran SM, Barrette TR, Ghosh D, Shah R, Varambally S, Kurachi K, Pienta KJ, Rubin MA, Chinnaiyan AM. Delineation of prognostic biomarkers in prostate cancer. Nature 2001;412(6849):822-826.
26. Kim JH, Dhanasekaran SM, Mehra R, Tomlins SA, Gu W, Yu J, Kumar-Sinha C, Cao X, Dash A, Wang L, Ghosh D, Shedden K, Montie JE, Rubin MA, Pienta KJ, Shah RB, Chinnaiyan AM. Integrative analysis of genomic aberrations associated with prostate cancer progression. Cancer research 2007;67(17):8229-8239.
27. Luo JH. Gene expression alterations in human prostate cancer. Drugs Today (Barc) 2002;38(10):713-719.
28. Xu J, Stolk JA, Zhang X, Silva SJ, Houghton RL, Matsumura M, Vedvick TS, Leslie KB, Badaro R, Reed SG. Identification of differentially expressed genes in human prostate cancer using subtraction and microarray. Cancer research 2000;60(6):1677-1682.
29. Ernst T, Hergenhahn M, Kenzelmann M, Cohen CD, Bonrouhi M, Weninger A, Klaren R, Grone EF, Wiesel M, Gudemann C, Kuster J, Schott W, Staehler G, Kretzler M, Hollstein M, Grone HJ. Decrease and gain of gene expression are equally discriminatory markers for prostate carcinoma: a gene expression analysis on total and microdissected prostate tissue. The American journal of pathology 2002;160(6):2169-2180.
30. Tamura K, Furihata M, Tsunoda T, Ashida S, Takata R, Obara W, Yoshioka H, Daigo Y, Nasu Y, Kumon H, Konaka H, Namiki M, Tozawa K, Kohri K, Tanji N, Yokoyama M, Shimazui T, Akaza H, Mizutani Y, Miki T, Fujioka T, Shuin T, Nakamura Y, Nakagawa H. Molecular features of hormone-refractory prostate cancer cells by genome-wide gene expression profiles. Cancer research 2007;67(11):5117-5125.
31. True L, Coleman I, Hawley S, Huang CY, Gifford D, Coleman R, Beer TM, Gelmann E, Datta M, Mostaghel E, Knudsen B, Lange P, Vessella R, Lin D, Hood L, Nelson PS. A

molecular correlate to the Gleason grading system for prostate adenocarcinoma. Proceedings of the National Academy of Sciences of the United States of America 2006;103(29):10991-10996.
32. Setlur SR, Royce TE, Sboner A, Mosquera JM, Demichelis F, Hofer MD, Mertz KD, Gerstein M, Rubin MA. Integrative microarray analysis of pathways dysregulated in metastatic prostate cancer. Cancer research 2007;67(21):10296-10303.
33. Braakhuis BJ, Leemans CR, Brakenhoff RH. Using tissue adjacent to carcinoma as a normal control: an obvious but questionable practice. The Journal of pathology 2004;203(2):620-621.
34. Mehrotra J, Varde S, Wang H, Chiu H, Vargo J, Gray K, Nagle RB, Neri JR, Mazumder A. Quantitative, spatial resolution of the epigenetic field effect in prostate cancer. The Prostate 2008;68(2):152-160.
35. Chandran UR, Dhir R, Ma C, Michalopoulos G, Becich M, Gilbertson J. Differences in gene expression in prostate cancer, normal appearing prostate tissue adjacent to cancer and prostate tissue from cancer free organ donors. BMC cancer 2005;5(1):45.
36. Yu YP, Landsittel D, Jing L, Nelson J, Ren B, Liu L, McDonald C, Thomas R, Dhir R, Finkelstein S, Michalopoulos G, Becich M, Luo JH. Gene expression alterations in prostate cancer predicting tumor aggression and preceding development of malignancy. J Clin Oncol 2004;22(14):2790-2799.
37. Tuxhorn JA, Ayala GE, Rowley DR. Reactive stroma in prostate cancer progression. The Journal of urology 2001;166(6):2472-2483.
38. Condon MS. The role of the stromal microenvironment in prostate cancer. Seminars in cancer biology 2005;15(2):132-137.
39. Hanson JA, Gillespie JW, Grover A, Tangrea MA, Chuaqui RF, Emmert-Buck MR, Tangrea JA, Libutti SK, Linehan WM, Woodson KG. Gene promoter methylation in prostate tumor-associated stromal cells. Journal of the National Cancer Institute 2006;98(4):255-261.
40. Thiel G, Cibelli G. Regulation of life and death by the zinc finger transcription factor Egr-1. Journal of cellular physiology 2002;193(3):287-292.
41. Khachigian LM, Collins T. Early growth response factor 1: a pleiotropic mediator of inducible gene expression. Journal of molecular medicine (Berlin, Germany) 1998;76(9):613-616.
42. Matthews CP, Colburn NH, Young MR. AP-1 a target for cancer prevention. Current cancer drug targets 2007;7(4):317-324.
43. Ozanne BW, Spence HJ, McGarry LC, Hennigan RF. Transcription factors control invasion: AP-1 the first among equals. Oncogene 2007;26(1):1-10.
44. Cheng I, Krumroy LM, Plummer SJ, Casey G, Witte JS. MIC1 and IL1RN genetic variation and advanced prostate cancer risk. Cancer Epidemiol Biomarkers Prev 2007;16(6):1309-1311.
45. Selander KS, Brown DA, Sequeiros GB, Hunter M, Desmond R, Parpala T, Risteli J, Breit SN, Jukkola-Vuorinen A. Serum macrophage inhibitory cytokine-1 concentrations correlate with the presence of prostate cancer bone metastases. Cancer Epidemiol Biomarkers Prev 2007;16(3):532-537.
46. Huang CY, Beer TM, Higano CS, True LD, Vessella R, Lange PH, Garzotto M, Nelson PS. Molecular alterations in prostate carcinomas that associate with in vivo exposure to

chemotherapy: identification of a cytoprotective mechanism involving growth differentiation factor 15. Clin Cancer Res 2007;13(19):5825-5833.
47. Patrikainen L, Porvari K, Kurkela R, Hirvikoski P, Soini Y, Vihko P. Expression profiling of PC-3 cell line variants and comparison of MIC-1 transcript levels in benign and malignant prostate. European journal of clinical investigation 2007;37(2):126-133.
48. Dutsch-Wicherek M, Popiela TJ, Klimek M, Rudnicka-Sosin L, Wicherek L, Oudinet JP, Skladzien J, Tomaszewska R. Metallothionein stroma reaction in tumor adjacent healthy tissue in head and neck squamous cell carcinoma and breast adenocarcinoma. Neuro endocrinology letters 2005;26(5):567-574.
49. Zhang T, Kruys V, Huez G, Gueydan C. AU-rich element-mediated translational control: complexity and multiple activities of trans-activating factors. Biochemical Society transactions 2002;30(Pt 6):952-958.
50. Bouraoui Y, Ricote M, Garcia-Tunon I, Rodriguez-Berriguete G, Touffehi M, Rais NB, Fraile B, Paniagua R, Oueslati R, Royuela M. Pro-inflammatory cytokines and prostate-specific antigen in hyperplasia and human prostate cancer. Cancer detection and prevention 2008;32(1):23-32.
51. DeMarzo AM, Nelson WG, Isaacs WB, Epstein JI. Pathological and molecular aspects of prostate cancer. Lancet 2003;361(9361):955-964.
52. Suh J, Rabson AB. NF-kappaB activation in human prostate cancer: important mediator or epiphenomenon? Journal of cellular biochemistry 2004;91(1):100-117.
53. Menendez JA, Mehmi I, Atlas E, Colomer R, Lupu R. Novel signaling molecules implicated in tumor-associated fatty acid synthase-dependent breast cancer cell proliferation and survival: Role of exogenous dietary fatty acids, p53-p21WAF1/CIP1, ERK1/2 MAPK, p27KIP1, BRCA1, and NF-kappaB. International journal of oncology 2004;24(3):591-608.
54. Gallagher WM, Currid CA, Whelan LC. Fibulins and cancer: friend or foe? Trends in molecular medicine 2005;11(7):336-340.
55. Christian JD, Lamm TC, Morrow JF, Bostwick DG. Corpora amylacea in adenocarcinoma of the prostate: incidence and histology within needle core biopsies. Mod Pathol 2005;18(1):36-39.

Figure Legends

Fig. 1. H&E staining of 3 cancer-free normal prostate tissues (A-C) and 3 representative cases of tumor and tumor adjacent histologically normal (TAHN) tissues (D-F; cases 5, 6, and 8 in Table I). A-C are at 40x magnification; D-E are at 200x magnification; arrows and asterisks denote glandular (ductal epithelial) and stromal areas, respectively; diamonds in D-TAHN and E-TAHN denote *corpora amylacea* (sedimented sulfated glycosaminoglycans) often seen in normal prostatic tissues (55).

Fig. 2. Analysis of microarray expression. Scatter plot of 1810 transcripts (open circles) mutually expressed at >1.27 compared to cancer-free prostatic samples in tumor and TAHN tissues as analyzed by microarray analysis (unknown transcripts included). Expression in tumor and TAHN tissues is shown on the log-scaled x-axis and y-axis, respectively. The Cy3/Cy5 dye bias and the 2xSD thresholds (as defined in Table III) are indicated by arrows and dotted lines. The solid line shows the best fit by logistic regression analysis accompanied by correlation coefficient R^2. Quadrant I: Transcripts expressed at <2.0xSD of the mean expression (see Table III) of all transcripts expressed in tumor and TAHN tissues (i.e. <3.13 and <2.80, respectively); quadrant II: Transcripts expressed at >2.0xSD of the mean expression in TAHN and at >1.27 in tumor tissues; quadrant III: Transcripts expressed at >2.0xSD of the mean expression in both TAHN and tumor tissues; quadrant IV: Transcripts expressed at >2.0xSD of the mean expression in tumor and at >1.27 in TAHN tissues.

Fig. 3. RNA expression levels by qRT-PCR of FAS (A), TTP (B), EGR-1 (C), testican (D), and the control transcripts TIMP2 (E), and SOD2 (F) normalized to either GAPDH or TBP. The tissue groups are indicated on the y-axis (MA, microarray set; VA, validation set; TAHN, tumor adjacent histologically normal). Expression is shown on the y-axis relative to cancer-free normal prostatic tissues, dots represent the distribution, and the horizontal line indicates the median. The numbers represent the p-values for differences between indicated groups as determined by the unpaired (compared to cancer-free tissues) and paired (compared to matched tissues) *t*-test.

Fig. 4. Comparative microarray expression analysis between our study and the Gene Expression Omnibus (GEO) GSE6919 data set from the National Center for Biotechnology Information (NCBI) (http://www.ncbi.nlm.nih.gov/geo/). Expression levels of EGR-1, c-Fos, GDF-15, MT-1E, FAS, and testican are shown for tumor and tumor adjacent histologically normal (TAHN) tissues on the y-axis. The horizontal dotted line represents an expression level of 1 and indicates no change compared to cancer-free normal tissues.

Figure 1

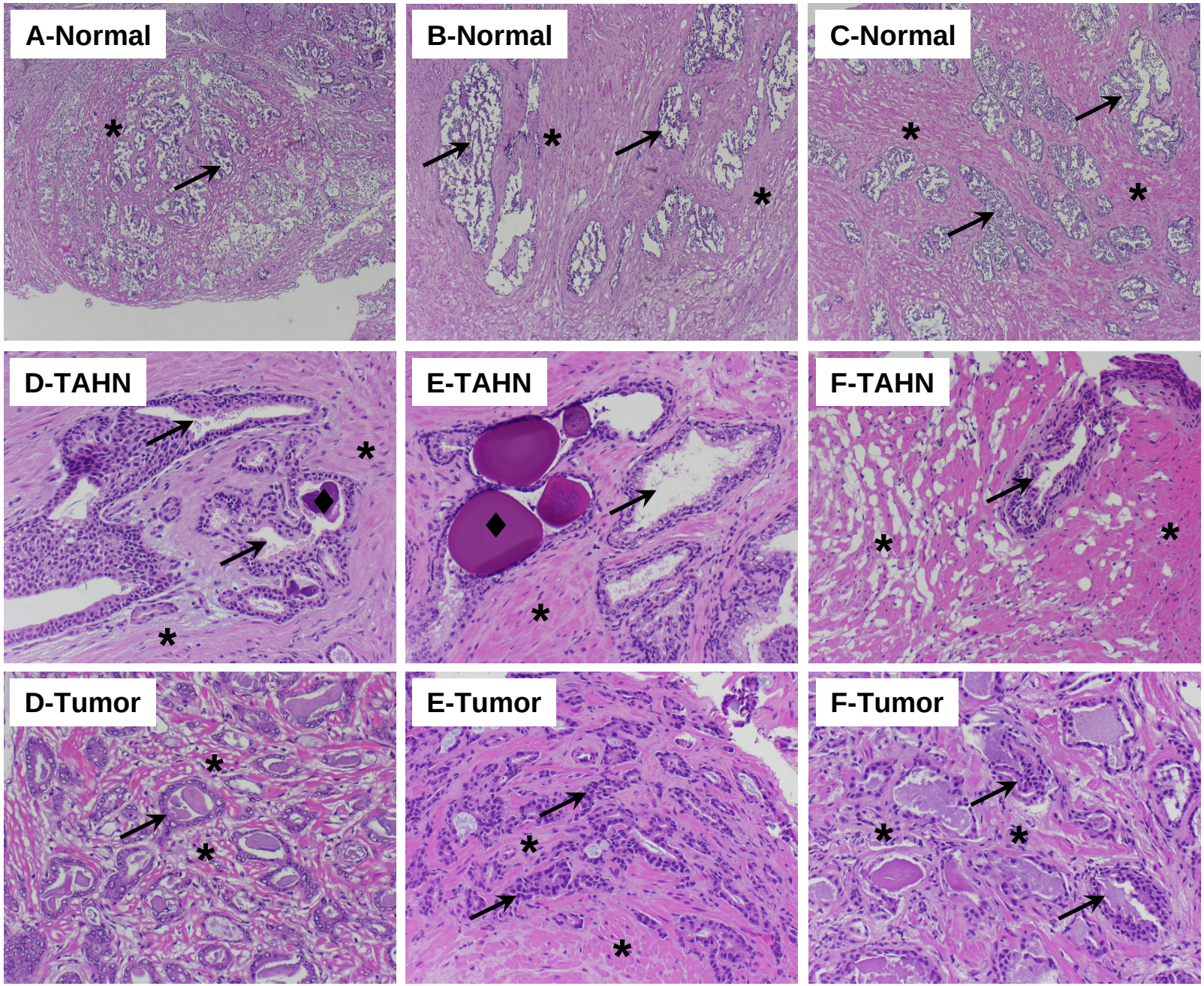
A-Normal
B-Normal
C-Normal
D-TAHN
E-TAHN
F-TAHN
D-Tumor
E-Tumor
F-Tumor

Figure 2

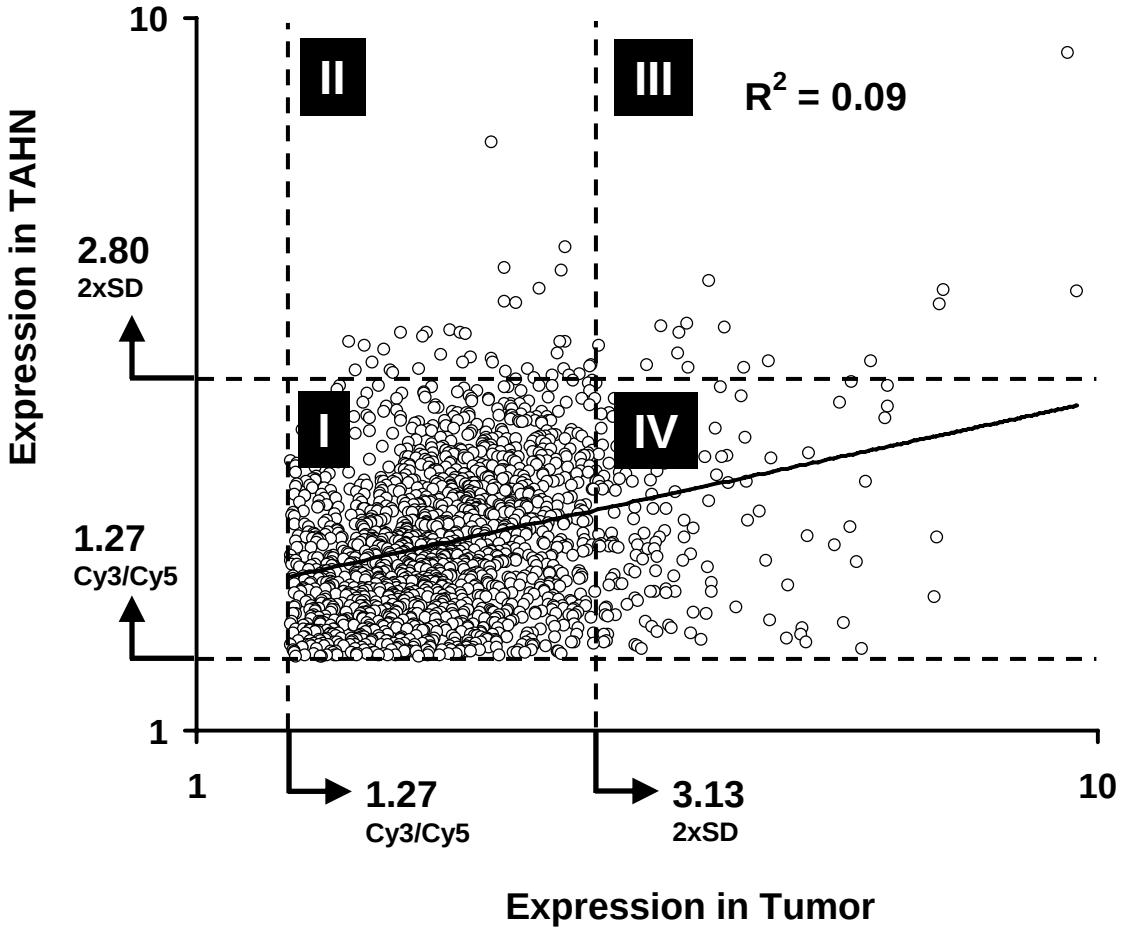
10
II
III
R^2 = 0.09
Expression in TAHN
2.80
2xSD
I
IV
1.27
Cy3/Cy5
1
1
1.27
Cy3/Cy5
3.13
2xSD
10
Expression in Tumor

Figure 3

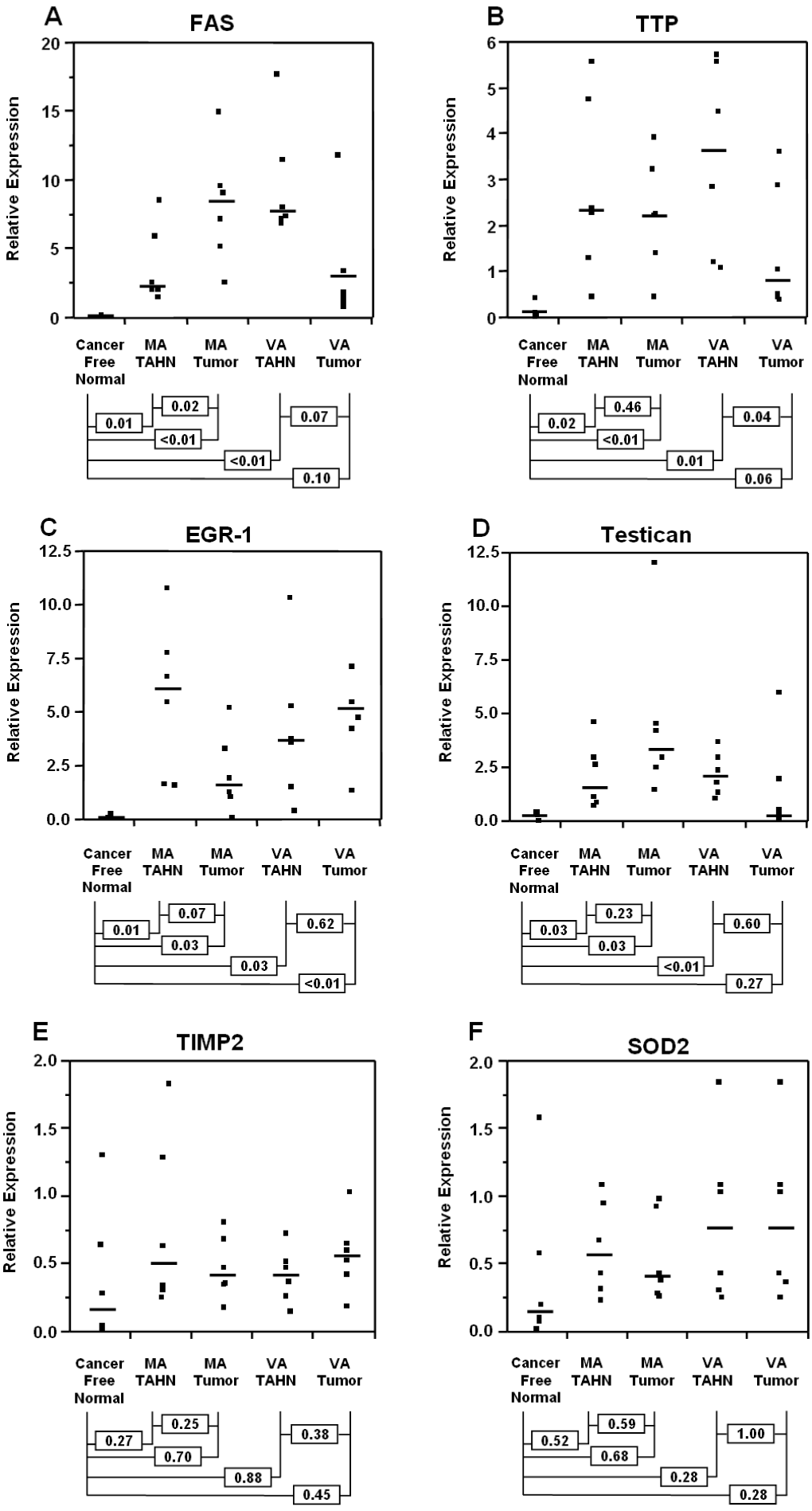
A
FAS
Relative Expression
20
15
10
5
0
Cancer Free Normal
MA TAHN
MA Tumor
VA TAHN
VA Tumor
0.01
0.02
<0.01
<0.01
0.07
0.10
B
TTP
Relative Expression
6
5
4
3
2
1
0
Cancer Free Normal
MA TAHN
MA Tumor
VA TAHN
VA Tumor
0.02
0.46
<0.01
0.01
0.04
0.06
C
EGR-1
Relative Expression
12.5
10.0
7.5
5.0
2.5
0.0
Cancer Free Normal
MA TAHN
MA Tumor
VA TAHN
VA Tumor
0.01
0.07
0.03
0.03
0.62
<0.01
D
Testican
Relative Expression
12.5
10.0
7.5
5.0
2.5
0.0
Cancer Free Normal
MA TAHN
MA Tumor
VA TAHN
VA Tumor
0.03
0.23
0.03
<0.01
0.60
0.27
E
TIMP2
Relative Expression
2.0
1.5
1.0
0.5
0.0
Cancer Free Normal
MA TAHN
MA Tumor
VA TAHN
VA Tumor
0.27
0.25
0.70
0.88
0.38
0.45
F
SOD2
Relative Expression
2.0
1.5
1.0
0.5
0.0
Cancer Free Normal
MA TAHN
MA Tumor
VA TAHN
VA Tumor
0.52
0.59
0.68
0.28
1.00
0.28

Figure 4

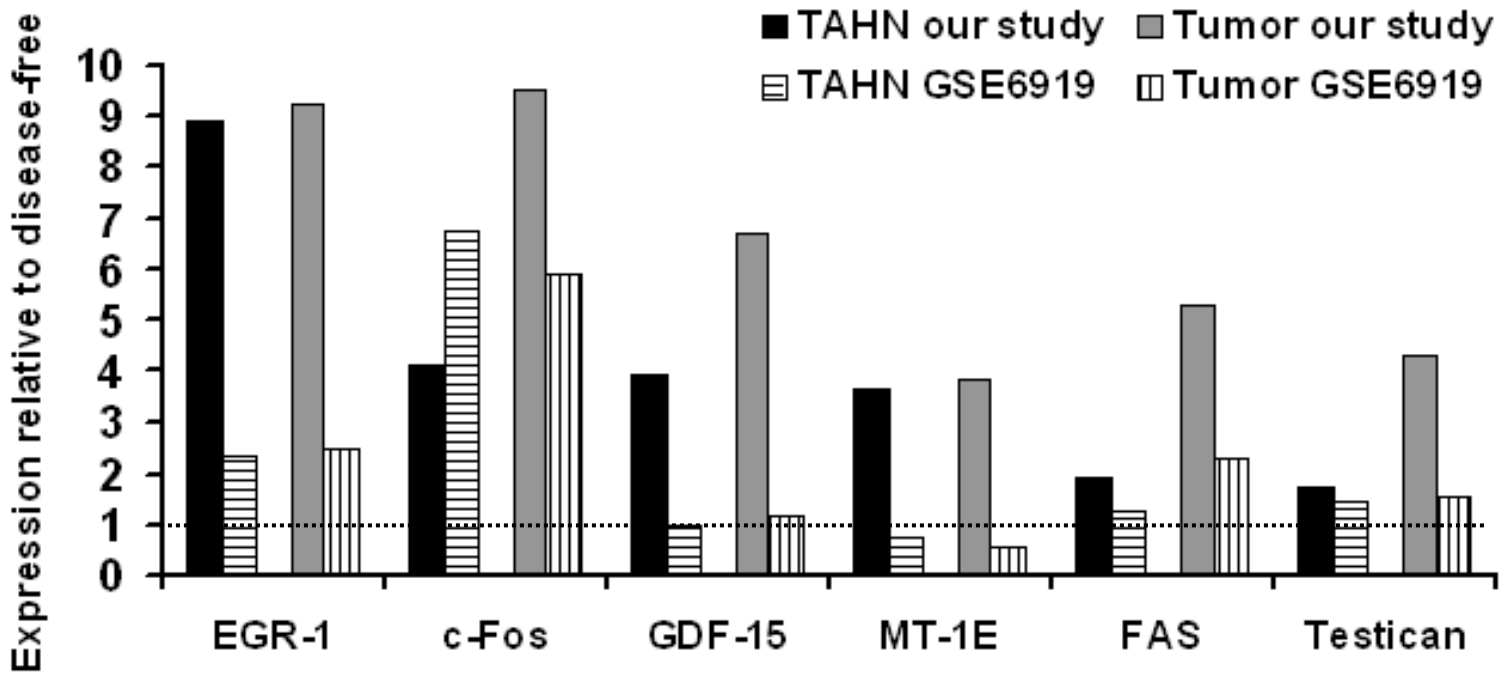
TAHN our study
Tumor our study
TAHN GSE6919
Tumor GSE6919
Expression relative to disease-free
10
9
8
7
6
5
4
3
2
1
0
EGR-1
c-Fos
GDF-15
MT-1E
FAS
Testican

Table I. Description of prostate samples used in this study. The cohort consisted of (i) 12 tumor and matched tumor adjacent histologically normal (TAHN) human tissues collected at the University of New Mexico Health Sciences Center and (ii) 6 normal, cancer-free prostates obtained from the Cooperative Human Tissue Network.

Sample	Patient's Age	Gleason Score[1]	TNM Stage[1]
Tumor/TAHN			
1	58	3+3	T3/III
2	57	3+3	T2/II
3	71	3+4	T3 N0/III
4	64	3+3	T2a N0/II
5	53	3+3	T2c N0/II
6	57	3+4	T2c N0/II
7	51	3+4	T2c/II
8	60	3+4	T2a N0/II
9	50	3+3	T2c N0/II
10	55	3+3	T2c/II
11	64	3+3	T2 N0/II
12	53	3+4	T2c/II
Normal			
13	46	na[2]	na
14	55	na	na
15	43	na	na
16	79	na	na
17	26	na	na
18	43	na	na

[1] Tumor Nodes Metastasis (TNM) stage was assigned using criteria published by the American Joint Committee on Cancer (http://www.cancerstaging.org/index.html). Gleason scores and Stages were determined from the prostatectomy samples.

[2] Not applicable.

Table II. Primers used for qRT-PCR validation of microarray experiments.

Gene	Forward Primer (5'-3')	Reverse Primer (5'-3')	Product (basepairs)
Gene of Interest			
EGR-1	GAGCAGCCCTACGAGCAC	AGCGGCCAGTATAGGTGATG	130
FAS	AGAACTTGCAGGAGTTCTGGGACA	TCCGAAGAAGGAGGCATCAAACCT	149
Testican	TGGAACCGCTTTCGAGACGATGAT	CACACACTTTGTGAGGGCTGCATT	124
TTP	GTTACACCATGGATCTGACTGCCA	AGTCCCTCCATGGTCGGATGG	86
TIMP2	TGCAATGCAGATGTAGTGATCAGGGC	GGGTTGCCATAAATGTCGTTTCCAG	80
SOD2	AGCATGTTGAGCCGGGCAGTGT	TGCTTCTGCCTGGAGCCCAGATAC	74
Loading Control			
TBP	CACGAACCACGGCACTGATT	TTTTCTTGCTGCCAGTCTGGAC	112
GAPDH	ACCACAGTCCATGCCATCAC	TCCACCACCCTGTTGCTGTA	70

Table III. Cy3/Cy5 fluorescent dye bias control microarray hybridization compared to experimental set using tumor and matched tumor adjacent histologically normal (TAHN) tissues.

	TAHN	**Tumor**	**Cy3/Cy5 Dye Bias Test**
Mean[1] ± SD	1.58 ± 0.61	1.63 ± 0.75	1.27 ± 0.35
Median	1.49	1.51	1.22
Coefficient of Variation (%)[2]	38.6*	46.1*	27.3

[1] Mean ± standard deviation (SD) for all transcripts detected.

[2] * denotes significant difference ($p<0.05$) from Cy3/Cy5 dye bias test.

Table IV. Top 40 transcripts mutually up-regulated in tumor and corresponding matched tumor adjacent histologically normal (TAHN) tissues compared to normal cancer-free prostatic tissues.

Gene ID[1]	Gene Description	TAHN[2]	Tumor[2]
H200019156	**Early growth response protein 1 (EGR-1)[3]**	**8.92[4]**	**9.27**
H200003548	Proto-oncogene protein c-Fos	4.13[4]	9.50
H200009720	Growth/differentiation factor 15 (GDF-15), macrophage inhibitory cytokine-1 (MIC1)	3.96[4]	6.68
H300013105	ETS-domain protein ELK-4	3.70[4]	3.28
H200005926	Metallothionein-1E (MT-1E)	3.68[4]	3.86
H300013389	Copine IV	3.62[4]	3.43
H300011237	Ergic-53-like protein precursor	3.37[4]	3.43
H300020290	Molecule possessing ankyrin repeats induced by lipopolysaccharide	3.09[4]	5.33
H300017466	Early response protein NAK1, TR3 orphan receptor	2.94[4]	4.03
H200000319	Aminopeptidase N	2.85[4]	5.85
H200019945	**Tristetraprolin (TTP)[3]**	**2.75[4]**	**5.81**
H300015296	Casein kinase I (CK1)	2.66	3.77
H200000676	Transcription factor Jun-D	2.64	3.45
H200006111	BTG2 protein	2.60	3.40
H200012441	Glandular kallikrein 1 precursor	2.58	4.06
H200020421	Paired immunoglobulin-like receptor beta	2.54	3.36
H300005679	Calreticulin precursor (CRP55), calregulin	2.45	4.79
H300014629	Tumor protein D52	2.43	3.88
H300022633	Similar to postmeiotic segregation increased 2-like 5	2.42	3.83
H300014182	Neprilysin	2.41	4.34
H300012307	Vascular endothelial growth factor A precursor (VEGF-A)	2.37	3.32
H300015765	Colorectal mutant cancer protein (MCC protein)	2.31	3.25
H300016106	Transcription factor EB	2.24	3.19
H300021922	Ubiquitin-protein ligase NEDD4-like	2.23	5.52
H300014306	HTPAP protein	2.23	4.08
H200014240	Poliovirus Receptor related protein (CD112 antigen)	2.10	3.71
H300004950	Claudin-4	1.97	4.09
H300017343	**Fatty acid synthase (FAS)[3]**	**1.93**	**5.31**
H200017342	Prostein protein	1.92	3.56
H300005700	Keratin, cytokeratin 8 (CK 8)	1.90	3.31
H300012280	Prostate specific antigen (PSA) precursor, kallikrein 3	1.89	3.15
H200003843	Diamine acetyltransferase	1.87	6.63
H300016780	Dolichyl-diphosphooligosaccharide-protein glycosyltransferas, 63 KD subunit	1.86	3.27
H200006197	NDRG1 protein	1.86	3.48
H300016292	Ubiquitin-conjugating enzyme E2-like	1.83	3.24
H200013682	X box binding protein-1 (XBP-1)	1.82	5.12
H300014868	KIAA0220-like protein (similar to nuclear pore complex interacting protein)	1.77	3.54
H300004833	**Testican (SPOCK-1)**	**1.73**	**4.29**
H200019551	Sialidase 1 precursor	1.72	5.40

[1] Gene identification number according to the Ensembl Human 13.31 Database (http://www.ensembl.org/).

[2] Cy3/Cy5 ratios of tumor or TAHN (Cy3) compared to cancer-free normal (Cy5) tissues.

[3] The 4 transcripts evaluated by qRT-PCR (Figure 3) are in bold.

[4] The shaded area represents transcripts above the 2xSD of the mean in TAHN tissues.

Appendix C

Int. J. Cancer: **119,** 108–116 (2006)

Telomere DNA content and allelic imbalance demonstrate field cancerization in histologically normal tissue adjacent to breast tumors

Christopher M. Heaphy[1], Marco Bisoffi[1,2], Colleen A. Fordyce[1], Christina M. Haaland[1], William C. Hines[1], Nancy E. Joste[2,3] and Jeffrey K. Griffith[1,2]*

[1]*Department of Biochemistry and Molecular Biology, University of New Mexico School of Medicine, Albuquerque, NM, USA*
[2]*Cancer Research and Treatment Center, University of New Mexico School of Medicine, Albuquerque, NM, USA*
[3]*Department of Pathology, University of New Mexico School of Medicine, Albuquerque, NM, USA*

Cancer arises from an accumulation of mutations that promote the selection of cells with progressively malignant phenotypes. Previous studies have shown that genomic instability, a hallmark of cancer cells, is a driving force in this process. In the present study, two markers of genomic instability, telomere DNA content and allelic imbalance, were examined in two independent cohorts of mammary carcinomas. Altered telomeres and unbalanced allelic loci were present in both tumors and surrounding histologically normal tissues at distances at least 1 cm from the visible tumor margins. Although the extent of these genetic changes decreases as a function of the distance from the visible tumor margin, unbalanced loci are conserved between the surrounding tissues and the tumors, implying cellular clonal evolution. Our results are in agreement with the concepts of ''field cancerization'' and ''cancer field effect,'' concepts that were previously introduced to describe areas within tissues consisting of histologically normal, yet genetically aberrant, cells that represent fertile grounds for tumorigenesis. The finding that genomic instability occurs in fields of histologically normal tissues surrounding the tumor is of clinical importance, as it has implications for the definition of appropriate tumor margins and the assessment of recurrence risk factors in the context of breast-sparing surgery.

Key words: telomere loss; allelic imbalance; genomic instability; cancer field effect; breast cancer

Genomic instability is an important factor in the progression of human cancers.[1–4] One mechanism that underlies genomic instability is loss of telomere function.[5–7] Telomeres are nucleoprotein complexes located at the ends of eukaryotic chromosomes. Telomeres in human somatic cells are composed of 1,000 to 2,000 tandemly repeated copies of the hexanucleotide DNA sequence, TTAGGG.[8] Numerous telomere binding proteins are associated with these repeat regions and are important for telomere maintenance.[9,10] Telomeres stabilize chromosome ends and prevent them from being recognized by the cell as DNA double-strand breaks, thereby preventing degradation and recombination.[11] However, telomeres can be critically shortened, and thereby become dysfunctional, by several mechanisms, including incomplete replication of the lagging strand during DNA synthesis,[12] loss or alterations of telomere-binding proteins involved in telomere maintenance,[13] and oxidative stress leading to DNA damage.[14] Alternatively, telomere loss may be compensated for by recombination[15,16] or, as seen in the majority of human cancers, by the enzyme telomerase.[17,18]

Telomeres in tumors are frequently shorter than in the matched adjacent normal tissues, presumably reflecting their extensive replicative histories.[19–21] The cause-and-effect relation between dysfunctional telomeres and genomic instability implies that shortened telomeres are also associated with altered gene expression. The latter is a primary source of phenotypic variability, which in turn drives the development of cell clones displaying progressively malignant traits, such as the potential for invasion and metastasis.[22] In agreement with this sequence of events, we and others have shown that telomere length, or its surrogate, telomere DNA content (TC), predicts the course of disease in several different malignancies, including leukemias,[23] non-small cell lung cancers,[24] neuroblastomas,[25] prostatic adenocarcinomas,[26–28] and breast carcinomas.[29,30]

Recently, Meeker and colleagues observed that telomere length abnormalities are early and frequent events in the malignant transformation of several types of cancer, including breast.[27,31,32] In addition, telomere attrition and other measures of genomic instability, such as allelic imbalance (AI) and loss of heterozygosity, demonstrate that genomic instability occurs within atypical breast hyperplasias,[33–35] histologically normal tissue proximal to breast tumors,[36–42] and, in some instances, breast tissue from women with benign breast disease.[43] Loss of heterozygosity and AI have also been found in the stromal compartment of cancer-associated breast tissues.[41,44] In addition, our own recent results identified fields of telomerase-positive cells within histologically normal tissues adjacent to breast tumors that could represent areas of premalignant cell populations.[45] Similarly, we have recently reported on the occurrence of telomere attrition in histologically normal prostatic tissue proximal to prostate adenocarcinomas.[28] These data imply that there is a reservoir of genetically unstable cell clones within histologically normal breast and prostate tissues that may represent fertile ground for tumor development. The origin and extent of this reservoir are presently undefined. However, the existence of fields of genetically altered cells, appearing histologically normal and disease-free, is consistent with the hypothesis that genomic instability arises early in breast tumorigenesis.

The primary goal of the present study was to define the extent and spatial distribution of genomic instability in histologically normal tissues surrounding breast tumors. A secondary goal was to investigate the relationship between genetic alterations in tumors and matched tumor-adjacent histologically normal (TA-HN) tissues. Towards these ends, two independent, yet conceptually linked markers of genomic instability, TC and AI, were investigated in two independent cohorts of breast tumors and their matched TA-HN tissues. One cohort represented a controlled study with tumors and matched TA-HN tissues excised at sites 1 and 5 cm from the tumor margins. The second cohort consisted of archival tumor specimens and matched TA-HN tissues excised at unknown distances from the tumor margin. Our results show that breast tumors reflect the properties of the matched TA-HN breast tissues, including the conservation of unbalanced alleles. Furthermore, our results support the hypothesis that fields of histologically normal, but genetically unstable cells provide a fertile ground for tumorigenic events in breast tissues.

Materials and methods

Breast tissue samples

Four independent cohorts of human breast tissues were used in this study. The characteristics of each of these cohorts are sum-

***Correspondence to:** Department of Biochemistry and Molecular Biology, MSC08 4670, 1 University of New Mexico, Albuquerque, NM, 87131-0001, USA. Fax: +1-505-272-6587.
E-mail: jkgriffith@salud.unm.edu
C.A. Fordyce's current address is Department of Pathology, University of California at San Francisco, San Francisco, CA, USA.
Grant sponsor: DOD BCRP grants; Grant numbers: DAMD-17-01-1-0572, DAMD 17-00-1-0370, DAMD17-02-1-0514; Grant sponsor: NIH grants; Grant numbers: R25 GM60201, T34 GM08751.
Received 17 August 2005; Accepted after revision 9 December 2005
DOI 10.1002/ijc.21815
Published online 31 January 2006 in Wiley InterScience (www.interscience.wiley.com).

TABLE I – CLINICAL CHARACTERISTICS OF TUMOR COHORTS

Cohort	*N*	Age at Dx[1]			Dx[1]			Size[2]		Node[3]		TNM Stage						
		Range	Median	Mean	IDC	LC	DCIS	S	L	N	P	n/av	I	IIA	IIB	IIIA	IIIB	IV
1	12	26–61	53	49	10	1	1	n/av		2	10	2	0	3	2	2	3	0
2	38	35–75	48	50	36	2	0	4	32	7	29	2	2	5	14	11	0	2
3	48	31–89	54	56	44	4	0	8	40	19	29	0	11	13	15	8	1	0
4 (Normal)	20	15–48	30	29	n/a	n/a	n/a	n/a		n/a		n/a						

TNM, Tumor-Nodes-Distant Metastasis; n/a, not applicable; n/av, not available.
[1]Dx, Diagnosis of invasive ductal carcinoma (IDC), lobular carcinoma (LC), ductal carcinoma in situ (DCIS).–[2]S = small (≤2 cm), L = large (>2 cm).–[3]N = negative, P = positive.

marized in Table I. The first cohort consisted of 12 full mastectomy cases obtained consecutively from the University of New Mexico (UNM) Hospital Surgical Pathology Laboratory in 2003 and 2004. Approximately 500 mg of tissue was excised from the tumors and sites 1 and 5 cm from the visible tumor margins. After resection, the tissues were immediately frozen in liquid nitrogen. Sections (10–12 μm) were prepared and stained with hematoxylin and eosin by the Human Tissue Repository Service of the UNM Department of Pathology. The sections were examined microscopically to define their histological status. In addition, serial sections of the breast tumors were collected and stored at −70°C until used for isolation of genomic DNA.

The second cohort was provided by the New Mexico Tumor Registry (NMTR) and consisted of 38 archival, paraffin-embedded ductal or lobular carcinomas and matched, histologically normal breast tissues from women who had undergone radical mastectomies or lumpectomies between 1982 and 1993. The histologically normal breast tissues originated from different blocks than the tumor tissues and were obtained at the time of dissection from sites outside the visible tumor margins. Generally, the sections were selected to contain high epithelial cell fractions.

The third cohort was obtained from the University of New Mexico Solid Tumor Facility and consisted of 48 frozen archival invasive ductal or lobular carcinomas from women who had radical mastectomies or lumpectomies between 1982 and 1993. Unlike cohorts 1 and 2, matched, histologically normal breast tissues were not available for the tumors in cohort 3.

The fourth cohort was obtained from the National Cancer Institute Cooperative Human Tissue Network (Nashville, TN) and contained 20 normal, disease-free breast tissue samples from women undergoing reduction mammoplasty (NBRST-RM). In addition, peripheral blood lymphocytes (PBLs) were obtained from 59 women previously diagnosed with breast cancer. The women ranged in age from 25 to 74 years, with a mean of 53 years. All tissues used in this study were anonymous, and experiments were performed in accordance with all federal guidelines as approved by the University of New Mexico Health Science Center Human Research Review Committee.

TC assay

Telomere length measurements can be affected by both extraneous factors, such as tissue specimens' age and means of preservation and storage, and inherent properties, such as patients' ages and health status, and the organ sites from which the tissue specimens were collected. To minimize the confounding effects of extraneous factors, we previously described a slot blot method for titrating the TC in fresh, frozen or paraffin-embedded tissues up to 20 years old.[46,47] TC measured by this method is directly proportional to telomere length measured by Southern blot.[47] However, in contrast to Southern blotting, the TC assay can be performed with as little as 5 ng of genomic DNA,[46] and is insensitive to fragmentation of DNA to less than 1 kb in length.[47] Thus, there is excellent agreement between TC measured in paired tissues stored either frozen, or formalin-fixed in paraffin at room temperature.[28,30] Therefore, TC is a sensitive and convenient proxy for telomere length, particularly for applications where genomic DNA is fragmented or scant, such as in sections of archival, paraffin-embedded tissues comprising the second cohort of breast tumors, which contains specimens that are over 20 years old.

TC was measured as described previously.[46] Briefly, DNA was isolated from frozen or paraffin-embedded tissues and blood samples, using Qiagen DNeasy Tissue kits (Qiagen, Valencia, CA) and the manufacturer's protocols. DNA was denatured at 56°C in 0.05 M NaOH/1.5 M NaCl, neutralized in 0.5 M Tris/1.5 M NaCl, and applied and UV cross-linked to Tropilon-Plus blotting membranes (Applied Biosystems, Foster City, CA). A telomere-specific oligonucleotide, end-labeled with fluorescein, (5′-TTAGGG-3′)$_4$-FAM (IDT, Coralville, IA), was hybridized to the genomic DNA, and the membranes were washed to remove nonhybridizing oligonucleotides. Hybridized oligonucleotides were detected by using an alkaline phosphatase-conjugated anti-fluorescein antibody that produces light when incubated with the CDP®-Star substrate (Applied Biosystems, Foster City, CA). Blots were exposed to Hyperfilm® for 2–10 min (Amersham Pharmacia Biotech, Buckinghamshire, UK) and digitized by scanning. The intensity of the telomere hybridization signal was measured from the digitized images, using Nucleotech Gel Expert Software 4.0 (Nucleotech, San Mateo, CA). TC is expressed as a percentage of the average chemiluminescent signal of three replicate tumor DNAs compared to the same amount of a placental DNA standard (typically 20 ng). In addition to placental DNA, DNA purified from HeLa cells, which has approximately 30% of placental TC was frequently included to confirm the reproducibility of the assay.

AI assay

DNA (approximately 1 ng) was amplified using the AmpFlSTR Identifiler PCR Amplification Kit (Applied Biosystems, Foster City, CA), using the manufacturer's protocol. Each multiplex PCR reaction amplifies 16 short tandem repeat (STR) microsatellite loci from independent locations in the genome (Amelogenin, CSF1PO, D2S1338, D3S1358, D5S818, D7S820, D8S1179, D13S317, D16S539, D18S51, D19S433, D21S11, FGA, TH01, TPOX and vWA). Each of the PCR primers is labeled with one of four fluorescent dyes (6-FAM, PET, VIC and NED), each with a unique emission profile, allowing the simultaneous resolution of 16 amplicons of similar size. PCR products were resolved by capillary gel electrophoresis and detected using an ABI Prism 377 DNA Sequencer (Perkin Elmer, Foster City, CA). The height of each fluorescence peak in the electropherograms was quantitated using the ABI Prism GeneScan and Genotype Analysis software (Applied Biosystems, Foster City, CA) and a ratio of the peak heights of each pair of heterozygous allelic amplicons was calculated. By convention, the allele with the greater fluorescence intensity was designated the numerator. Thus, the ratio was always ≥1.0, with 1.0 representing the theoretical ratio for normal alleles.

Statistical analysis

Statistical analyses were performed using the JMP® statistical package (SAS Institute, Cary, NC), choosing a significance level of 0.01. The nonparametric two-sided Wilcoxon/Kruskal–Wallis log rank test was used to determine the comparative distribution of TC and AI in the breast tumor and TA-HN tissue specimens, as well as associations between TC and AI in the paraffin-embedded breast tumor samples of cohort 2.

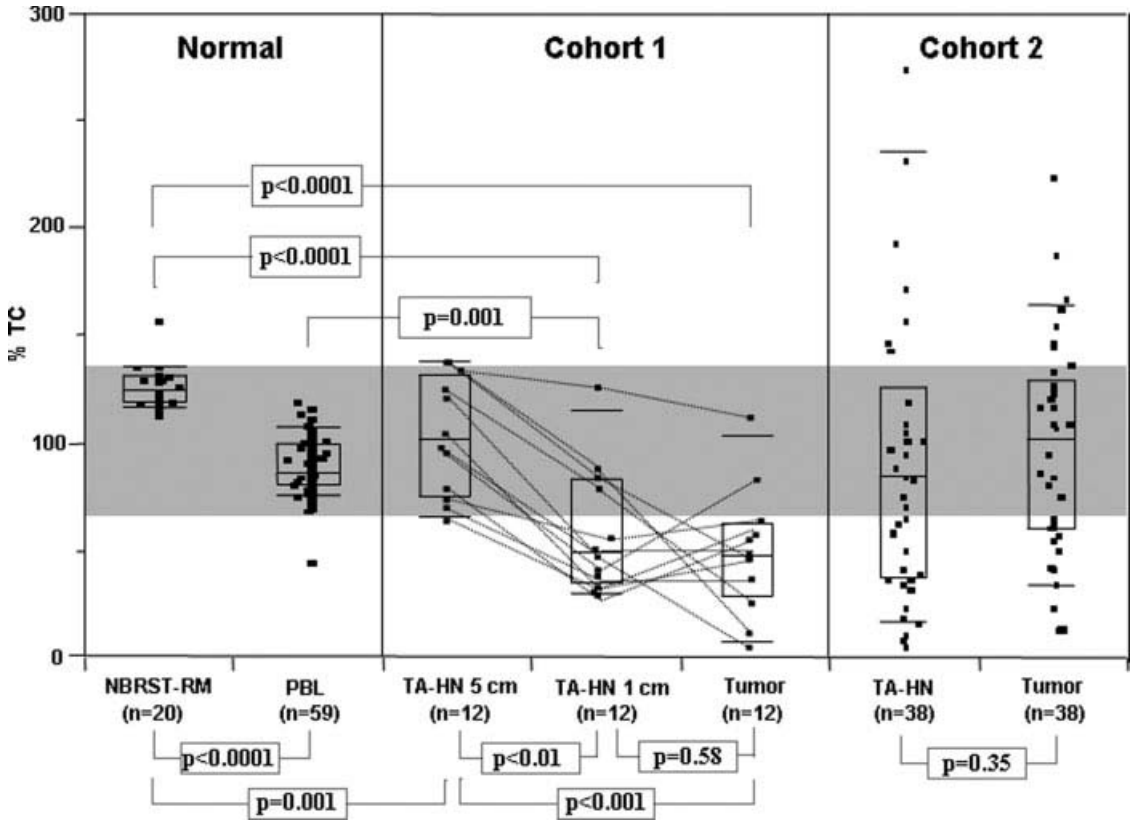

Figure 1 – Distribution of telomere DNA content (TC) in disease-free normal breast tissues from reduction mammoplasties (NBRST-RM), in peripheral blood lymphocytes (PBL), and in the breast tumor cohorts 1 and 2, including their tumor-adjacent histologically normal (TA-HN) tissues. TA-HN was excised at 1 and 5 cm from the tumor margin in cohort 1, and at unknown distances from the tumor margin in cohort 2. The number of tissues analyzed is indicated (*n*). TC is expressed as percentage of TC in placental control. The boxes represent group median (line across middle) and quartiles (25th and 75th percentiles) at its ends. Lines below and above boxes indicate 10th and 90th percentiles, respectively. In cohort 1, TC values of the individual matched samples are connected by thin lines. The gray shaded area indicates 95% of TC measurement for all normal specimens (NBRST-RM and PBLs). The *p*-values indicate comparisons between different tissue cohorts calculated by the two-sided Wilcoxon Kruskal/Wallis rank sums test. Additional statistical comparisons are mentioned in the text. *Note:* (i) Although the data points are horizontally shifted, some are still overlapping, and therefore not visible; (ii) due to the scale of the figure, two data points at values of 404% and 480% in the TA-HN set of cohort 2 are not shown.

Results

TC in normal breast tissues

To define the normal range of TC in disease-free breast tissues, the TC, a proxy for telomere length,[46,47] was measured in normal breast tissues obtained from 20 women (mean age 29) undergoing reduction mammoplasty (NBRST-RM). TC ranged from 114% to 158%, with a mean of 127% and a median of 126%, of TC in the placental DNA standard (Fig. 1). The interquartile variation (IQR), a statistical measure of the dispersion of the data, was only 12%, indicating little variation in telomere length in normal breast tissue. For comparison, TC was also measured in PBLs from 59 women (mean age 53) with a previous diagnosis of breast cancer. TC in PBLs ranged from 46% to 120%, with a mean of 90%, a median of 87% and an IQR of 19%, of the standard. The mean TC in normal breast was significantly higher than mean TC in PBLs ($p > 0.0001$). However, greater than 95% of all normal specimens (NBRST-RM and PBLs) had TC values within 70–137% of the standard. This range is interpreted to include the effects of all extraneous and inherent factors on observed TC in normal tissue, including age, tissue site, sample source and experimental variation.

Histology of cancerous and adjacent histologically normal breast tissues

The histologies of the tissues comprising two representative cases from the two independent cohorts of breast tumor tissues and matched tumor adjacent histologically normal (TA-HN) tissues are shown in Figure 2. The first cohort was composed of 12 sets of breast tumor tissues and TA-HN tissues excised 1 cm (TA-HN-1) and 5 cm (TA-HN-5) from the tumor margins. Frozen sections were stained with hematoxylin and eosin and examined microscopically. Sections of the tumors contained variable amounts of infiltrating carcinoma and ductal carcinoma *in situ* (Fig. 2*A* and 2*D*). In contrast, both TA-HN-1 and TA-HN-5 tissues had normal architecture, lobular units, ducts, and adipose tissue (Fig. 2*B*, 2*C* and 2*E*, 2*F*, respectively). Unlike the first cohort, which was composed of snap frozen tissues derived from contemporary mastectomies, the second was composed of paraffin-embedded archival tissues derived from women who had radical mastectomies or lumpectomies between 1982 and 1993. Fig. 2 shows two representative pairs of hematoxylin and eosin stained tumor (Fig. 2*G* and 2*I*) and TA-HN tissues (Fig. 2*H* and 2*J*). Infiltrating carcinoma can be seen in the tumors, while the TA-HN tissues show normal lobular architecture. Although tumor and TA-HN tissues comprising the second cohort came from different paraffin blocks, and the TA-HN tissues were obtained from sites outside the visible tumor margins, the exact distances between the sites of the TA-HN tissues and the tumors' margins are not known.

TC in tumor and adjacent histologically normal breast tissues

The spatial distribution of TC was examined in the 12 groups of breast tissues comprising the first cohort and compared with TC in the normal, disease-free breast tissues from radical mastectomy (Fig. 1). The mean TC values in the TA-HN-5 and TA-HN-1 tissues

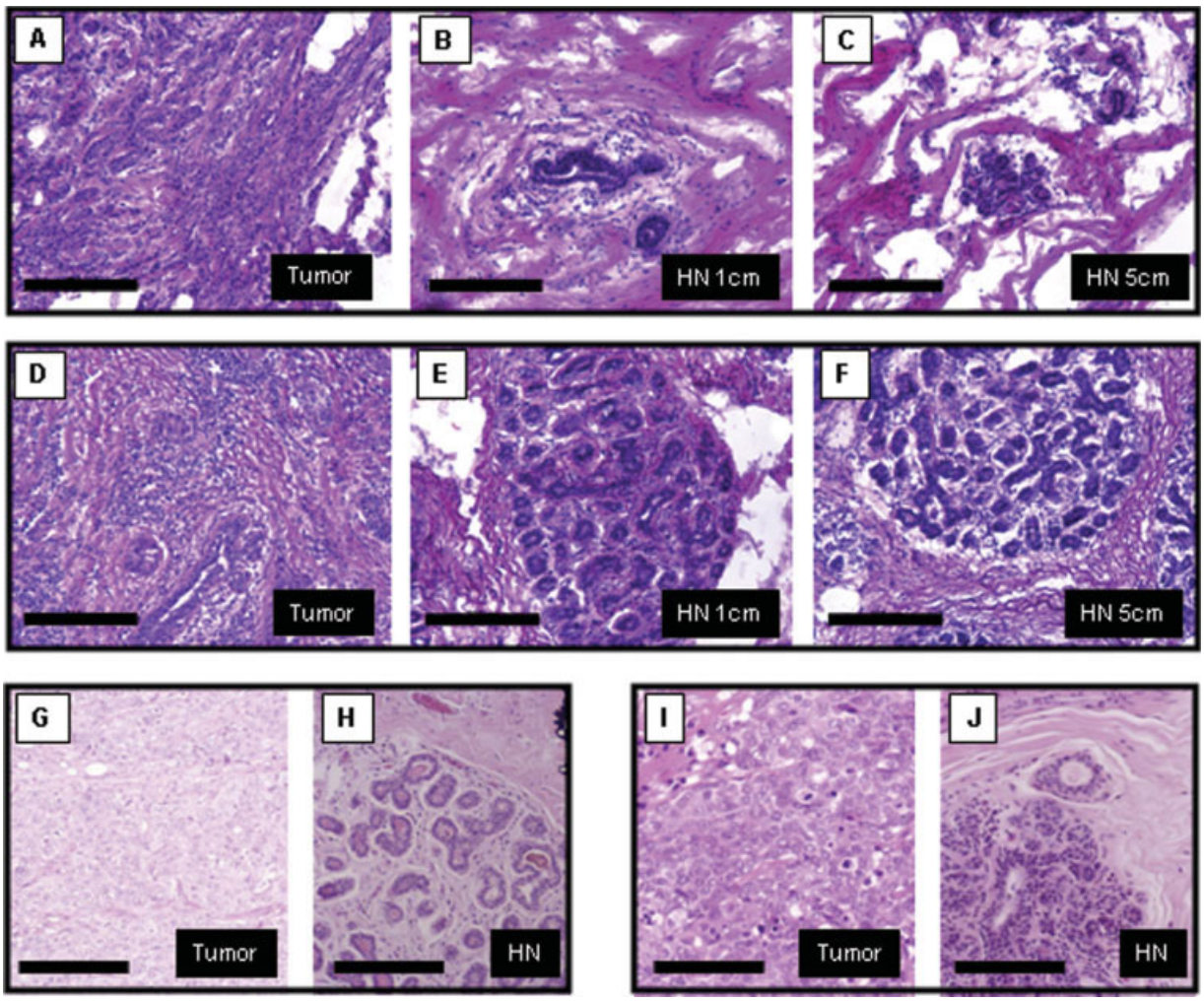

FIGURE 2 – Hematoxylin and eosin staining of human breast tissue sample sections. Two representative cases from the first (*A–F*) and second (*G–J*) cohorts are shown. Abnormal architecture with fields of infiltrating ductal carcinoma and ductal carcinoma *in situ* are seen in the tumor sections (A, D, G and I). Normal lobular and ductal architecture and adipose tissue are seen in the tumor-adjacent tissues at the indicated distance from the visible tumor margin (first cohort: B, C and E, F), or at unknown distances (second cohort: H and J). HN, histologically normal tissue; bars represent 200 μm.

were 101% and 66% of TC in the normal placental DNA standard, respectively. The mean TC value in tumors was 59%. Although the mean TC in TA-HN-5 tissues was significantly less than in NBRST-RM tissues ($p = 0.001$), it was not significantly different than the mean TC in PBLs from women of similar age ($p = 0.16$). Moreover, TC values in each of the TA-HN-5 tissues were within the range that defined >95% of all normal tissues. Since telomere length decreases with age,[48,49] it is likely that the difference between TC in the normal and TA-HN-5 tissues is due to the different ages of the two groups of women (27 *vs.* 49 years).

In contrast, mean TC in TA-HN-1 tissues was significantly less than TC in NBRST-RM tissues ($p < 0.0001$) and PBLs ($p = 0.001$), and TA-HN-5 tissues ($p < 0.01$). Mean TC in tumors also was significantly less than those in NBRST-RM tissues ($p < 0.0001$), PBLs ($p < 0.0001$) and TA-HN-5 tissues ($p < 0.001$). However, mean TC in tumor and TA-HN-1 tissues was indistinguishable ($p = 0.58$). Consistent with these findings, TC was, on average, 35% lower in each TA-HN-1 sample than in the paired TA-HN-5 sample, while the differences in TC between the TA-HN-1 and matched tumor specimens were varied, encompassing decrease, stabilization, and increase of TC with an average change of only 3% (lines in middle panel of Fig. 1). In total, TC values in 8 of 12 specimens of TA-HN-1 and 10 of 12 specimens of paired tumor tissues were outside the range that defined >95% of all normal tissues (NBRST-RM and PBLs).

Similarly, TC distribution was examined in a second, independent cohort (Fig. 1). Although the distributions of TC values in the 38 matched pairs of TA-HN and tumor tissues were broader than those measured in the first cohort (IQR = 88% and 69%, respectively), 16 of 38 TA-HN and 14 of 38 tumor specimens, respectively, had TC values less than those found in NBRST-RM tissues and PBLs, and only 9 of 38 TA-HN and 7 of 38 tumor specimens had TC values exceeding those found in all normal tissues (NBRST-RM and PBLs). A similar TC distribution was observed in a third collection of 48 frozen breast tumors (Table II), and in a collection of archival tumor and matched TA-HN prostate tissues, each collected between 1982 and 1993.[28] As observed in the comparison between tumor and TA-HN-1 specimens in the first cohort, there was no difference in mean TC in tumors and TA-HN tissues ($p = 0.35$). However, there was greater heterogeneity in the samples of the second as compared to the first cohort. Nevertheless, data from both cohorts are consistent with the conclusion that significant telomere attrition, comparable to that observed in tumors, occurs in TA-HN breast tissue. Significant telomere attrition (to a level outside the range seen in >95% of all normal tissues) occurred (i) in almost 50% (24/50) of TA-HN-1 and TA-HN

specimens, (ii) at sites at least 1 cm from the tumors' margins, and (iii) since TC is measured in bulk tissue that has not been microdissected, in a substantial fraction of the cells in the samples.

AI in tumor and adjacent histologically normal breast tissues

To investigate the extent of genomic instability in cohorts 1 and 2, tumor and TA-HN tissues were screened for AI at 16 unlinked microsatellite loci. Unlike the TC assay, which utilizes a slot blot methodology to titrate the quantity of telomere DNA in a defined amount of genomic DNA, the AI is defined by the ratio of the peak heights of allelic amplicons after PCR. Thus, it is unlikely that inherent or extrinsic factors that affect measurement of TC would similarly affect the determination of AI. To establish a baseline for the incidence of AI in normal breast tissue, 201 heterozygous loci in the 20 specimens of NBRST-RM tissues were analyzed by this approach. The mean peak height ratio was determined to be 1.18 (SD = 0.166). On the basis of these values, a highly conservative, operational definition of AI was established as a ratio of peak heights $\geq$1.68, *i.e.*, the mean + 3.0 SD. This threshold excluded more than 99% of the allelic ratios observed in the NBRST-RM tissues, and established a baseline incidence of 0.1 unbalanced loci per specimen of normal breast tissue. As shown in Figure 3, a virtually identical value, 0.08 loci per specimen, was measured in the TA-HN-5 tissues. In contrast, the mean numbers of unbalanced loci in the TA-HN-1 and tumor tissues were 0.42 and 1.25 loci per specimen, respectively, approximately 5 and 15 times higher than the incidence in the TA-HN-5 tissues. The baseline incidence of 0.1 unbalanced loci per specimen predicts that approximately 10% and 1% of normal tissues will have one and two unbalanced loci, respectively. Consistent with this prediction, 3 of 20 and 1 of 12 NBRST-RM and TA-HN-5 tissues, respectively, had one site of AI. Only one of more than 120 normal samples we have analyzed to date had 2 unbalanced loci, and none had more than 2 unbalanced loci. Accordingly, neither the NBRST-RM nor the TA-HN-5 specimens had more than one unbalanced locus. In contrast, one TA-HN-1, and 5 tumor tissues had 2 or more unbalanced loci. These data are consistent with the conclusion drawn from the TC analysis that both tumors and TA-HN-1 tissues are genetically distinct from TA-HN-5 tissue, and that both are genetically unstable.

TABLE II – TC VALUES IN NORMAL, TUMOR AND TUMOR ADJACENT, HISTOLOGICALLY NORMAL (TA-HN) TISSUES[1]

	N	Median	Mean	Min	Max	IQR
Normal tissues						
NBRST-RM	20	126	127	114	158	12
PBL	59	87	90	46	120	19
Cohort 1						
TA-HN-5	12	100	101	70	128	44
TA-HN-1	12	59	66	43	119	38
Tumor	12	57	59	24	108	27
Cohort 2						
TA-HN	38	85	106	6	480	88
Tumor	38	102	98	14	224	69
Cohort 3						
Tumor	48	105	118	65	247	60

IQR, interquartile range; NBRST-RM, normal breast tissue from reduction mammoplasty; PBL, peripheral blood lymphocytes.
[1]Data from Figure 1.

This conclusion is further supported by results obtained with the second cohort. Microsatellite alleles were successfully amplified in 23 pairs of the 38 samples. As with the TC determinations, the distribution of the numbers of unbalanced loci was much broader in the second cohort than in the first. The mean numbers of unbalanced loci in the TA-HN tissues and matched tumors were 2.61 and 2.48 loci per specimen, respectively (Fig. 3). The mean numbers of unbalanced loci in TA-HN and tumor tissues were significantly greater than the numbers in either NBRST-RM or TA-HN-5 tissues ($p < 0.01$). The extent of AI in the tumors and their matched TA-HN tissues of the second cohort were indistinguishable ($p = 0.88$). Significantly, 74% (17/23) of TA-HN tissues and 70% (16/23) of matched tumors had 2 or more sites of AI, and 57% (13/23) and 40% (9/23), respectively, had 3 or more sites. Like the TC measurements, the independent measurement of AI, performed in two independent cohorts of paired breast tissues, indicates that at least 1 unbalanced locus is present (i) in more than 74% (26/35) of TA-HN-1 and TA-HN specimens, (ii) at sites at least 1 cm from the tumors' margins and (iii) since AI was measured in bulk tissue that was not microdissected, and the threshold for detecting AI requires that approximately 40% of the cells have lost the specific allele (see later), specific sites of AI are present in a substantial fraction of the cells.

Conservation of unbalanced alleles in tumor and adjacent breast tissues

To investigate the possibility that TA-HN and tumor tissues represented early and late stages, respectively, in the clonal evolution of the cancers, we measured the frequency of conservation of unbalanced loci in the 2 cohorts of paired tumor and TA-HN tissues. As shown in Figure 4, in the first cohort, 2 of the 6 (33%) sites of AI present in TA-HN tissues were conserved in the paired tumors (left panel). Likewise, in the second cohort, 21 of the 60

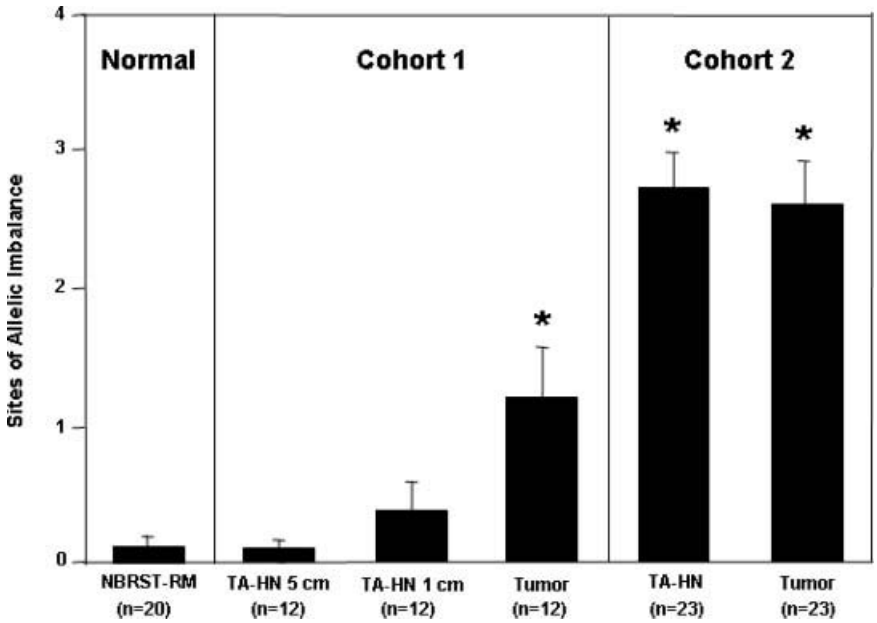

FIGURE 3 – Extent of allelic imbalance (AI) in disease-free normal breast tissues from reduction mammoplasties (NBRST-RM), and in the breast tumor cohorts 1 and 2, including their tumor-adjacent histologically normal (TA-HN) tissues. TA-HN was excised at 1 and 5 cm from tumor margin in cohort 1, and at unknown distances from the tumor margin in cohort 2. The number of tissues analyzed is indicated (*n*). The bars indicate the mean number of unbalanced loci ± standard errors. The stars indicate statistically significant differences ($p < 0.01$) from both NBRST-RM and TA-HN-5 (two-sided Wilcoxon Kruskal/Wallis rank sums test).

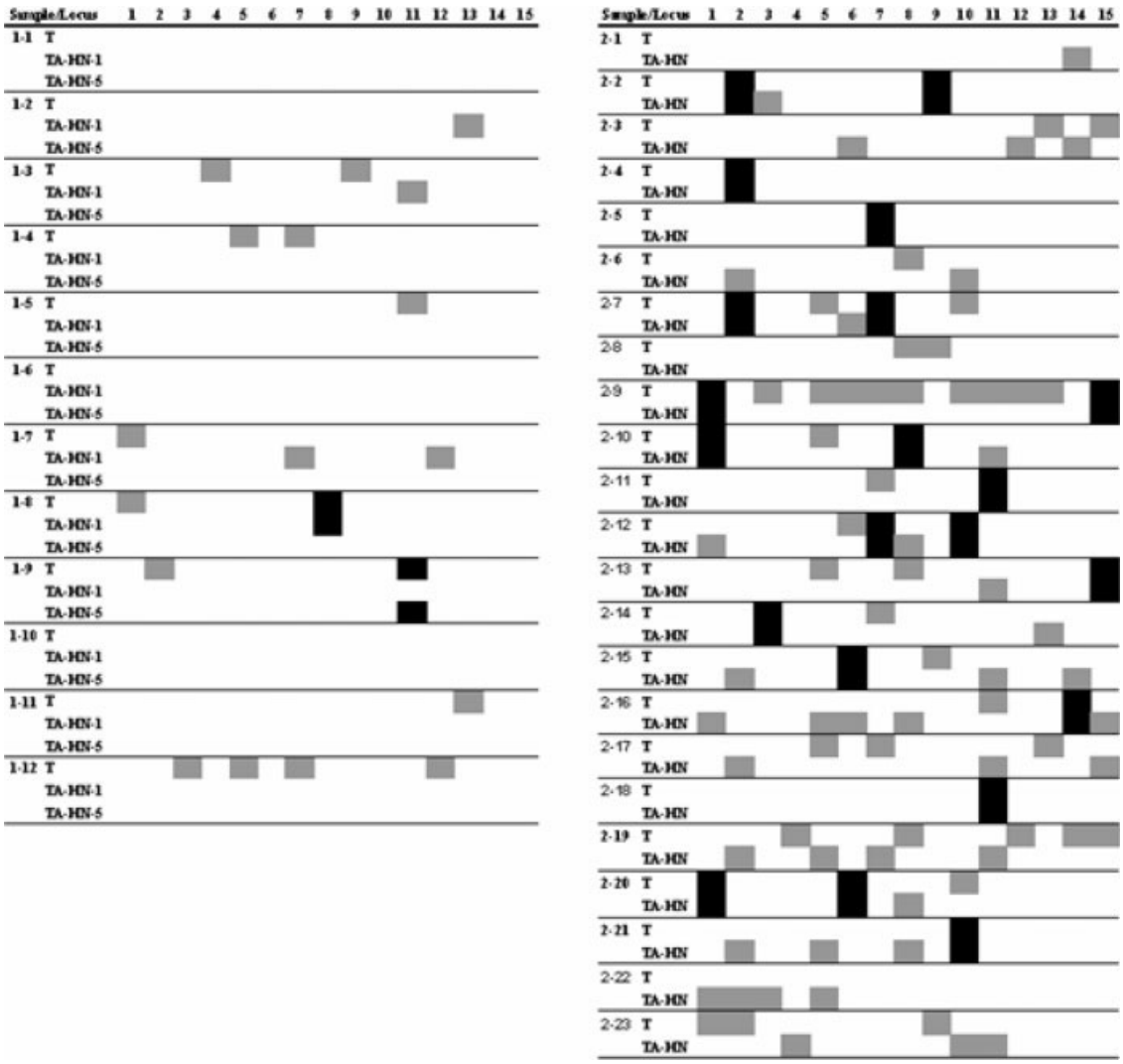

FIGURE 4 – Conservation of unbalanced alleles in matched tumor (T) and tumor-adjacent histologically normal (TA-HN) breast tissues of cohort 1 (left panel) and cohort 2 (right panel). Sites of allelic imbalances are indicated by gray boxes; sites of allelic imbalances conserved between tumor and TA-HN tissues are indicated by black boxes. The unlinked chromosomal loci are designated 1–15 and are as following (1) D8S1179, (2) D21S11, (3) D7S820, (4) CSF1PO, (5) D3S1358, (6) TH01, (7) D13S317, (8) D16S539, (9) D2S1338, (10) D19S433, (11) vWA, (12) TPOX, (13) D18S51, (14) D5S818, (15) FGA. *Note:* Homozygous amelogenin (all female samples) is not shown.

(35%) sites of AI present in TA-HN tissues were conserved in the paired tumors (right panel). The odds of this occurring by chance are estimated to be approximately 3×10^{-2} and 10^{-7} for the first and second cohorts, respectively.

Association between TC and AI in breast tumor tissues

Since telomere attrition is a source of genomic instability, and since we observed telomere attrition and increased AI in breast tumors, we determined the association between TC and AI (Fig. 5). For this analysis, microsatellite alleles were successfully amplified in 30 of the 38 breast tumor samples of cohort 2. Nonparametric 2-sided Wilcoxon/Kruskal–Wallis log rank analysis revealed a significant difference in TC in tumors with high ($\geq$3 sites) as compared to low ($\leq$2 sites) AI ($p = 0.002$).

Discussion

Although mechanistic insights into the molecular pathology of sporadic breast cancers are increasing, the question of how carcinogenesis is initiated in human breast tissues remains largely unanswered.[50–53] However, it is widely accepted that genomic instability is a prerequisite of virtually all tumors, including breast cancers, and that this instability facilitates the accumulation of further genetic alterations that result in cancer progression through clonal expansion of cells with a proliferative advantage.[1–3,51–53]

Two independent, quantitative measures of genomic instability, TC and AI, were used in this study to demonstrate that genomic instability occurs in histologically normal breast tissues adjacent to the corresponding tumors. These studies show that shortened telomeres (to a level outside the range seen in >95% of all normal tissues) and unbalanced allelic loci are present (i) in 50–75% of TA-HN and TA-HN-1 specimens, (ii) at sites at least 1 cm from the tumor margins and (iii) in a substantial fraction of the cells comprising the TA-HN tissue. This finding parallels our previous studies on tumors of the prostate and their matched TA-HN tissues,[28] and is in agreement with the work of previous investigators who reported that genetic alterations, including telomere attrition and loss of heterozygosity, occur in histologically normal tissues adjacent to breast tumors.[34–38,41–44] In these previous studies, the sites of telomere attrition, loss of heterozygosity and AI were physically distant from one another and from the tumors, albeit in most cases at undefined distances from the corresponding tumor lesions.[24,42–44] In contrast, and to our knowledge, the findings in cohort 1 represent the first

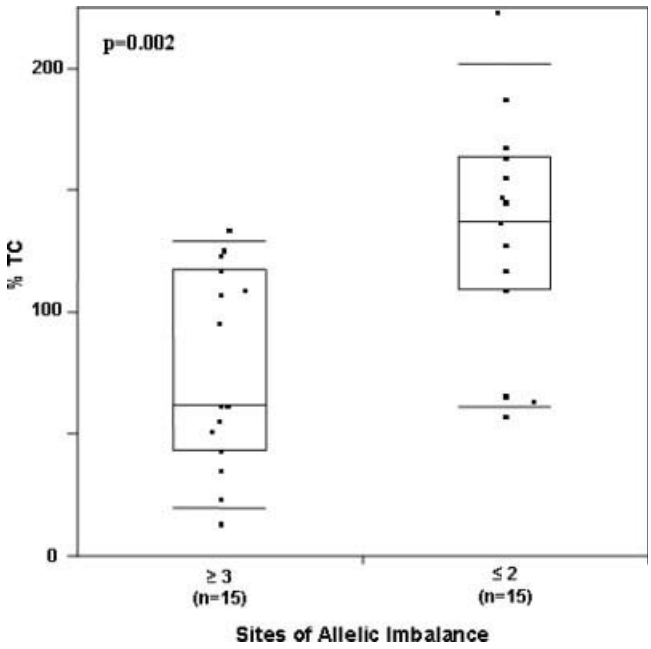

FIGURE 5 – Association between telomere DNA content and allelic imbalance in 30 breast tumor samples of cohort 2. The samples were dichotomized according to the number of genomic sites affected by allelic imbalance, i.e. ≥ 3 or ≤ 2 sites. The number of tissues analyzed is indicated (*n*). TC is expressed as percentage of TC in placental control. The boxes represent group median (line across middle) and quartiles (25th and 75th percentiles) at its ends. Lines below and above boxes indicate 10th and 90th percentiles, respectively. The nonparametric two-sided Wilcoxon/Kruskal–Wallis log rank test was used to assess the statistical significance of the difference between the means.

study in breast cancers that analyzes genomic instability at defined distances (1 and 5 cm) from the visible tumor margins. Consequently, this study reveals that genomic instability in tumor adjacent, histologically normal breast tissues is a function of distance from the tumor lesion, showing decreasing extent of genomic instability with increasing distance from the tumor margin. One explanation for these findings is that breast tumor cells exert a transforming effect on surrounding cells, leading to genetic alterations in adjacent tissues, as has been proposed for prostate cancer cells.[54,55] However, we prefer the alternate hypothesis, that breast epithelial carcinogenesis occurs at higher frequency in fields of cells with elevated genomic instability. This is supported by our observation that the occurrence of two independent markers of genomic instability, telomere attrition and unbalanced allelic loci, are highest in the tumor lesions and decrease with increasing distance from the tumor. In addition, analysis of tumors reveals an association between TC and extent of AI. Thus, we argue that telomere attrition induces genomic instability in breast tissues, and while this may not necessarily be apparent in histologically normal precancerous tissue, it is strongly displayed in tumor lesions.

Although similar conclusions can be drawn from the TC and AI analyses in each of the two cohorts, the range of TC values and the number of unbalanced loci per specimen were both greater in the second cohort. In this context, it is important to emphasize that both TC and AI reflect the average TC and peak height ratios in the cells comprising the sample; they do not provide information about the variability of TC or AI *between* individual cells. Consequently, the ability to detect specific changes in TC or AI diminishes as the number and types of cells in the sample increases. On the basis of the DNA yields, we estimate that there were approximately 20 times more cells in the samples comprising the first cohort (median $\sim 10^6$ cells), than the second cohort (median $\sim 5 \times 10^4$ cells). This difference reflects the relative amounts of tissue available from the fresh surgical specimens comprising the first cohort versus the sections of paraffin-embedded tissue blocks comprising the second cohort. This consideration is particularly significant in the case of the AI assay. On the basis of theoretical considerations and mixing experiments (data not shown), we estimate that imbalance at a specific locus must occur in ~40% of the cells in the sample to generate an allelic ratio of 1.68, the threshold for significance used in these studies. Thus, sites of AI that are not prevalent in the cell population are not detected, even if there are many such individual sites. In this context, it is not surprising that specific sites of AI are detectable in breast tumors, which evolve clonally.[51] However, it is remarkable that AI is detected in TA-HN tissue, as it not only reflects underlying genomic instability, but also requires *clonal* expansion of genetically altered, premalignant cell clones within histologically normal breast tissues. This interpretation is further corroborated by the fact that more than a third of unbalanced alleles in adjacent, histologically normal tissues are conserved in the matched tumors. The latter has important practical implications, as it indicates that it is not necessary to micro-dissect tissues, for example using laser capture microscopy, to detect genomic instability, using the assays described in the present study. In fact, these assays allow the selective detection of changes in cell clones undergoing expansion because of proliferative advantages.

Taken together, our results are in agreement with the concept of ''field cancerization,'' introduced by Slaughter and colleagues in 1953,[56] and more recently reviewed by others.[57–59] These authors developed the term to explain the multifocal and seemingly independent areas of histologically precancerous alterations occurring in oral squamous cell carcinomas.[56] Organ systems in which field cancerization has been implied include lung, colon, cervix, bladder, skin and breast.[57] The concept of field cancerization has also been used to explain the occurrence of genetic and epigenetic mosaicism in cancer precursor tissues.[60] Based on our results, we propose to extend the concept of field cancerization to genetic alterations in otherwise histologically normal breast tissues, and our study is the first to include TC.

In head and neck squamous carcinoma, field cancerization has been shown for relatively large tissue areas, *i.e.* up to 7 cm in diameter.[61] It is thus not surprising that our data show extensive field cancerization in tissues 1 cm outside breast tumor margins. In the present study, TC was also different between disease-free NBRST-RM tissues and TA-HN tissues excised at 5 cm from the tumor margin. However, TC was similar in TA-HN-5 tissues and PBLs from women of similar age. Since telomere length decreases with age,[48,49] the observed difference in TC between NBRST-RM and TA-HN-5 tissues is likely due to the age discrepancy between the two cohorts of women (27 *vs*. 49 years).

The existence of fields of genomic instability that support tumorigenic events also has important clinical implications. First, such fields could give rise to clonal selection of precursor cells that ultimately lead to the development of cancer.[62] In this context, our recent studies have identified the presence of telomerase-positive cell populations within histologically normal tissues adjacent to breast tumors that could represent fields of premalignant cells.[45] Second, the presence of such fields, even after surgical resection of primary tumors, may represent an ongoing risk factor for cancer recurrence or formation of secondary lesions, which occurs in up to 22% of women undergoing breast conservation therapies for small invasive and noninvasive breast cancers.[58,63,64] For these reasons, our study has practical implications for the assessment of appropriate tumor margins for breast cancer surgical procedures, secondary treatment options and prognosis, possibly including the risk for the development of new primary tumors in the contra-lateral breast.[65–67] Thus, our study also suggests that evaluation of surgical margins should include molecular, in addition to histological, techniques, thus warranting further investigations.

Acknowledgements

We thank Myra Zucker from the University of New Mexico Pathology Laboratory for excision of the fresh breast tissues. We thank Kelly Salceies from the Human Tissue Repository for preparing and staining breast tissue sections.

References

1. Gollin SM. Chromosomal instability. Curr Opin Oncol 2004;16:25–31.
2. Charames GS, Bapat B. Genomic instability and cancer. Curr Mol Med 2003;3:589–96.
3. Nojima H. G1 and S-phase checkpoints, chromosome instability, and cancer. Methods Mol Biol 2004;280:3–49.
4. Lengauer C, Kinzler KW, Vogelstein B. Genetic instabilities in human cancers. Nature 1998;396:643–9.
5. Desmaze C, Soria JC, Freulet-Marriere MA, Mathieu N, Sabatier L. Telomere-driven genomic instability in cancer cells. Cancer Lett 2003;194:173–82.
6. Callen E, Surralles J. Telomere dysfunction in genome instability syndromes. Mutat Res 2004;567:85–104.
7. Hackett JA, Feldser DM, Greider CW. Telomere dysfunction increases mutation rate and genomic instability. Cell 2001;106:275–86.
8. Moyzis RK, Buckingham JM, Cram LS, Dani M, Deaven LL, Jones MD, Meyne J, Ratliff RL, Wu JR. A highly conserved repetitive DNA sequence, $(TTAGGG)_n$, present at the telomeres of human chromosomes. Proc Natl Acad Sci U S A. 1988;85:6622–6.
9. de Lange T. Protection of mammalian telomeres. Oncogene 2002;21:532–40.
10. Smogorzewska A, de Lange T. Regulation of telomerase by telomeric proteins. Ann Rev Biochem 2004;73:177–208.
11. Maser RS, DePinho RA. Telomeres and the DNA damage response: why the fox is guarding the henhouse. DNA Repair 2004;3:979–88.
12. Olovnikov AM. Principle of marginotomy in template synthesis of polynucleotides. Dokl Akad Nauk 1971;201:1496–9.
13. Smogorzewska A, van Steensel B, Bianchi A, Oelmann S, Schaefer MR, Schnapp G, de Lange T. Control of human telomere length by TRF1 and TRF2. Mol Cell Biol 2000;20:1659–68.
14. Bohr VA, Anson RM. DNA damage, mutation and fine structure DNA repair in aging. Mutat Res 1995;338:25–34.
15. Neumann AA, Reddel RR. Telomere maintenance and cancer—look, no telomerase. Nat Rev Cancer 2002;2:879–84.
16. Reddel RR. Alternative lengthening of telomeres, telomerase, and cancer. Cancer Lett 2003;194:155–62.
17. Greider CW, Blackburn EH. Identification of a specific telomere terminal transferase activity in tetrahymena extracts. Cell 1985;43:405–13.
18. Kim NW, Piatyszek MA, Prowse KR, Harley CB, West MD, Ho PL, Coviello GM, Wright WE, Weinrich SL, Shay JW. Specific association of human telomerase activity with immortal cells and cancer. Science 1994;266:2011–5.
19. Hastie N, Dempster M, Dunlop M, Thompson A, Green D, Alshire R. Telomere reduction in human colorectal carcinoma and with ageing. Nature 1990;346:866–8.
20. Furugori E, Hirayama R, Nakamura KI, Kammori M, Esaki Y, Takubo K. Telomere shortening in gastric carcinoma with aging despite telomerase activation. J Cancer Res Clin Oncol 2000;126:481–5.
21. Mehle C, Ljungberg B, Roos G. Telomere shortening in renal cell carcinoma. Cancer Res 1994;54:236–41.
22. Albertson DG, Collins C, McCormick F, Gray JW. Chromosome aberrations in solid tumors. Nat Genet 2003;34:369–76.
23. Ohyashiki JH, Sashida G, Tauchi T, Ohyashiki K. Telomeres and telomerase in hematologic neoplasia. Oncogene 2002;21:680–7.
24. Hirashima T, Komiya T, Nitta T, Takada Y, Kobayashi M, Masuda N, Matui K, Takada M, Kikui M, Yasumitu T, Ohno A, Nakagawa K, et al. Prognostic significance of telomeric repeat length alterations in pathological stage I–IIIA non-small cell lung cancer. Anticancer Res 2000;20:2181–7.
25. Hiyama E, Hiyama K, Yokoyama T, Ichikawa T, Matsuura Y. Length of telomeric repeats in neuroblastoma: correlation with prognosis and other biological characteristics. Jpn J Cancer Res 1992;83:159–64.
26. Donaldson L, Fordyce C, Gilliland F, Smith A, Feddersen R, Joste N, Moyzis R, Griffith J. Association between outcome and telomere DNA content in prostate cancer. J Urol 1999;162:1788–92.
27. Meeker AK, Hicks JL, Platz EA, March GE, Bennett CJ, Delannoy MJ, De Marzo AM. Telomere shortening is an early somatic DNA alteration in human prostate tumorigenesis. Cancer Res 2002;62:6405–9.
28. Fordyce CA, Heaphy CM, Joste NE, Smith AY, Hunt WC, Griffith JK. Association between cancer-free survival and telomere DNA content in prostate tumors. J Urol 2005;173:610–4.
29. Odagiri E, Kanada N, Jibiki K, Demura R, Aikawa E, Demura H. Reduction of telomeric length and c-erbB-2 gene amplification in human breast cancer, fibroadenoma, and gynecomastia. Relationship to histologic grade and clinical parameters. Cancer 1994;73:2978–84.
30. Griffith JK, Bryant JE, Fordyce CA, Gilliland FD, Joste NE, Moyzis RK. Reduced telomere DNA content is correlated with genomic instability and metastasis in invasive human breast carcinoma. Breast Cancer Res Treat 1999;54:59–64.
31. Meeker AK, Hicks JL, Iacobuzio-Donahue CA, Montgomery EA, Westra WH, Chan TY, Ronnett BM, De Marzo AM. Telomere length abnormalities occur early in the initiation of epithelial carcinogenesis. Clin Cancer Res 2004;10:3317–26.
32. Meeker AK, Argani P. Telomere shortening occurs early during breast tumorigenesis: a cause of chromosome destabilization underlying malignant transformation? J Mammary Gland Biol Neoplasia 2004;9:285–96.
33. O'Connell P, Pekkel V, Fuqua SA, Osborne CK, Clark GM, Allred DC. Analysis of loss of heterozygosity in 399 premalignant breast lesions at 15 genetic loci. J Natl Cancer Inst 1998;90:697–703.
34. Aubele MM, Cummings MC, Mattis AE, Zitzelsberger HF, Walch AK, Kremer M, Hofler H, Werner M. Accumulation of chromosomal imbalances from intraductal proliferative lesions to adjacent in situ and invasive ductal breast cancer. Diagn Mol Pathol 2000;9:14–9.
35. Farabegoli F, Champeme MH, Bieche I, Santini D, Ceccarelli C, Derenzini M, Lidereau R. Genetic pathways in the evolution of breast ductal carcinoma in situ. J Pathol 2002;196:280–6.
36. Deng G, Lu Y, Zlotnikov G, Thor AD, Smith HS. Loss of heterozygosity in normal tissue adjacent to breast carcinomas. Science 1996;274:2057–9.
37. Forsti A, Louhelainen J, Soderberg M, Wijkstrom H, Hemminiki K. Loss of heterozygosity in tumour-adjacent normal tissue of breast and bladder cancer. Eur J Cancer 2001;37:1372–80.
38. Lakhani SR, Chaggar R, Davies S, Jones C, Collins N, Odel C, Stratton MR, O'Hare MJ. Genetic alterations in 'normal' luminal and myoepithelial cells of the breast. J Pathol 1999;189:496–503.
39. Kurose K, Hoshaw-Woodard S, Adeyinka A, Lemeshow S, Watson PH, Eng C. Genetic model of multi-step breast carcinogenesis involving the epithelium and stroma: clues to tumor-microenvironment interactions. Hum Mol Gen 2001;10:1907–13.
40. Moinfar F, Man YG, Arnould L, Bratthauer GL, Ratschek M, Tavassoli FA. Concurrent and independent genetic alterations in the stromal and epithelial cells of mammary carcinoma: implications for tumorigenesis. Cancer Res 2000;60:2562–6.
41. Larson PS, de las Morenas A, Bennett SR, Cupples LA, Rosenberg CL. Loss of heterozygosity or allele imbalance in histologically normal breast epithelium is distinct from loss of heterozygosity or allele imbalance in co-existing carcinomas. Am J Pathol 2002;161:283–90.
42. Meeker AK, Hicks JL, Gabrielson E, Strauss WM, De Marzo AM, Argani P. Telomere shortening occurs in subsets of normal breast epithelium as well as in situ and invasive carcinoma. Am J Pathol 2004;164:925–35.
43. Euhus DM, Cler L, Shivapurkar N, Milchgrub S, Peters GN, Leitch AM, Heda S, Gazdar AF. Loss of heterozygosity in benign breast epithelium in relation to breast cancer risk. J Natl Cancer Inst 2002;94:858–60.
44. Ellsworth DL, Ellsworth RE, Love B, Deyarmin B, Lubert SM, Mittal V, Shriver CD. Genomic patterns of allelic imbalance in disease-free tissue adjacent to primary breast carcinomas. Breast Cancer Res Treat 2004;88:131–9.
45. Hines WC, Fajardo AM, Joste NE, Bisoffi M, Griffith JK. Quantitative and spatial measurements of telomerase reverse transcriptase expression within normal and malignant human breast tissues. Mol Cancer Res 2005;3:503–9.
46. Fordyce CA, Heaphy CM, Griffith JK. Chemiluminescent measurement of telomere DNA content in biopsies. Biotechniques 2002;33:144–6, 8.
47. Bryant JE, Hutchings KG, Moyzis RK, Griffith JK. Measurement of telomeric DNA content in human tissues. Biotechniques 1997;23:476–8, 80, 82.
48. Baird DM, Kipling D. The extent and significance of telomere loss with age. Ann N Y Acad Sci 2004;1019:265–8.
49. Aviv A. Telomeres and human aging: facts and fibs. Sci Aging Knowl Environ 2004;51:43.
50. Mathieu N, Pirzio L, Freulet-Marriere MA, Desmaze C, Sabatier L. Telomeres and chromosomal instability. Cell Mol Life Sci 2004;61:641–56.
51. Simpson PT, Reis-Filho JS, Gale T, Lakhani SR. Molecular evolution of breast cancer. Mol J Pathol 2005;205:248–54.
52. Kenemans P, Verstraeten RA, Verheijen RH. Oncogenic pathways in hereditary and sporadic breast cancer. Maturitas 2004;49:34–43.
53. O'Connell P. Genetic and cytogenetic analyses of breast cancer yield different perspectives of a complex disease. Breast Cancer Res Treat 2003;78:347–57.
54. Pathak S, Nemeth MA, Multani AS, Thalmann GN, von Eschenbach AC, Chung LW. Can cancer cells transform normal host cells into malignant cells? Br J Cancer 1997;76:1134–8.

55. Ozen M, Multani AS, Kuniyasu H, Chung LW, von Eschenbach AC, Pathak S. Specific histologic and cytogenetic evidence for in vivo malignant transformation of murine host cells by three human prostate cancer cell lines. Oncol Res 1997;9:433–8.
56. Slaughter DP, Southwick HW, Smejkal W. Field cancerization in oral stratified squamous epithelium; clinical implications of multicentric origin. Cancer 1953;6:963–8.
57. Braakhuis BJ, Tabor MP, Kummer JA, Leemans CR, Brakenhoff RH. A genetic explanation of Slaughter's concept of field cancerization: evidence and clinical implications. Cancer Res 2003;63:1727–30.
58. Garcia SB, Park HS, Novelli M, Wright NA. Field cancerization, clonality, and epithelial stem cells: the spread of mutated clones in epithelial sheets. J Pathol 1999;187:61–81.
59. Hockel M, Dornhofer N. The hydra phenomenon of cancer: why tumors recur locally after microscopically complete resection. Cancer Res 2005;65:2997–3002.
60. Tycko B. Genetic and epigenetic mosaicism in cancer precursor tissues. Ann N Y Acad Sci 2003;983:43–54.
61. Braakhuis BJ, Leemans CR, Brakenhoff RH. Expanding fields of genetically altered cells in head and neck squamous carcinogenesis. Semin Cancer Biol 2005;15:113–20.
62. Ellsworth DL, Ellsworth RE, Liebman MN, Hooke JA, Shriver CD. Genomic instability in histologically normal breast tissues: implications for carcinogenesis. Lancet Oncol 2004;5:753–8.
63. Li Z, Moore DH, Meng ZH, Ljung BM, Gray JW, Dairkee SH. Increased risk of local recurrence is associated with allelic loss in normal lobules of breast cancer patients. Cancer Res 2002;62:1000–3.
64. Huston TL, Simmons RM. Locally recurrent breast cancer after conservation therapy. Am J Surg 2005;189:229–35.
65. Klimberg VS, Harms S, Korourian S. Assessing margin status. Surg Oncol 1999;8:77–84.
66. Singletary SE. Surgical margins in patients with early-stage breast cancer treated with breast conservation therapy. Am J Surg 2002;184:383–93.
67. Meric-Bernstam F. Breast conservation in breast cancer: surgical and adjuvant considerations. Curr Opin Obstet Gynecol 2004;16:31–6.

Appendix D

Journal of Molecular Diagnostics, Vol. 9, No. 2, April 2007

DOI: 10.2353/jmoldx.2007.060115

Assessment of the Frequency of Allelic Imbalance in Human Tissue Using a Multiplex Polymerase Chain Reaction System

Christopher M. Heaphy,* William C. Hines,* Kimberly S. Butler,* Christina M. Haaland,* Glenroy Heywood,[†‡] Edgar G. Fischer,[§] Marco Bisoffi,*[‡] and Jeffrey K. Griffith*[‡]

From the Departments of Biochemistry and Molecular Biology, Surgery,[†] and Pathology,[§] and the Cancer Research and Treatment Center,[‡] University of New Mexico School of Medicine, Albuquerque, New Mexico*

Genomic instability can generate chromosome breakage and fusion randomly throughout the genome, frequently resulting in allelic imbalance, a deviation from the normal 1:1 ratio of maternal and paternal alleles. Allelic imbalance reflects the karyotypic complexity of the cancer genome. Therefore, it is reasonable to speculate that tissues with more sites of allelic imbalance have a greater likelihood of having disruption of any of the numerous critical genes that cause a cancerous phenotype and thus may have diagnostic or prognostic significance. For this reason, it is desirable to develop a robust method to assess the frequency of allelic imbalance in any tissue. To address this need, we designed an economical and high-throughput method, based on the Applied Biosystems AmpF*l*STR Identifiler multiplex polymerase chain reaction system, to evaluate allelic imbalance at 16 unlinked, microsatellite loci located throughout the genome. This method provides a quantitative comparison of the extent of allelic imbalance between samples that can be applied to a variety of frozen and archival tissues. The method does not require matched normal tissue, requires little DNA (the equivalent of ~150 cells) and uses commercially available reagents, instrumentation, and analysis software. Greater than 99% of tissue specimens with ≥2 unbalanced loci were cancerous. ***(J Mol Diagn 2007, 9:266–271; DOI: 10.2353/jmoldx.2007.060115)***

It is widely accepted that genomic instability—the duplication, loss, or structural rearrangement of a critical gene(s)—occurs in virtually all cancers[1] and in some instances has diagnostic, prognostic, or predictive significance. Thus, it is not surprising that tumor progression is reflected by allelic losses or gains in genes that regulate aspects of cell proliferation, apoptosis, angiogenesis, invasion, and, ultimately, metastasis.[2,3]

There are several technologies available to detect chromosomal copy number changes in tumor cells. For example, chromosome painting techniques can identify chromosomal copy number changes in cytological preparations.[4,5] Segmental genomic alterations can be identified by comparative genomic hybridization (CGH). CGH identifies copy number changes by detecting DNA sequence copy variations throughout the entire genome and mapping them onto a cytogenetic map supplied by metaphase chromosomes.[6] On the other hand, array CGH maps copy number aberrations relative to the genome sequence by using arrays of bacterial artificial chromosome or cDNA clones as the hybridization target instead of the metaphase chromosomes.[7–11] However, these methods cannot identify all cases of allelic imbalance (AI), which is a deviation from the normal 1:1 ratio of maternal and paternal alleles, for instance, in cases with uniparental disomy. In addition, these methods are poorly suited for high-throughput applications, and analysis is limited to a relatively small cellular field, thus increasing potential sampling error.

Single nucleotide polymorphism (SNP) arrays can be used for high-resolution genome-wide genotyping and loss of heterozygosity detection.[12–14] For example, the development of a panel of 52 microsatellite markers that detects genomic patterns of loss of heterozygosity[15–17] has been used for breast cancer diagnosis and prognosis. However, this approach requires matched referent (normal) DNA, typically blood or buccal samples, and these cancer-type-specific panels may not be informative for other cancers, thus limiting their applicability across multiple tumor types. Larger panels of SNPs may be used for genome-wide analysis, for example, the Affymetrix 10K and 100K SNP mapping arrays.[18,19] Likewise, Illumina BeadArrays with a SNP linkage-mapping panel[20] allow allelic discrimination directly on short genomic seg-

Supported by the Department of Defense (Breast Cancer Research Program: DAMD17-02-1-0514, W81XWH-05-1-0273, and W81XWH-04-1-0370; Prostate Cancer Research Program: W81XWH-04-1-0831 and W81XWH-06-1-0120) and the National Institutes of Health (grant RR0164880).

Accepted for publication November 17, 2006.

Address reprint requests to Jeffrey K. Griffith, Ph.D., Department of Biochemistry and Molecular Biology, MSC08 4670, 1 University of New Mexico, Albuquerque, NM 87131-0001. E-mail: jkgriffith@salud.unm.edu.

ments surrounding the SNPs of interest, thus overcoming the need for high-quality DNA.[14] Lips and colleagues[21] have shown that Illumina BeadArrays can be used to obtain reliable genotyping and genome-wide loss of heterozygosity profiles from formalin-fixed, paraffin-embedded (FFPE) normal and tumor tissues. However, all these approaches, although robust, require costly reagents and specialized equipment, and the sheer amount of data produced from these analyses complicate the interpretation of results.

For these reasons, and as outlined by Davies and colleagues,[22] it is desirable to develop a general, economical, and high-throughput method to assess the frequency of AI in any tissue, independent of the nature and composition of the specimen and the availability of matched, normal tissue. To address this need, we developed a method to measure the ratio of maternal and paternal alleles at 16 unlinked, microsatellite short tandem repeat (STR) loci in a single multiplexed polymerase chain reaction (PCR). The assay, which is based on the Applied Biosystems AmpF/STR Identifiler system, can be performed with only 1 ng of genomic DNA and uses commercially available primers and reagents as well as common instrumentation and analysis software. Thus, it is an attractive alternative to current methods and is readily adaptable to most clinical laboratory environments.

Materials and Methods

Tissue Acquisition

All tissues were provided by the University of New Mexico Solid Tumor Facility, unless otherwise specified. Buccal cells were collected from oral rinses of volunteers. The Cooperative Human Tissue Network (Western Division, Nashville, TN) provided frozen normal and tumor renal tissues obtained by radical nephrectomy, frozen normal breast tissues obtained by reduction mammoplasty, and normal frozen prostate tissues obtained through autopsy. A set of FFPE prostate tumors obtained by radical prostatectomy was provided by the Cooperative Prostate Cancer Tissue Resource (*http://www.cpctr.cancer.gov*). Duodenal FFPE tumor tissues were obtained from the Mayo Clinic (Rochester, MN). Pancreatic FFPE normal and tumor tissues were obtained from the Department of Pathology at the University of New Mexico. Frozen endometrial tumor tissues were obtained through the Gynecologic Oncology Group (Philadelphia, PA). All specimens lacked patient identifiers and were obtained in accordance with all federal guidelines, as approved by the University of New Mexico Human Research Review Committee.

DNA Isolation and Quantification

DNA was isolated from all tissue samples using the DNeasy silica-based spin column extraction kit (Qiagen, Valencia, CA) and the manufacturer's suggested animal tissue protocol. FFPE samples were treated with xylene and washed with ethanol before DNA extraction. DNA concentrations were measured using the Picogreen dsDNA quantitation assay (Molecular Probes, Eugene, OR) using a λ phage DNA as the standard as directed by the manufacturer's protocol.

Multiplex PCR Amplification of STR Loci

The AmpF/STR Identifiler kit (Applied Biosystems, Foster City, CA) was used to amplify genomic DNA at 16 different STR microsatellite loci (Amelogenin, CSF1PO, D2S1338, D3S1358, D5S818, D7S820, D8S1179, D13S317, D16S539, D18S51, D19S433, D21S11, FGA, TH01, TPOX, and vWA) in a single multiplexed PCR reaction, according to the supplier's protocol. Linear amplification of allelic PCR products is a prerequisite for ratiometric determination of AI. Therefore, each PCR reaction was limited to 28 cycles, as determined in preliminary studies. The 16 primer sets are designed and labeled with either 6-FAM, PET, VIC, or NED to permit the discrimination of all amplicons in a single electrophoretic separation. The PCR products were resolved by capillary electrophoresis using an ABI Prism 377 DNA sequencer (Applied Biosystems). Fluorescent peak heights were quantified using ABI Prism GeneScan analysis software (Applied Biosystems). Allelic ratios were calculated using the peak height, rather than the peak area, as suggested in previous studies.[23–25] For simplicity, the allele with the greater fluorescence was always made the numerator, as to always generate a ratio ≥ 1.0.

Statistical Analysis

A Pearson χ^2 test was performed using SAS JMP software version 9.1 (SAS Institute Inc., Cary, NC) to examine the relationship between the extent of AI and tissue type, using a significance level of 0.05.

Results

The 16 allelic microsatellite loci amplified by the AmpF/STR Identifiler primer sets are unlinked and can be used to assess AI simultaneously at multiple heterozygous sites throughout the genome. This is technically possible because each amplicon is labeled with one of four fluorescent dyes (6-FAM, PET, VIC, and NED), each with a unique emission profile, thus allowing the resolution of amplicons of similar size. Figure 1 shows the sizes of VIC-labeled amplicons derived from a representative specimen of matched normal and tumor renal tissue (the fluorescent channels showing the PET-, 6-FAM-, and NED-labeled products are not shown). Within Figure 1A, illustrating the results from the normal tissue specimen, two of the allelic pairs are homozygous (D13S317, D16S539), as indicated by a single peak, and three of the allelic pairs are heterozygous (D3S1358, TH01, D2S1338), as indicated by two peaks. Although the peak heights varied between different loci, ostensibly because of different PCR efficiencies, the peak heights of the paired alleles were similar. Theoretically, the ratio of any

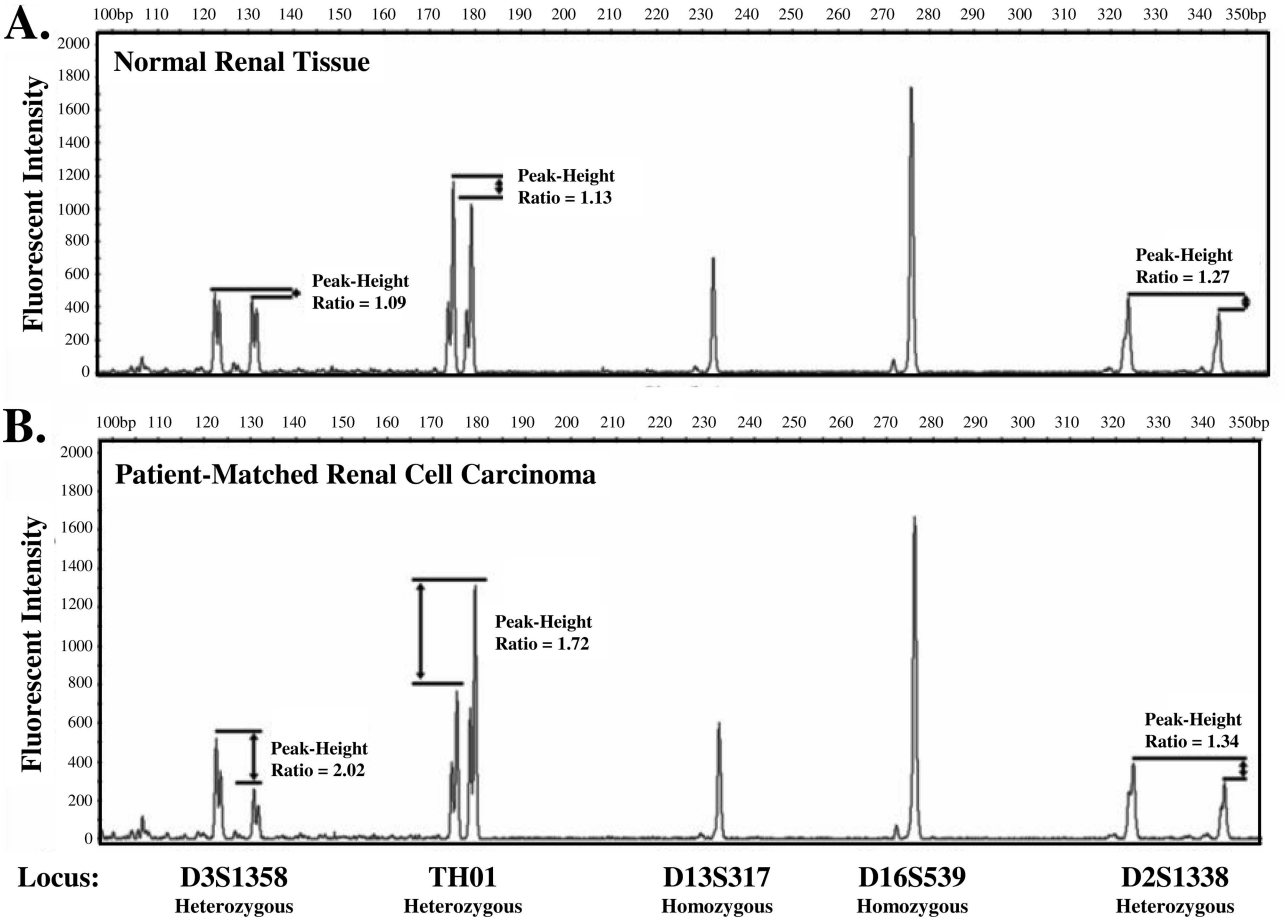

Figure 1. Electropherograms of VIC-labeled amplicons from a matched normal and renal carcinoma sample. PCR was performed and the resulting amplicons resolved as described in Materials and Methods. Only VIC-labeled amplicons are shown. In this particular sample, the D3S1358, THO1, and D2S1338 loci are heterozygous, and D13S317 and D16S539 loci are homozygous. Fluorescence intensity is shown on the *y* axis, and amplicon size, in bp, is shown on the *x* axis. The ratios of the fluorescent intensities of each allelic pair of heterozygous loci are shown. Loci with allelic ratios of >1.60 are defined as sites of AI for matched normal (**A**) or tumor (**B**) tissue.

two heterozygous alleles is 1.0 in normal tissues. However, differences in PCR efficiency between different length alleles and random experimental variation resulting from instruments, reagents, and personnel may affect the observed ratio of heterozygous alleles. To assess these sources of potential variation, the ratios of paired alleles' signal intensities were compared at 320 heterozygous loci in buccal cells from 27 healthy individuals. Across all loci, the mean ratio was near 1.0 (mean, 1.15; SD, 0.18). We expect that ~97.5% of all allelic ratios in normal tissues would fall within 2.5 SD of the mean and therefore operationally defined an allelic ratio of >1.60 (mean +2.5 SD) as a site of AI. Applying this threshold to the 27 analyzed buccal samples, only eight sites of AI were detected of the 320 heterozygous loci, thus representing a mean of 0.30 unbalanced loci per sample. Figure 1B illustrates the results of the tumor tissue matched to the normal sample in Figure 1A. Within this sample, two of the three heterozygous loci in the renal tumor tissue amplified by the VIC-labeled primer sets have peak height ratios of >1.60, identifying them as sites of AI.

To determine whether AI determinations were reproducible, the assay was repeated within a random subset of the buccal samples. The mean absolute variation of the allelic ratios for the repeated samples was 10% and 193 of the 198 (97.5%) loci measured were correctly categorized on repeating the experiment; however, only five of the 198 (2.5%) loci initially designated as sites of AI could not be confirmed (Figure 2A). Two loci changed from sites without AI (≤1.60) to sites of AI (>1.60), and three loci changed from sites of AI to sites without AI.

We next confirmed that the differences in AI detected by this approach reflected true differences in the ratio of the alleles, not experimental artifact (eg, differential PCR amplification efficiency). We constructed defined mixtures of DNAs from the paired normal and tumor tissue shown in Figure 1. As shown in Figure 2B for the D3S1358 locus, there was a linear relationship (R^2 = 0.965) between the ratio of alleles measured in the assay and the composition of the mixture. Similar results were obtained for each of the other loci exhibiting a site of AI (TH01, R^2 = 0.973; VWA, R^2 = 0.981; D18S541, R^2 = 0.953). In contrast, the composition of the mixture had no effect on the allelic ratios of loci not exhibiting AI (data not shown).

The operationally defined threshold for AI was validated by measuring the allelic ratios for 1382 heterozygous loci in an independent test set comprised of 118

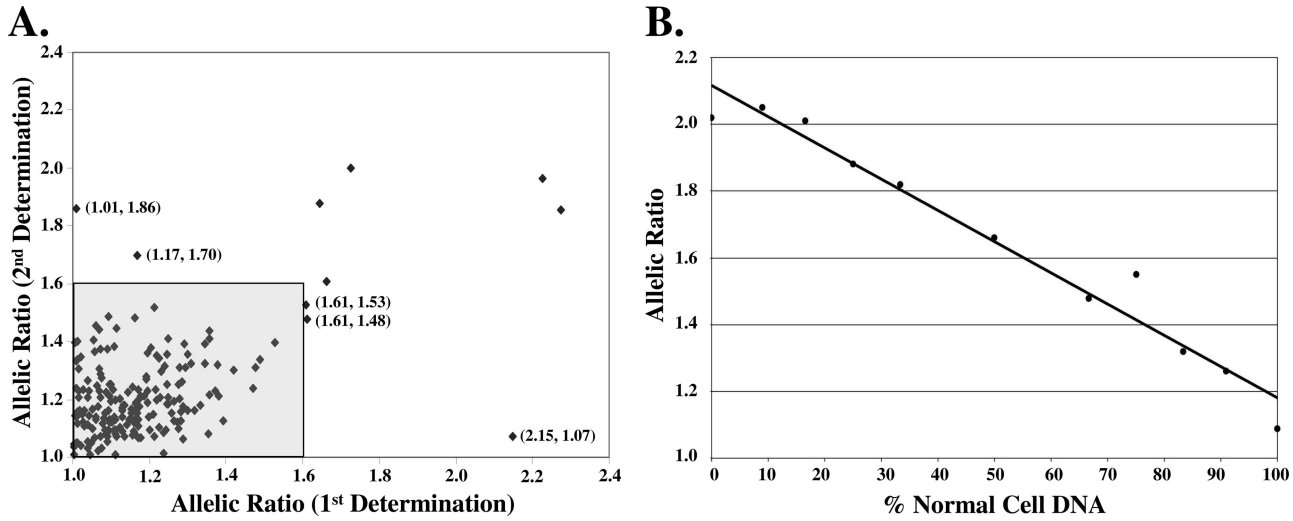

Figure 2. Reproducibility and effect of admixtures of matched normal and renal carcinoma DNA on allelic peak height ratios. **A:** Allelic peak height ratios were determined for 198 heterozygous loci in 16 normal buccal samples. The plot represents the first determination (*x* axis) and the second determination (*y* axis). The region defined by the **gray shaded box** represents all of the loci that were determined not to be a site of AI on both determinations. The labeled points (allelic peak height ratios for both determinations) represent the five loci that were not correctly identified on repeating the experiment. **B:** The specified admixtures were generated using DNA from a matched pair of normal renal tissue and renal cell carcinoma as shown in Figure 1. Data from the heterozygous D3S1358 locus are shown. The allelic ratios are 1.09 in the normal renal tissue and 2.02 in the renal carcinoma. The best-fit line was generated by linear regression and has a correlation coefficient (R^2) of 0.965.

normal samples consisting of bone (n = 2), breast (n = 10), buccal (n = 53), lymph node (n = 5), peripheral blood lymphocytes (n = 18), pancreas (n = 6), placenta (n = 3), prostate (n = 4), renal (n = 16), and tonsil (n = 1) tissues (Figure 3A). In this sample set of normal tissues, only 32 of 1382 heterozygous loci were designated sites of AI, thus representing a mean of 0.27 unbalanced loci per sample, comparable with the 0.30 unbalanced loci per sample in the original normal sample set. In summary, 88 (74.6%), 29 (24.6%), and one (0.8%) of the 118 normal tissues specimens contained zero, one, and two loci with AI, respectively.

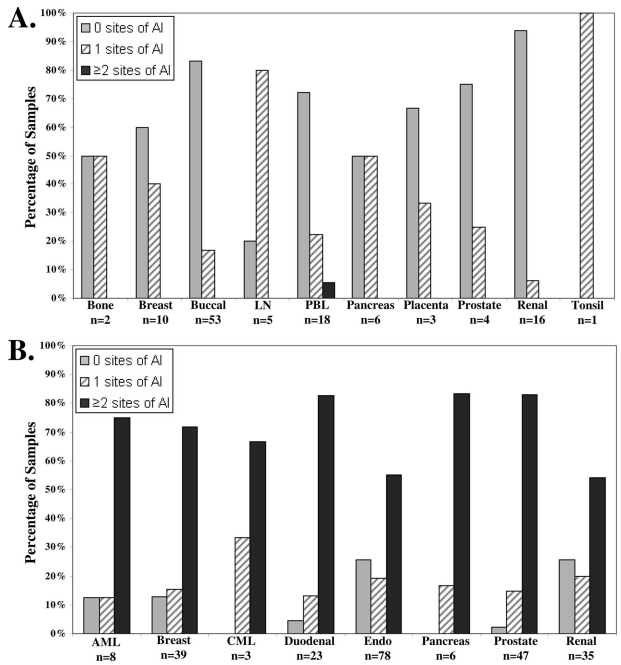

Figure 3. Frequency of AI in normal and tumor tissues. The numbers of sites of AI (ie, 0, 1, ≥2) were determined in 118 samples of normal tissue (**A**) and in 239 samples of tumor tissue (**B**). The number of specimens in each tissue set (n) is indicated below the set designation. LN, lymph node; PBL, peripheral blood lymphocytes; AML, acute myelogenous leukemia; CML, chronic myelogenous leukemia; Endo, endometrial. See Materials and Methods for additional details.

It is well established that cancerous tissues have more sites of AI than normal tissues. To validate our assay in this context, we next measured the frequency of AI in 2792 heterozygous loci in a set of 239 frozen or FFPE tumor samples consisting of acute myelogenous leukemia (n = 8), breast (n = 39), chronic myelogenous leukemia (n = 3), duodenal (n = 23), endometrial (n = 78), pancreas (n = 6), prostate (n = 47), and renal (n = 35) tissues. As shown in Figure 3B, 37 (15.5%), 41 (17.2%), and 161 (67.4%) of the 239 tumor tissues specimens contained zero, one, and more than or equal to two loci with AI, respectively. In contrast to the normal tissues, 611 sites of AI were detected, thus representing a mean of 2.56 unbalanced loci per sample, nearly 10 times greater than the frequency in the normal tissues ($P < 0.0001$). In summary, 162 of 357 tissue specimens had ≥2 unbalanced loci, of which >99% were cancerous.

Discussion

The frequency of AI reflects the karyotypic complexity of the cancer genome and such manifestations are widespread in solid tumors.[1] There have been numerous studies of these abnormalities and several techniques, including chromosome painting, array CGH, and SNP arrays, have emerged to analyze these differences between normal and tumor tissues.[4–21] However, these methods are typically costly, time intensive, and need a matched referent (normal) DNA sample for analysis. For this reason,

it is desirable to develop general, economical, high-throughput methods to quantify the extent of AI in the genome of any tissue, independent of the nature and composition of the specimen and the availability of matched, normal tissue.

Using our newly developed assay and interpretation scheme to assess the frequency of AI in human tissues, we have shown in a set of 239 samples that 67% of the tumors contained two or more sites of AI, as compared with 0.8% of the normal samples, which represents an almost 84-fold difference. It must be noted that tissue heterogeneity, such as a preponderance of normal cells within the tumor, may quench peak-height ratios below the 1.60 threshold, thus obscuring AI in a particular sample. In addition, the assay cannot discriminate between homozygous alleles and complete loss of heterozygosity in the absence of matched normal tissue. However, the latter limitation is mitigated by the near ubiquitous presence of normal tissue within tumors, which allows for the assessment of AI in samples without requiring analysis of matched normal tissue. This is an important consideration in the potential evaluation of biopsy tissue, which may contain multiple clones of genetically altered cells superimposed on a background of normal stromal and epithelial cells, and obtaining matched normal tissue may be difficult.

Altered gene expression resulting from genomic instability is a cause of cancer progression; therefore, cancerous tissues have more sites of AI than normal tissues. Consistent with this observation, >99% of tissues with ≥2 sites of AI were cancerous. We are currently investigating the possibility that the number of sites of AI in cancer tissue is a reflection of its stage of progression and therefore may correlate with clinical parameters or prognosis.

Existing alternative methods identify AI as a difference in the allelic ratios in the sample of interest (eg, tumor) relative to the allelic ratios in a patient-matched referent DNA. These methods allow for the distinction between complete loss of heterozygosity and a constitutive homozygous allele and are able to control for PCR efficiency differences of alleles of dissimilar length. In contrast, the present method identifies AI as a deviation from a 1:1 ratio between alleles within the sample of interest only. Thus, the assay described herein can be performed on specimens for which a reliable referent sample is not available. In addition, we have determined that the mean absolute variation of the allelic ratios for all microsatellite loci in our panel is ~15% in normal tissues. This variation represents the combined effects of 1) random experimental error resulting from instruments, reagents, and personnel; 2) copy number polymorphisms; and 3) inherent differences in the PCR efficiencies of microsatellite alleles of dissimilar lengths. Based on replicate experiments of the same sample (Figure 2A), we have determined that random experimental variation resulting from instruments, reagents, and personnel accounts for ~10% of the overall variation. Therefore, variation resulting from differences in PCR efficiencies is ~5%. Although the latter variation is excluded by comparison to a referent DNA, the requirement for two determinations (sample of interest and referent), each with an average variation of at least 10%, minimizes the benefit gained by controlling for PCR efficiency.

In conclusion, we describe here a simple method for assessing the extent of AI throughout the genome. This method has a number of significant advantages over existing technologies, such as chromosome painting, array CGH, and SNP arrays and, as a molecular-based assay, may be used clinically in conjunction with histological techniques. The advantages of this method are that 1) it is robust, reproducible, and provides a quantitative basis for comparing the extent of AI between samples; 2) it does not require matched normal tissue; 3) it utilizes commercially available reagents, instrumentation, and analysis software;, 4) it can be applied to a variety of fresh, frozen, and archival tissues; 5) it requires very little DNA (the equivalent of ~150 cells); and 6) >99% of tissues with ≥2 sites of AI were cancerous.

Acknowledgments

We thank Terry Mulcahy and Phillip Enriquez III, from the DNA Research Services of the University of New Mexico Health Sciences Center for gel capillary analysis; and Dr. Artemis Chakerian from the University of New Mexico Experimental Pathology Laboratory for tissue sectioning.

References

1. Lengauer C, Kinzler KW, Vogelstein B: Genetic instabilities in human cancers. Nature 1998, 396:643–649
2. Payne SR, Kemp CJ: Tumor suppressor genetics. Carcinogenesis 2005, 26:2031–2045
3. Hanahan D, Weinberg RA: The hallmarks of cancer. Cell 2000, 100:57–70
4. Mundle SD, Sokolova I: Clinical implications of advanced molecular cytogenetics in cancer. Expert Rev Mol Diagn 2004, 4:71–81
5. Gray JW, Collins C: Genome changes and gene expression in human solid tumors. Carcinogenesis 2000, 21:443–452
6. Kallioniemi A, Kallionemi OP, Sudar D, Rutovitz D, Gray JW, Waldman F, Pinkel D: Comparative genomic hybridization for molecular cytogenic analysis of solid tumors. Science 1992, 258:818–821
7. Solinas-Toldo S, Lampel S, Stilgenbauer S, Nickolenko J, Benner A, Dohner H, Cremer T, Lichter P: Matrix-based comparative genomic hybridization: biochips to screen for genomic imbalances. Genes Chromosom Cancer 1997, 20:399–407
8. Pinkel D, Segraves R, Sudar D, Clark S, Poole I, Kowbel D, Collins C, Kuo WL, Chen C, Zhai Y, Dairkee SH, Ljung BM, Gray JW, Albertson DG: Quantitative high resolution analysis of DNA copy number variation in breast cancer using comparative genomic hybridization to DNA microarrays. Nat Genet 1998, 20:207–211
9. Pollack JR, Perou CM, Alizadeh AA, Eisen MB, Pergamenschikov A, Williams CF, Jeffrey SS, Botstein D, Brown PO: Genome-wide analysis of DNA copy-number changes using cDNA microarrays. Nat Genet 1999, 23:41–46
10. Snijders AM, Nowak N, Segraves R, Blackwood S, Brown N, Conroy J, Hamilton G, Hindle AK, Huey B, Kimura K, Law S, Myambo K, Palmer J, Ylstra B, Yue JP, Gray JW, Jain AN, Pinkel D, Albertson DG: Assembly of microarrays for genome-wide measurement of DNA copy number. Nat Genet 2001, 29:263–264
11. Albertson DG: Profiling breast cancer by array CGH. Breast Cancer Res Treat 2003, 78:289–298
12. Rauch A, Ruschendorf F, Huang J, Trautmann U, Becker C, Thiel C, Jones KW, Reis A, Nurnberg P: Molecular karyotyping using an SNP array for genomewide genotyping. J Med Genet 2004, 41:916–922
13. Zhao X, Li C, Paez JG, Chin K, Janne PA, Chen TH, Girard L, Minna J, Christiani D, Leo C, Gray JW, Sellers WR, Meyerson M: An inte-

grated view of copy number and allelic alterations in the cancer genome using single nucleotide polymorphism arrays. Cancer Res 2004, 64:3060–3071
14. Fan JB, Oliphant A, Shen R, Kermani BG, Garcia F, Gunderson KL, Hansen M, Steemers F, Butler SL, Deloukas P, Galver L, Hunt S, McBride C, Bibikova M, Rubano T, Chen J, Wickham E, Doucet D, Chang W, Campbell D, Zhang B, Kruglyak S, Bentley D, Haas J, Rigault P, Zhou L, Stuelpnagel J, Chee MS: Highly parallel SNP genotyping. Cold Spring Harb Symp Quant Biol 2003, 68:69–78
15. Ellsworth RE, Ellsworth DL, Lubert SM, Hooke J, Somiari RI, Shriver CD: High-throughput loss of heterozygosity mapping in 26 commonly deleted regions in breast cancer. Cancer Epidemiol Biomarkers Prev 2003, 129:915–919
16. Ellsworth DL, Ellsworth RE, Love B, Deyarmin B, Lubert SM, Mittal V, Hooke JA, Shriver CD: Outer breast quadrants demonstrate increased levels of genomic instability. Ann Surg Oncol 2004, 11:861–868
17. Ellsworth RE, Ellsworth DL, Deyarmin B, Hoffman LR, Love B, Hooke JA, Shriver CD: Timing of critical genetic changes in human breast disease. Ann Surg Oncol 2005, 12:1054–1060
18. Zhou X, Mok SC, Chen Z, Li Y, Wong DT: Concurrent analysis of loss of heterozygosity (LOH) and copy number abnormality (CNA) for oral premalignancy progression using the Affymetrix 10K SNP mapping array. Hum Genet 2004, 115:327–330
19. Meaburn E, Butcher LM, Schalkwyk LC, Plomin R: Genotyping pooled DNA using 100K SNP microarrays: a step towards genomewide association scans. Nucleic Acids Res 2006, 34:e27
20. Murray SS, Oliphant A, Shen R, McBride C, Steeke RJ, Shannon SG, Rubano T, Kermani BG, Fan JB, Chee MS, Hansen MS: A highly informative SNP linkage panel for human genetic studies. Nat Methods 2004, 1:113–117
21. Lips EH, Dierssen JW, van Eijk R, Oosting J, Eilers PH, Tollenaar RA, de Graaf EJ, van't Slot R, Wijmenga C, Morreau H, van Wezel T: Reliable high-throughput genotyping and loss-of-heterozygosity detection in formalin-fixed, paraffin-embedded tumors using single nucleotide polymorphism arrays. Cancer Res 2005, 65:10188–10191
22. Davies JJ, Wilson IM, Lam WL: Array CGH technologies and their applications to cancer genomes. Chromosome Res 2005, 13:237–248
23. Paulson TG, Galipeau PC, Reid BJ: Loss of heterozygosity analysis using whole genome amplification, cell sorting, and fluorescence-based PCR. Genome Res 1999, 9:482–491
24. Medintz IL, Lee CC, Wong WW, Pirkola K, Sidransky D, Mathies RA: Loss of heterozygosity assay for molecular detection of cancer using energy-transfer primers and capillary array electrophoresis. Genome Res 2000, 10:1211–1218
25. Skotheim RI, Diep CB, Kraggerud SM, Jakobsen KS, Lothe RA: Evaluation of loss of heterozygosity/allelic imbalance scoring in tumor DNA. Cancer Genet Cytogenet 2001, 127:64–70